Unravelling the presynaptic connectome of adult-generated neurons: Rabies virus-mediated tracing of monosynaptic connections onto newborn neurons

Aditi Deshpande

Dissertation of the Graduate School of Systemic Neurosciences
Ludwig Maximilians University Munich

Munich, 2012

Supervisor	Prof. Benedikt Berninger
Second reviewer	Prof. Magdalena Götz
Date of oral defense	10th December 2012

“Mühsam ernährt sich das Eichhörnchen”

For my grandfather,

Table of Contents

1 Introduction 3

1.1 Neurogenesis in the adult brain 3

1.1.1 Historical perspective 3

1.1.2 Cellular perspective: Adult neural stem cells 4

1.2 Hippocampal Neurogenesis 6

1.2.1 Dentate gyrus: Anatomical structure 7

1.2.2 Dentate gyrus: Synaptic connectivity 8

1.2.3 Dentate gyrus: Overview of adult neurogenesis 10

1.2.4 Dentate gyrus: Synaptic integration and functional relevance of adult neurogenesis 12

1.3 Olfactory Neurogenesis 18

1.3.1 Olfactory system: Anatomical structure 18

1.3.2 Olfactory system: Synaptic connectivity 21

1.3.3 Olfactory system: Overview of adult neurogenesis 23

1.3.4 Olfactory system: Synaptic integration and functional relevance of adult neurogenesis 25

1.4 Watching new neurons 'listen' 29

1.5 Neuronal tracers 29

1.5.1 Non-viral Transneuronal Tracers 30

1.5.2 Viral Transneuronal Tracers 31

1.5.2.1 Herpes viruses 32

1.5.2.2 Rabies virus 33

1.5.2.3 Lifecycle of the rabies virion. 34

1.5.2.4 Monosynaptic tracing using rabies virus 37

2 Results 43

2.1 In vitro validation of the monosynaptic tracing technique. 43

2.1.1 Embryonic cortical culture 43

2.1.2 Postnatal astroglial culture 50

2.2 In vivo implementation of the monosynaptic tracing technique 53

2.2.1 Tracing the connectivity of adult-generated neurons in the dentate 53

2.2.2 Tracing the connectivity of adult-generated neurons in the dentate 63

2.3 In vivo implementation of the monosynaptic tracing technique 73

2.3.1 Tracing of presynaptic partners of adult-generated neurons in the olfactory bulb. 73

3 Discussion 81

3.1 Rabies virus to reveal the presynaptic connectome of adult-generated . . . neurons 81

3.1.1 Specificity of retrovirus and RABV-based monosynaptic tracing: the pseudotransduction conundrum 82

3.2 Identifying the presynaptic partners of newborn neurons in the adult dentate gyrus 85

3.2.1 Local connectivity. 85

3.2.1.1 Hilar interneurons 85

3.2.1.2 Mossy cells 86

3.2.1.3 Glial cells 87

3.2.2 Influence of local interneurons and mossy cells on adult neurogenesis 87

3.2.3 Long-distance projections 89

3.2.4 Role of afferents in adult neurogenesis 92

3.3 Identification of the presynaptic partners of newborn neurons in the . . . . . olfactory bulb 95

3.3.1 Local connectivity and its influence on neurogenesis 95

3.3.2 Long distance connectivity 98

3.3.3 Influence of afferents on adult neurogenesis 100

3.4 Conclusion and future prospects 101

4 Methods 105

4.1 In vitro methods 105

4.1.1 Preparation and transduction of embryonic cortex cultures 105

4.1.2 Preparation and transduction of postnatal astrocytes 106

4.1.3 Treatment of cover slips and coating with PDL. 106

4.1.4 Immunocytochemistry 107

4.2 In vivo methods 107

4.2.1 Animals 107

4.2.2 Genotyping 108

4.2.3 Viral vector construction 109

4.2.3.1 Retroviral constructs 109

4.2.3.2 Rabies virus constructs 114

4.2.4 DNA preparation for retrovirus production (CsCl gradient) . .114

4.2.5 Retrovirus Production 116

4.2.5.1 Cells. 116

4.2.5.2 Retroviral Packaging 116

4.2.5.3 Retroviral Harvesting 117

4.2.5.4 Retroviral titering 117

4.2.6 Pseudotyped rabies virus production. 118

4.2.7 Stereotactic injections 119

4.2.8 Fixation and histology 120

4.2.9 Immunohistochemistry 120

4.2.10 Confocal imaging and cell counting 121

4.2.11 Electrophysiological recordings of neuronal cultures. 121

4.2.12 Statistical analysis 122

4.3 Materials 123

4.3.1 Primary antibodies 123

4.3.2 Secondary antibodies 124

4.3.3 Solutions 125

4.3.4 Media 127

5 Appendix 129

5.1 Appendix 1: List of abbreviations 129

5.2 Appendix 2: List of figures 133

6 Bibliography 136

List of publications

Acknowledgements

Introduction

Summary

Generation of new neurons in the adult brain of most mammals is restricted to the subgranular zone (SGZ) of the dentate gyrus (DG) of the hippocampus and the subependymal zone (SEZ) of the lateral ventricle. These newly generated neurons integrate into pre-existing networks and remodel the basic circuitry for information processing. This integration of newborn neurons is known to follow a distinct pattern compared to those generated during development. Even so, the final connectivity of these two populations is predicted to be very similar. However, the precise identity of the various synaptic partners, local and long-range, acquired during the process of maturation is not yet entirely known. In this study, a rabies virus (RABV)-based monosynaptic tracing technique was adapted to identify the presynaptic partners of adult-generated neurons. To specifically target newborn neurons a retrovirus, that selectively transduces proliferating cells, was engineered to express two key proteins - TVA, ligand for EnvA, the envelope protein of an avian virus, and the rabies virus (RABV) glycoprotein (G) – requisite for infection and subsequent retrograde transsynaptic spread of the EnvA-pseudotyped RABV, respectively. Thus, primary infection by the EnvA-pseudotyped RABV was restricted to "starter" cells ectopically expressing the TVA receptor. Providing these starter cells with G allowed for the subsequent retrograde transsynaptic virus transfer to presynaptic partners.

The strategy employed for identifying presynaptic partners of adult-born neurons in vivo consisted of stereotaxic injections of *G* and *TVA*-encoding retrovirus into the DG

of adult mice to transduce neuronal progenitors, followed by a second injection of EnvA-pseudotyped RABV at different time points. This resulted in the appearance of retrovirus and EnvA-pseudotyped RABV infected newborn granule neurons that retrogradely transported the RABV to their immediate presynaptic partners - local interneurons and mossy cells in the DG as well as long-distance projections originating in the entorhinal cortex, medial septum and nucleus of the diagonal band of Broca. Surprisingly, there was occasional labeling of neurons in the subiculum, a subdivision of the hippocampal formation whose projection to the DG has not been studied in detail.

Stereotactic injections of the *G* and *TVA*-encoding retrovirus into the SEZ followed by EnvA-pseudotyped RABV into the rostral migratory stream (RMS) 4 days later resulted in infection by EnvA-pseudotyped RABV of those migrating neuroblasts expressing the TVA receptor and G, having been previously transduced by the retrovirus. In the olfactory bulb, double-transduced newborn granule and periglomerular cells were observed in addition to EnvA-pseudotyped RABV-only infected cells within the olfactory bulb. These presumably belong to the heterogeneous population of short-axon cells, some of which are known to innervate granule cells. Monosynaptic tracing also revealed RABV-only labelled cells in the anterior olfactory nucleus (AON) and piriform cortex.

Studying the presynaptic connectivity of adult-generated neurons at different stages following their birth revealed increasingly diverse populations of presynaptic partners suggestive of the gradual incorporation of adult-generated neurons into functional neural circuits. The implications of newborn neurons receiving these various inputs is discussed in the context of the influence of afferents may have on neurogenesis and the contribution of adult neurogenesis to remodelling of pre-existing circuits.

1 Introduction

1.1 Neurogenesis in the adult brain

1.1.1 Historical perspective

"*Once the development was ended, the founts of growth and regeneration of the axons and dendrites dried up irrevocably. In the adult centers, the nerve paths are something fixed, ended, and immutable. Everything may die, nothing may be regenerated. It is for the science of the future to change, if possible, this harsh decree.*" (Cajal, 1928)

The fascinating discovery of neurogenesis, first in the postnatal brain and then in the adult, nearly five decades ago, challenged the harsh decree rendered by Cajal and altered a fundamental principle in the field of neuroscience that new neurons cannot be generated in the adult mammalian brain. Using autoradiographic labelling with 3H-thymidine, Altman and Das showed that new neurons are generated in the olfactory bulb and hippocampus of adult rats (Altman, 1969; Altman and Das, 1965). Tritiated thymidine is a nucleotide base analogue that gets incorporated into DNA during synthesis and hence can be used as a marker for cell proliferation (Sidman et al., 1959). These studies were corroborated by the work of Kaplan and Hinds in which they used 3H-Thymidine to reveal newly generated cells in the dentate gyrus and olfactory bulb of three month old rats and confirmed that they were neurons by electron microscopy (Kaplan and Hinds, 1977). Several following studies in the rodent and other mammals provided substantial evidence that new neurons are indeed added to the adult mammalian brain, that they receive synaptic inputs and extend axonal projections (Kaplan and Bell,

1984; Stanfield and Trice, 1988).

However, these pioneering studies were met with considerable scepticism and the final proof of neurogenesis in the adult rodent brain came only in the 1990s with the introduction of cell specific immunohistochemical markers that could be used to identify the newborn neurons (Cameron et al., 1993) and the development of Bromodeoxyuridine (BrdU) as a marker of proliferating cells (Kuhn et al., 1996; Miller and Nowakowski, 1988). BrdU, also a thymidine base analogue, gets incorporated into the DNA of proliferating cells and its advantage over 3H-thymidine is that it can be used in combination with other cell specific markers to establish the identity of dividing cells and their progeny by immunohistochemistry. Several laboratories since then have used innovative techniques such as retroviral labelling (Luskin, 1993), Cre-mediated fate mapping and transplantation experiments (Lois and Alvarez-Buylla, 1994; Ventura and Goldman, 2007) to unequivocally demonstrate that new neurons are generated in discrete regions of the adult rodent brain throughout life. Moreover, studies have shown that adult neurogenesis is not restricted to the rodent brain, but is found in other non-mammalian vertebrates such as birds, lizards and non-human primates (Goldman and Nottebohm, 1983; Gould et al., 1999; Lopez-Garcia et al., 1988). Although the presence of new neurons in the adult human olfactory bulb has been challenged by recent findings (Bergmann et al., 2012; Sanai et al., 2011), evidence from the seminal study by Eriksson et al (1995) and findings from other labs still strongly point towards neurogenesis in the adult hippocampus (**Fig.1.1**) (Eriksson et al., 1998; Knoth et al., 2010).

1.1.2 Cellular perspective: Adult neural stem cells

After the establishment of neurogenesis in the adult brain, the next question was - where are these neurons coming from? Consequently, the identity and location of the cells that give rise to the adult-generated neurons became a subject of intense research. It was discovered that new neurons in the adult mammalian central nervous system (CNS) are generated from a population of cells called adult neural stem cells

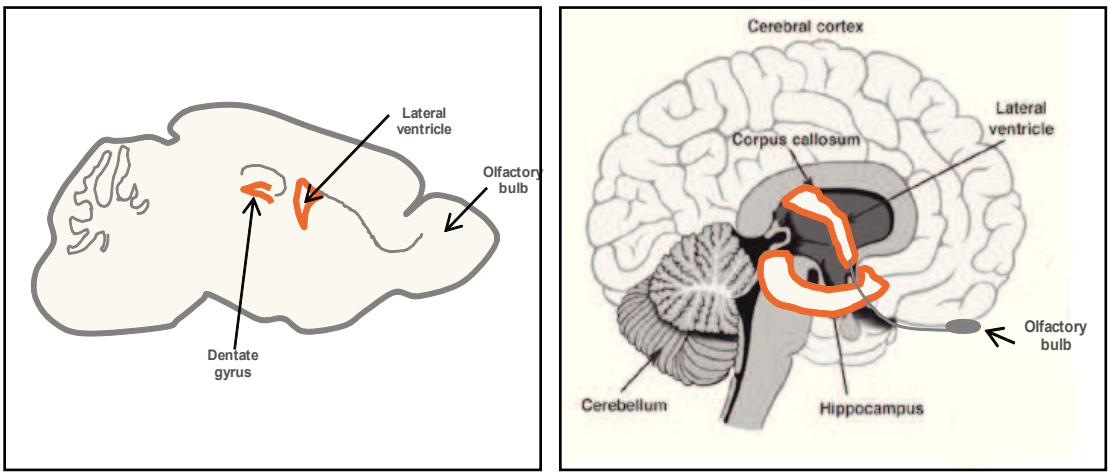

Fig. 1.1. Sites of neurogenesis in the adult brain.
Neurogenesis occurs in two regions in the adult brain. The subependymal zone (SEZ) of the lateral ventricles and in the dentate gyrus of the hippocampus. (A) Adult rodent brain. (B) Adult human brain. Neurogenic regions are indicated in orange (modified from Crews and Nixon, 2003).

(aNSCs), quiescent or slow-dividing multipotent progenitors that have the capacity to self-renew and give rise to neurons and glia throughout life (Doetsch et al., 1999; Johansson et al., 1999; Morshead et al., 1994). Different studies suggested various identities for aNSCs such as astrocytes or ependymal cells however the current evidence strongly favors the astrocytic/radial glial lineage of aNSCs, which are reminiscent of radial glia giving rise to neurons and glia in the developing brain (Pinto and Gotz, 2007; Kriegstein and Alvarez-Buylla, 2009). These aNSCs were isolated from adult rodent and human CNS and cultured in vitro to generate cells in the neural lineage (Kukekov et al., 1999; Reynolds and Weiss, 1992).

The two predominant neurogenic niches in the adult brain are - the subependymal zone (SEZ) of the lateral ventricle and the subgranular zone (SGZ) within the dentate gyrus of the hippocampus (Ming and Song, 2005). In the permissive microenvironment of the neurogenic niche comprising of astrocytes, ependymal cells, microglia, extracellular matrix and vasculature, aNSCs generate different types of progenitors called transit amplifying precursors (TAP) or intermediated precursors (IP) which in turn give rise to neuroblasts that finally mature into neurons (Ma et al., 2009). Adult NSCs are influenced by several common niche factors that regulate their self-renewal, fate specification, migration and differentiation. For example, astrocytes have been shown to regulate

nearly all aspects of adult neurogenesis (Barkho et al., 2006; Song et al., 2002); cells of the vasculature have been suggested to affect proliferation of aNSCs by providing blood-derived cues (Calvo et al., 2011; Palmer et al., 2000; Tavazoie et al., 2008); and molecules such as Wnt (Lie et al., 2005), Sonic hedgehog (Ahn and Joyner, 2005) and growth factors such as Fibroblast growth factor (FGF) and Brain-derived neurotrophic factor (BDNF) (Bergami et al., 2008; Yoshimura et al., 2001) influence proliferation and maintenance of aNSCs, survival, differentiation and even integration of newborn neurons in the adult brain. Besides these cues, the proliferation of aNSCs and survival of newly generated neurons is also affected by external stimuli such as exercise, enriched environment and stress (Kempermann et al., 1997; Rochefort et al., 2002; Tanapat et al., 1998).

While the identity of aNSCs was being investigated, studies on other fundamental questions in adult neurogenesis - what are these new neurons, why are they there, why only SEZ and SGZ? - had already begun. After decades of work, we have resolved some of these key questions and answers to many are just emerging. We now know that adult-generated neurons of the SEZ and SGZ have distinct terminal fates, they get fully integrated into the existing circuitry and contribute to various brain functions (Imayoshi et al., 2008). However the exact mechanisms of this process and its control remain to be fully elucidated.

1.2 Hippocampal Neurogenesis

Before delving into the complexities of hippocampal neurogenesis, a brief description of the structure and connectivity of this region is due. The hippocampus is one of the most well studied regions of the mammalian brain, in part because of its indisputable role in memory and learning and in part for its highly laminar organization. Along with the dentate gyrus, the subiculum, the presubiculum, the parasubiculum and the entorhinal cortex it forms a complex structure in the medial temporal lobe of the brain called hippocampal formation (Amaral et al., 2007).

1.2.1 Dentate gyrus: Anatomical structure

As an integral part of the hippocampal formation, the dentate gyrus functions as a continuous source of neurons throughout life that are required for information processing in hippocampal-dependent learning behaviours and formation of new memories (Kee et al., 2007; Tashiro et al., 2007). During development, the mouse dentate gyrus begins to form at about embryonic day 10 from progenitors in the primary dentate neuroepithelium located in the medial wall of the lateral ventricle (Sibbe et al., 2009). This progenitor pool further proliferates and migrates to give rise to the secondary proliferative matrix that begins to generate the granule cell layer (GCL) and a tertiary proliferative matrix that migrates into the hilus (Martin et al., 2002; Sibbe et al., 2009). The earliest-born granule neurons originate from the secondary proliferative matrix and poplulate the outermost region of the developing GCL while the later-born granule neurons derive from the tertiary proliferative matrix and form the inner core (Martin et al., 2002). Radial glial cells have been suggested to be the source of dentate stem cells as well as guiding the migration of granule neurons (Sibbe et al., 2009). The upper blade of the GCL is generated embryonically whereas the lower blade forms after birth. Stem cells in the tertiary proliferative matrix persist in the SGZ and continue to generate granule neurons during adulthood (Sibbe et al., 2009). The different cell types of the adult dentate gyrus are distributed into 3 layers :

Granule cell layer (GCL). The GCL is made up of densely packed excitatory, glutamatergic granule neurons. At the base of this layer lies the SGZ, the neurogenic niche harboring aNSCs that are responsible for generating newborn granule neurons (and astrocytes) in the adult mammalian brain (Ming and Song, 2005). Cell bodies of various γ-amino-butyric acid (GABA)ergic interneurons of the dentate gyrus are also often scattered along the GCL. The upper blade of the GCL is called the suprapyramidal blade and the lower blade is called the infrapyramidal blade (Amaral et al., 2007).

Hilus. It is also known as the polymorphic layer and it lies between the two blades of the dentate gyrus. It is occupied by different types of GABAergic interneurons, glutamatergic mossy cells, mossy fibres and glia (Amaral et al., 2007).

Molecular layer (ML). Above the GCL lies a relatively cell-free layer called the molecular layer which is occupied by interneurons, dendrites of granule neurons, axons of hilar interneurons and axons of pyramidal neurons in the entorhinal cortex, belonging to the perforant path (Amaral et al., 2007).

The hippocampus proper is divided into three subfields - CA3, CA2 and CA1. The CA3 subfield emerges between the two limbs of the dentate gyrus and continues into a narrow zone of cells termed as CA2. The pyramidal neurons of the CA3 and CA2 are similar in morphology but quite distinct in terms of their connectivity and function (Shepherd, 2003).

1.2.2 Dentate gyrus: Synaptic connectivity

The basic circuitry of the hippocampal formation comprises of unidirectionally connected excitatory circuits starting at the entorhinal cortex because most of the sensory information coming to the hippocampus enters from there. The perforant path, comprising of the axonal projections of excitatory, glutamatergic pyramidal neurons of the entorhinal cortex, provides the major input to dentate granule neurons. The mossy fibres, axons of granule neurons in the hilus, in turn terminate on the CA3 subfield of the hippocampus. They establish contact with the pyramidal neurons of CA3 which send their axons, called Schaeffer collaterals, to innervate the pyramidal neurons of CA1 (Shepherd, 2003). The CA1 subfield projects to the deeper layers of the entorhinal cortex and subiculum, thus completing a closed 'tripartite loop' of information flow from the cortex to the hippocampus and back to the cortex (Claiborne et al., 1986; Li et al., 2009). In addition to being a part of the trisynaptic circuit, the axons of CA3 pyramidal neurons send "backprojections" to the dentate gyrus and evidence strongly suggests that

this back projection innervates hilar mossy cells and GABAergic interneurons. Dentate granule neurons, on the other hand, receive inhibitory projections from interneurons in the CA3 subfield (Scharfman, 2007).

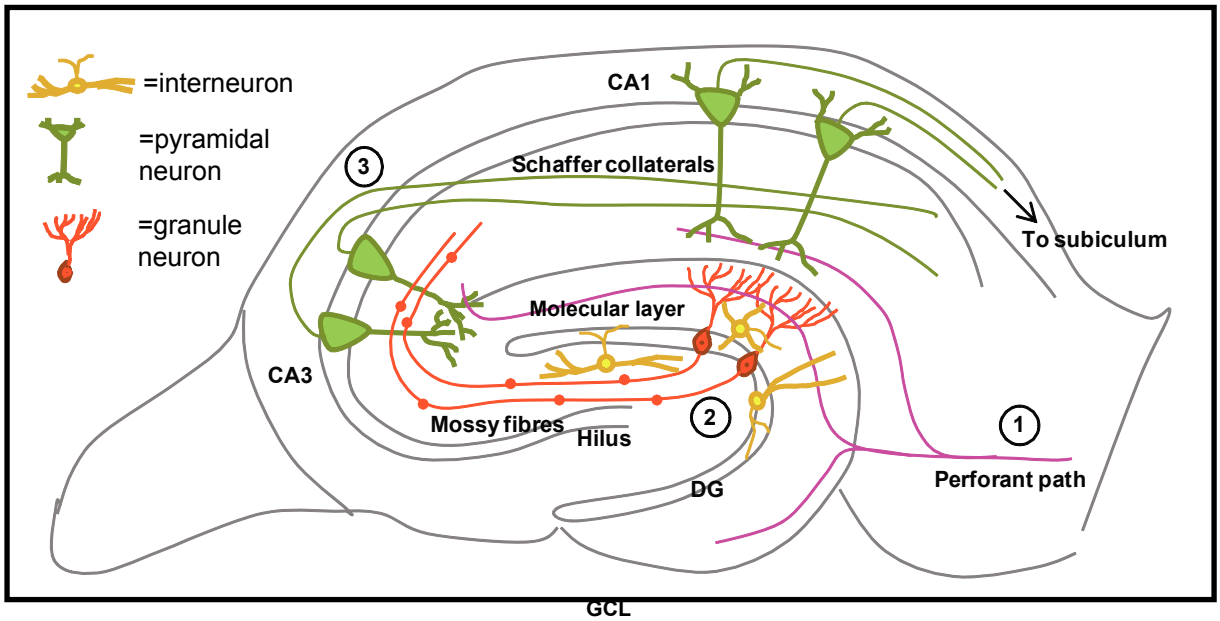

Fig. 1.2. Trisynaptic loop of hippocampal circuitry.
The entorhinal cortex provides the major synaptic input to the mature and newborn granule neurons [1]. Mossy fibres, axons of granule neurons, traverse through the hilus and innervate the proximal dendrites of CA3 [2] which in turn send their axons called Schaffer collaterals to the CA1 subfield [3], which projects back to the entorhinal cortex. Granule neurons are also innervated by different types of interneurons located in the hilus, granule cell layer and molecular layer. DG=dentate gyrus (adapted from Moser, E., 2011).

Besides the excitatory input via the perforant path, granule neurons receive local inhibitory inputs from interneurons in the hilus and ML (**Fig. 1.2**) (Houser, 2007). In addition, mossy fibres also have large boutons all along their length which form synapses with proximal dendrites of mossy cells in the hilus (Ribak et al., 1985), basal dendrites of basket cells and other GABAergic interneurons in the hilus. The local excitatory input to granule neurons arises from the mossy cells (Amaral et al., 2007) and extrinsic regulation to the adult hippocampal circuitry is provided via afferent systems from the medial septum/nucleus of the diagonal band of Broca (MS-NDB; cholinergic), raphe nucleus (serotonergic), locus coeruleus (noradrenergic) and ventral tegmental area (dopaminergic) (**Fig. 1.3**) (Leranth and Frotscher, 1983; Leranth and Hajszan, 2007). The newborn granule neurons have to integrate into this existing circuitry while maintaining its integrity and at the same time remodelling distinct networks important

for processing new information in the hippocampus.

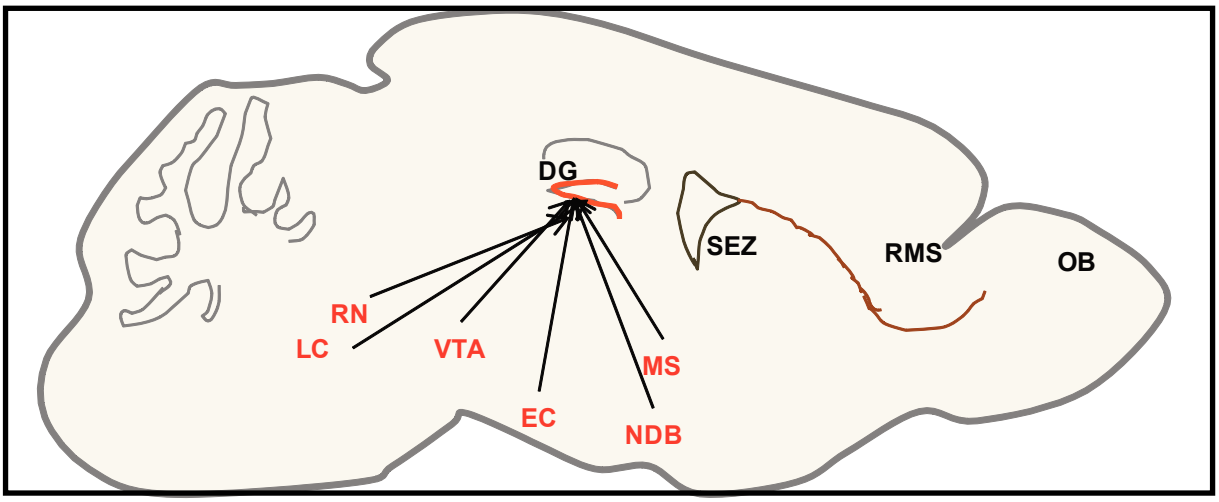

Fig. 1.3. Schematic of afferent inputs to the dentate gyrus.
Arrows extending to the olfactory bulb (OB) originate from brain structures that project to these areas. DG=dentate gyrus; MS=medial septum; NDB=diagonal band nucleus; EC=entorhinal cortex; VTA=ventral tegmental area; RN=raphe nucleus; LC=locus coeruleus (modified from Arenkiel, B., 2011).

1.2.3 Dentate gyrus: Overview of adult neurogenesis

The SGZ of the adult dentate gyrus harbors aNSCs expressing glial fibrillary acidic protein (GFAP). Various fate mapping studies have identified two morphologically distinct types of aNSCs: the radial aNSC that has its cell body in the SGZ and extends a process through the GCL branching extensively in the inner ML (Lugert et al., 2010). The radial morphology appears to resemble that of radial glia which generate neurons in the developing CNS. The non-radial (or horizontal) aNSC has its cell body in the SGZ but lacks a radial process and often extends small processes parallel to the SGZ (Suh et al., 2007; Lugert et al., 2010). In addition to GFAP, aNSCs also express Nestin, SRY-related HMG transcription factor (Sox2), brain lipid binding protein (BLBP) and are responsive to canonical Notch signalling through Hes5 expression (Lugert et al., 2010; Bonaguidi et al., 2011). Radial aNSCs, referred to as type-1 cells, are considered to be the quiescent NSCs of the hippocampus. They give rise to type-2a IPs that continue to express Sox2 but not GFAP, start downregulating Nestin and BLBP and express proneural genes such as Mash1 (Seri et al., 2001; Suh et al., 2007). Although expression of Mash1 is predominantly observed in IPs, some aNSCs in the SGZ have been shown to express

Mash1 (Kim et al., 2011); F.Guillemot, personal communication). Encinas et al (2011) proposed the 'disposable stem cell' model according to which quiescent Nestin-positive aNSCs in the dentate gyrus when activated undergo a series of rapid asymmetric divisions to generate fast dividing IPs that give rise to neurons, and then permanently leave the stem cell lineage by differentiating into an astrocyte, which ultimately would be responsible for the age-related decline in neurogenesis (Encinas et al., 2011). The 'disposable stem cell' model contradicted the conventional model which suggests that activated aNSCs undergo asymmetrical division to produce an IP that differentiates into a neuron and return to the quiescent state to be activated again at later time points (Encinas et al., 2011). In a recent model of dentate neurogenesis, Lugert et al (2012) demonstrated that aNSCs generate type-2a IPs, which are self-renewing progenitors giving rise to type-2b early neuroblasts expressing Tbr2 and Doublecortin (Dcx) through a single asysmmetric division, i.e., without amplification. Type-2b cells then divide to amplify the precursor pool before generating post-mitotic neuroblasts (type-3 cells) and neurons (Lugert et al., 2012). Neuronal fate of type-3 cells is apparent by the overlapping expression of pro-neural genes Prox1, NeuroD1 and Dcx (**Fig. 1.4**; Bonaguidi et al., 2011). In contrast to the 'disposable stem cell' model, Lugert et al (2012) argued that, as they could observe self-renewing aNSCs even in the brains of old mice and as they could not observe an increase in aNSC-derived astrocytes (S100β-positive) over time, the age-related decline in neurogenesis would, at least partially, be due to quiescence of aNSCs (Lugert et al., 2012).

Although it appears that the process of generation of granule neurons in vivo is highly debated, all of the above studies concur at one point, i.e., aNSCs in the adult dentate gyrus do generate granule neurons. The entire process of granule neuron development is supposed to take about 7-8 weeks in mice. Upon maturation, these newborn neurons exhibit dendritic and axonal distributions comparable to fully mature dentate granule neurons (Bergami and Berninger, 2012; Zhao et al., 2006).

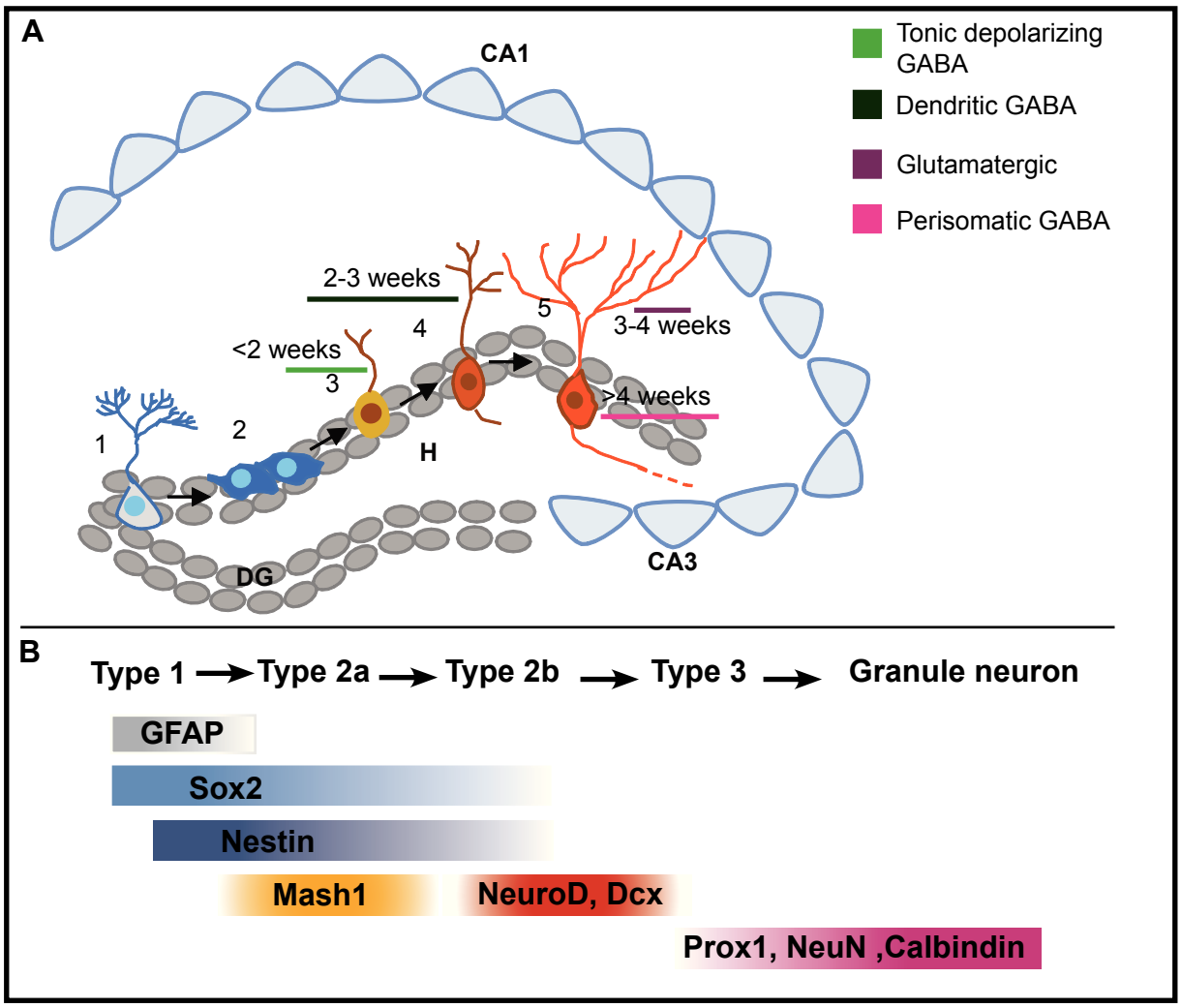

Fig. 1.4. Hippocampal neurogenesis.
(A) Radial glial-like cells of the subgranular zone of the dentate gyrus are the self-renewing stem cells, type-1 cells that give rise to intermediate precursor type 2 cells which in turn can generate immature neurons, express $GABA_A$ receptors and respond tonically to GABA released from local interneurons. GABA-mediated depolarization regulates the synaptic maturation and integration of granule neurons into the existing circuit. This is followed by formation of GABAergic dendritic synaptic inputs and finally perisomatic GABAergic inputs. Glutamatergic synapse formation starts after initial synaptogenesis of GABAergic dendritic synaptic inputs and before synaptogenesis of perisomatic GABAergic synaptic inputs. (B) Sequence of marker expression in the different cell types invoved in dentate neurogenesis. DG=dentate gyrus; H=hilus; 1=stem cells; 2=intermediate progenitor cells; 3=neuroblasts; 4=immature granule neuron; 5=mature granule neuron (adapted from Ming and Song, 2011 and Imayoshi and Kageyama, 2011).

1.2.4 Dentate gyrus: Synaptic integration and functional relevance of adult neurogenesis

The functional integration of adult-generated granule neurons has been studied extensively using classical electrophysiological recordings from newborn neurons labelled with retrovirus or in transgenic reporter mice (Ge et al., 2006; Markwardt et al., 2009). Newborn granule neurons in the adult dentate gyrus are activated by extrasynaptic

or tonic GABA as early as 3 days following their birth (Ge et al., 2006). Phasic (GABA release from synaptic vesicles) activation by GABA occurs only in the second week after birth when the first synapses are formed onto newborn neurons, involving mainly local interneurons. These synapses develop on the spineless dendrites of adult-generated neurons (Esposito et al., 2005). The initial tonic (or the early phasic) GABA release depolarizes immature neurons due to the high expression of the chloride (Cl^-) importer, NKCC1, on their surface which leads to an intracellular Cl^- concentration ($[Cl^-]i$) that is relatively high. The increased $[Cl^-]i$ establishes a transmembrane Cl^- equilibrium potential (E_{Cl}) that is positive with respect to the resting membrane potential. Activation by GABA leads to opening of $GABA_A$ channels on immature neurons causing the efflux of Cl^- and thereby membrane depolarization. As the neuron matures, there occurs downregulation of NKCC1 expression and increase in the expression of the Cl^- exporter, KCC2 resulting in a negative E_{Cl}. Opening of $GABA_A$ channels now leads to influx of Cl^- and membrane hyperpolarization (Ben-Ari and Cherubini, 1991; Ge et al., 2006). This progressive increase in KCC2 activity coupled with decreased NKCC1 activity causes the GABAergic switch from excitatory to inhibitory and it is an important step in maturation of newborn neurons. This GABA-mediated excitation has been shown to play an important role in neuronal differentiation (Masiulis et al., 2011).

By the third week after birth, newborn granule neurons exhibit spines and start receiving excitatory contacts from the entorhinal cortex (Mongiat and Schinder, 2011). Electron microscopy combined with retroviral labelling techniques have demonstrated that newborn granule neurons extend filopodia towards a bouton already involved in a synapse with another neuron, forming a multi-synapse bouton (Toni et al., 2007). According to this model, the dendritic spine from the newborn neuron competes with the existing contact and eventually eliminates it, forming a single-synapse bouton. At about the same time, mossy fibre terminals begin forming contacts with neurons in the CA3 region, some of which are shared with the pre-existing contacts (Toni et al., 2008). Maturation is complete with the appearance of perisomatic GABAergic contacts (Esposito

et al., 2005). Synaptic integration of adult-generated granule neurons follows a sequence similar to that observed in embryonic and postnatal development, albeit at a slower rate (Esposito et al., 2005). Given that these newly generated granule neurons integrate into pre-existing networks, they are likely to fulfil functions other than replacement of neurons lost in the hippocampus and contribute to changes in global network activity and higher brain functions. Indeed, young neurons display a lower threshold for long term potentiation (LTP) induction and reduced GABAergic inhibition compared to their mature counterparts. The LTP of perforant path inputs onto newborn granule neurons is almost double that of synapses on mature granule neurons. It is mediated by NR2B subunit of the N-Methyl-D-aspartate receptor (NMDAR) and is not affected by GABA antagonists, in contrast to LTP at synapses onto mature granule neurons (Ge et al., 2007). Moreover, since it was shown that this enhancement of LTP takes place in a narrow time window of 4-6 weeks after birth, adult-born neurons may exert a specific role in the activity-dependent synaptic plasticity in the hippocampus and adult neurogenesis may be a prerequisite for acquiring this synaptic plasticity (Mongiat and Schinder, 2011). Indeed, a recent study demonstrated that mice lacking the NR2B-containing NMDAR specifically in adult-born granule neurons were impaired in discrimination of highly similar contexts (Kheirbek et al., 2012).

Functionally, synaptic plasticity contributes in the form of hippocampus-dependent learning and memory. The dentate gyrus has been implicated to be involved in separation of very similar events, better known as pattern separation (Aimone et al., 2011; Sahay et al., 2011). Computational models of pattern separation have suggested that, in the dentate gyrus, granule neurons can bring about strong and domain-specific pattern separation on overlapping representations arriving from the entorhinal cortex and project this signal onto the CA3 subfield of the hippocampus (Yassa and Stark, 2011). This occurs via the mossy fibre pathway from the dentate gyrus (receiving input via the perforant path) to the CA3 subfield resulting in a new memory. On the other hand, axon collaterals of neurons in the entorhinal cortex that directly reach CA3, bypassing the dentate

gyrus, facilitate memory retrieval (Yassa and Stark, 2011). Indeed, electrophysiological recordings have shown that mossy fibre input from dentate granule neurons can act as 'detonator' synapses and strongly depolarize CA3 neurons (Henze et al., 2002). In agreement with this idea, inactivation of the mossy fibre pathway interferes with new learning while leaving retrieval intact (Yassa and Stark, 2011).

Electrophysiological evidence has also revealed that granule neurons fire in a spatially selective manner. Grid cells in the entorhinal cortex are known to fire at different regularly spaced regions (forming a 'grid') in a particular environment (Hafting et al., 2005) and they project to granule neurons in the dentate gyrus. Like place cells in the CA1 and CA3 subfields, dentate granule neurons (place cells) too exhibit place fields (a specific location in a given environment where place cells exhibit a high firing rate), although they are more localized compared to those in the CA1 and CA3 (Schmidt et al., 2012). Leutgeb et al (2007) have shown that granule neurons are very sensitive to changes in spatial configuration. In their experiments, they found that in different environments, the dentate gyrus responded by changing the population of neurons recruited to fire within a particular environment (global remapping) while with subtle changes in the same environment, granule neurons exhibited gradual changes in their firing rates (rate remapping; Leutgeb et al., 2007; Schmidt et al., 2012). This remapping response in granule neurons occurred even when grid cells in the entorhinal cortex did not change their firing patterns, indicating that pattern separation occurred within the dentate gyrus. In addition to remapping, pattern separation may be brought about by the sparse firing of granule neurons. Only 2-4% of granule neurons are active in any given environment, i.e., only a small proportion of these cells have place fields, due to inhibition from hilar interneurons (Leutgeb et al., 2007). Interestingly, in a new environment the same set of place cells, that were active in the old environment, is active in the new one (Lisman, 2011). Therefore, inspite of having nearly tenfold more granule neurons in the dentate gyrus than its cortical input, there exist specific populations of granule neurons that are predisposed to being activated repeatedly in several physically distinct

environments (Schmidt et al., 2012). This is directly correlated to the firing thresholds of granule neuron populations which is highly variable meaning that neurons having a lower threshold have a higher potential of being activated, irrespective of the environment (the animal is in) (Schmidt et al., 2012).

In this context, why there should be such a high density of granule neurons in the dentate gyrus when the "functional pool" is so limited and its relation to pattern separation is unclear (Lisman, 2011). It should also be taken into consideration that new neurons are continually added to the dentate gyrus and they must be involved in the process of pattern separation. Recent evidence has indeed shown that neurogenesis is required for discrimination between highly similar stimuli. For example, mice with reduced neurogenesis have impairments in location discrimination tasks in which the stimuli were presented with little spatial separation (Clelland et al., 2009) or in other studies, mice with ablated neurogenesis are impaired in discriminating similar contexts in a fear conditioning task (Tronel et al., 2012). On the other hand, increasing neurogenesis in mice leads to enhanced pattern separation capability in location discrimination and contextual fear conditioning tasks (Creer et al., 2010; Sahay et al., 2011). Several models proposing a role for adult-generated neurons in pattern separation have been put forth. Data from one study has indicated that immature granule neurons are highly excitable and would be activated in response to a wide range of stimuli but as they mature, they would fire selectively in response to events that were experienced when they were immature (Schmidt et al., 2012; Tashiro et al., 2007). However, electrophysiological recordings and gene expression data from another study suggest granule neuron "retirement", meaning that the highly excitable newborn granule neurons (activated in response to a wide range of stimuli) instead of getting selectively tuned to specific stimuli, become more and more inhibited and eventually reach a threshold where they are no longer excitable in response to a wide range of physiological stimuli (Alme et al., 2010; Schmidt et al., 2012). This means that neurons mediating pattern separation would be lost from the "functional pool" which can then be eventually replenished by newly arriving neurons. A

recent study investigating the pattern separation capability of transgenic mice in which output of mature granule neurons was specifically inhibited by tetanus toxin reported that distinguishing two very similar experiences would involve a greater participation by adult-born granule neurons within the first few weeks after birth while discriminating two dissimilar experiences would involve mainly mature granule neurons. Moreover, pattern completion, required for memory recall, would be accomplished by old granule neurons that can rapidly reactivate specific networks related to a particular memory (Nakashiba et al., 2012). Thus, the exact role of newborn neurons in mediating pattern separation within the hippocampal network is not clear, although their involvement in this function is highly suggestive.

In addition, newborn granule neurons may also play an important role in other microcricuits involving local circuitry as they are known to innervate hilar interneurons which in turn inhibit mature granule neurons or newborn granule neurons. They also innervate hilar mossy cells which can excite many mature granule neurons (Song et al., 2012). A computational study has suggested that two of the major subtypes of hilar cells, i.e., excitatory hilar mossy cells and inhibitory hilar perforant path-associated interneurons (HIPP cells), that receive input from and project to the perforant path could mediate dynamic regulation of pattern separation in response to environmental and task demands. The model proposes that due to the connectivity of mossy cells and HIPP neurons in the dentate gyrus, which includes direct innervation of granule neurons, pattern separation by dentate granule neurons could be strongly decreased by decreasing mossy cell function or by increasing HIPP cell function. Conversely, pattern separation could be increased by the opposite manipulations. The authors propose that the "backprojection" from CA3 pyramidal neurons could be strongly involved since they directly modulate hilar mossy cells and HIPP cells (Myers and Scharfman, 2009; Yassa and Stark, 2011).

In summary, although individual properties of adult-generated granule neurons that enable them to integrate into networks within and outside the hippocampal formation

have been elucidated and the emerging role of these neurons in hippocampal function is becoming evident, factors controlling integration of new neurons into the existing circuits remain largely elusive. Understanding the impact of this integration on the circuit level would give some insight into the role of newborn neurons in hippocampal functions.

1.3 Olfactory Neurogenesis

1.3.1 Olfactory system: Anatomical structure

The olfactory bulb is an extension of the forebrain, occupying the rostral-most position in the mammalian brain. It is integrally connected to the SEZ, the second neurogenic region of the mammalian brain that continues to generate new neurons during adulthood (Alvarez-Buylla and Lim, 2004). The olfactory system differs from the dentate gyrus in the process of neurogenesis in that new neurons in the olfactory bulb are born from aNSCs located in the SEZ and have to migrate a long distance (up to 5 mm in the mouse) in order to reach the olfactory bulb and differentiate into various subtypes of neurons to participate in olfactory processing. It is similar to the dentate gyrus in its ability to receive and integrate new neurons as well as in its highly laminar structure.

Subependymal zone (SEZ). The mouse SEZ derives from progenitors in the lateral ganglionic eminence (LGE) at approximately embryonic day 13.5 and during embryogenesis the SEZ is responsible for generating a large population of cortical neurons and glia (Anderson et al., 1997; Molyneaux et al., 2007). The adult SEZ lies just adjacent to the ependymal layer lining the walls of the lateral ventricle and harbors distinct populations of stem cells that give rise to different subtypes of interneurons in the olfactory bulb. Until recently, it was believed that the lateral wall (facing the striatum) of the ventricle is the only proliferative zone in the adult SEZ but now it is clear that the medial wall (facing the septum), the dorsal wall (below the corpus callosum) and even the rostral migratory stream (RMS) contain proliferative neural stem cells (NSC) that have the

capacity to self renew and are multipotent, in vitro and in vivo (Gritti et al., 2002; Hack et al., 2005; Merkle et al., 2007).

The olfactory bulb is subdivided into several layers, each harboring specific subtypes of cells or their processes and fulfilling a particular part of olfactory processing (**Fig. 1.5**). Surrounding the olfactory bulb is the olfactory nerve layer which comprises of unmyelinated axons of sensory neurons in the olfactory epithelium expressing odorant receptors (Carleton et al., 2002).

Glomerular layer (GL). The olfactory nerve projects to the outermost region of the olfactory bulb that comprises of spherical neuropile structures called glomeruli which harbor the apical dendrites of mitral or tufted cells, the principle neurons of the olfactory bulb (Ennis et al., 1996). Olfactory neurons expressing the same odorant receptor converge onto the same glomeruli in the olfactory bulb (Carleton et al., 2002). The GL contains a heterogeneous mixture of periglomerular cells (PGC) that also receive excitatory input from sensory axons and/or form dendrodendritic reciprocal synapses with mitral and tufted cells. They are one of the two predominant interneuron types generated from progenitors in the adult SEZ and comprise of about 5% of the newly generated cells. All of them express GABA and many co-express dopamine in the mouse (Lledo et al., 2008). The PGCs can be classified based on expression of calretinin or calbindin (Kosaka et al., 1998). Besides these, there are also several types of short-axon cells in the GL that extend their axons to the external plexiform layer or GCL (Kosaka and Kosaka, 2011).

External plexiform layer (EPL). It is a relatively cell-free layer lying immediately below the GL and comprises mainly of lateral dendrites of mitral and tufted cells, axon collaterals of mitral cells, apical dendrites of granule cells and cell bodies of tufted cells as well as different types of superficial short-axon cells scattered among them (Shepherd, 2003).

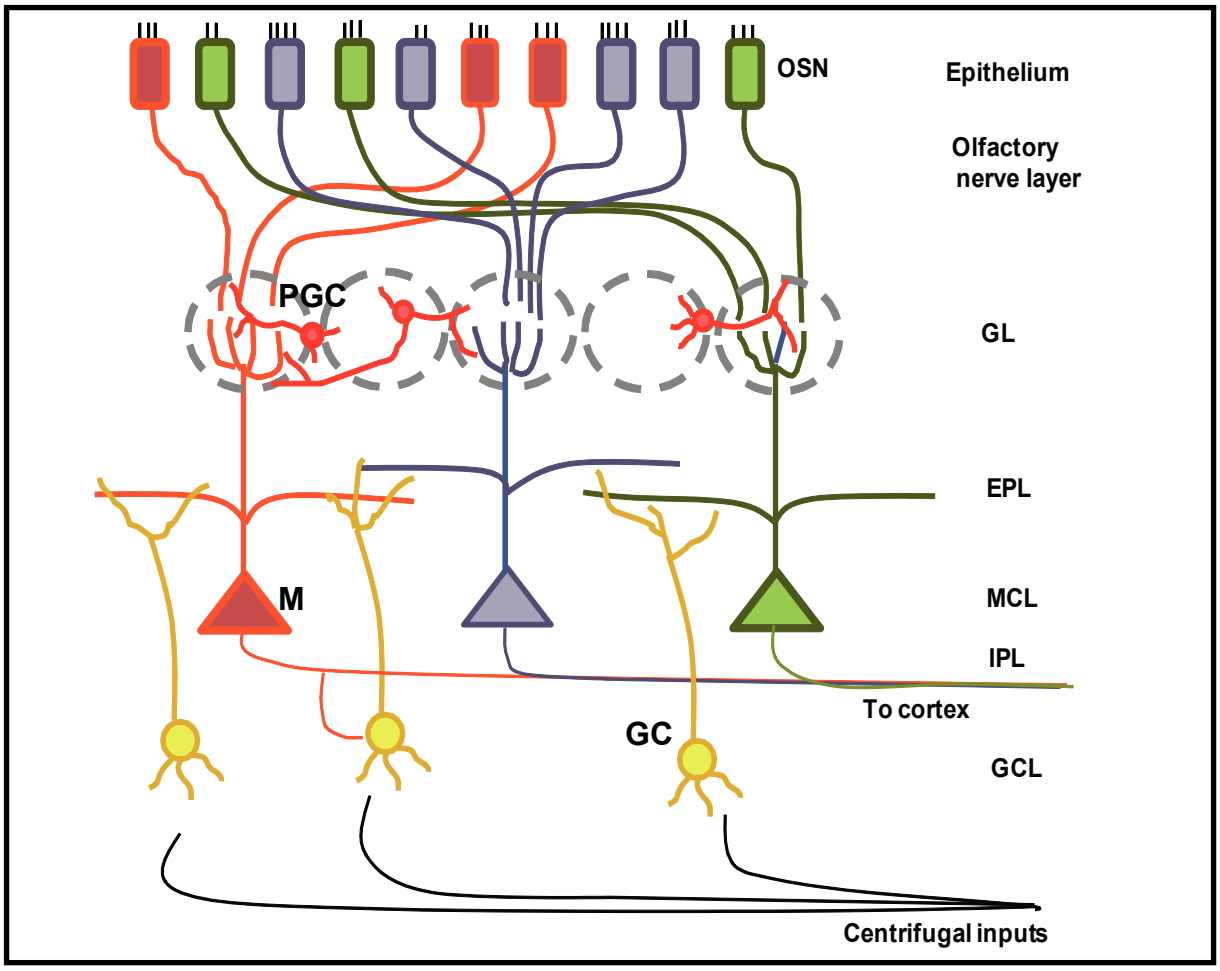

Fig. 1.5. Cellular organization of the olfactory bulb.
Axons of different subtypes of OSNs innervate specific glomeruli. Mitral and tufted cells extend a single apical dendrite which arborizes in the glomerulus and has lateral dendrites in the EPL. Within a glomerulus, OSN axons make excitatory synapses onto mitral and tufted cells as well as PGC dendrites. PGCs in turn make reciprocal dendrodendritic synapses with mitral and tufted cells. Axons of mitral and tufted cells project to the olfactory cortex via the lateral olfactory tract. Cell bodies of granule cells are located in the GCL and they extend an apical spiny dendrite that arborizes in the EPL, where they establish dendrodendritic synapses with lateral dendrites of mitral and tufted cells. Granule cells receive centrifugal input from the olfactory cortex. OSN=olfactory sensory neuron; GL=glomerular layer; EPL=external plexiform layer; MCL=mitral cell layer; IPL=internal plexiform layer; GCL=granule cell layer; PGC=periglomerular cell; M=mitral cell; GC=granule cell (adapted from Whitman and Greer, 2009).

Mitral cell layer (MCL). Lying below the EPL, the MCL contains cell bodies of mitral and tufted cells arranged in a dense layer, 2-3 cell diameters in length. Mitral and tufted cells are the two relay cells of the olfactory bulb and their axons project via the lateral olfactory tract (LOT) to the piriform cortex. The activity of mitral and tufted cells is modulated by periglomerular and granule cells through dendrodendritic synapses. This reciprocal synapse typically occurs between a specialized dendritic spine on the interneuron (granule cell or PGC) and the dendritic shaft of the projection neuron (mitral or tufted cell). It includes an inhibitory interneuron-mitral cell synapse immediately adjacent to

an excitatory mitral-interneuron synapse (Shepherd, 2003).

Internal plexiform layer (IPL). It is the region separating the MCL and GCL. Similar to the EPL, the IPL is relatively less cell-dense and mostly contains fibres of mitral cells, granule cells and cell bodies as well as dendritic and axonal arbors of various types of short-axon cells.

Granule cell layer (GCL). It is the innermost layer of the olfactory bulb comprising of densely packed cell bodies of the largest population of bulbar interneurons, the granule cells. It is also the layer into which the newborn neurons migrating along the RMS enter and commence their radial migration. They extend one long apical dendrite covered with spines to the EPL, where it branches profusely. There are three subtypes of granule cells, classified according to their dendritic arbors - deep granule cells extending their dendritic arbor in the deep EPL, close to the lateral dendrites of mitral cells, superficial granule cells with their dendrites arborizing in the superficial EPL, close to lateral dendrites of tufted cells and the third subtype of granule cells having their dendritic distribution all over the EPL (Whitman and Greer, 2009). Adult-generated granule cells comprise of almost 95% of the SEZ-derived cells. Other than granule cells, the GCL also harbors several types of calbindin-positive short-axon cells such as Blanes cells, Golgi cells, van Gehutchen cells and other short-axon cells (Kosaka and Kosaka, 2010).

1.3.2 Olfactory system: Synaptic connectivity

The axons of the sensory neurons arising from the sensory epithelium form excitatory, glutamatergic synapses with the apical dendrites of mitral and tufted cells in the glomerulus. Thus, the glomerulus is the first centre for processing sensory information in the olfactory bulb. Synaptic transmission between the olfactory nerve and mitral cells is mediated via α-amino-3-hydroxy-5-methyl-4-isoxazolepropionic acid (AMPA)/Kainate receptors and NMDAR (Desmaisons et al., 1999). It has been suggested that the olfactory

bulb amplifies sensory signals coming from the olfactory sensory neurons (Carleton et al., 2002). The next step of sensory information processing is accomplished by PGCs. They modulate synaptic signalling within a glomerulus and between glomeruli. Periglomerular cells receive excitatory input from the sensory neurons and form dendrodendritic synapses with mitral and tufted cells. The GABAergic PGCs inhibit the mitral and tufted cells while the dopaminergic PGCs release dopamine which activates D2 receptors on sensory axons thus modulating synaptic transmission between them and mitral cells (Hsia et al., 1999).

In addition, granule cells deeper within the bulb also form dendrodendritic synapses with the lateral dendrites mitral and tufted cells. Granule cells are depolarized by glutamate released from mitral cells which triggers inhibition of mitral cells by GABA released from granule cells resulting in regulation of mitral cell firing by negative feedback (Carleton et al., 2002). Each granule cell contacts the dendrites of several mitral and tufted cells and the dendrodendritic synapse may be responsible for recurrent inhibition of one mitral cell and lateral inhibition of mitral cells innervating different glomeruli, in response to odorant stimulation (Nissant and Pallotto, 2011). Granule cells (and perhaps PGCs) receive additional inputs at their cell bodies and basal dendrites from many intrabulbar and centrifugal sources. GABAergic inputs arise from axons of many short-axon cells in the olfactory bulb (Eyre et al., 2008) while glutamatergic inputs originate from within the bulb as axon collaterals of mitral and tufted cells or centrifugal connections (**Fig. 1.5**). Excitatory centrifugal fibres entering the olfactory bulb through the anterior commissure originate in the anterior olfactory nucleus, piriform cortex, periamygdaloid and lateral entorhinal cortex while cholinergic and GABAergic innervation comes from the nucleus of the diagonal band of Broca, serotonergic input from the raphe nuclei and noradrenergic fibres from locus coeruleus (**Fig. 1.6**; Whitman and Greer, 2007). The neuronal circuitry in the olfactory system is highly dynamic with continuous replacement of olfactory sensory nerves in the olfactory epithelium that must find the correct glomerulus and synaptic targets and the continuous genesis of granule cells and PGCs that integrate into the

existing circuitry without disturbing its function (Lledo et al., 2006).

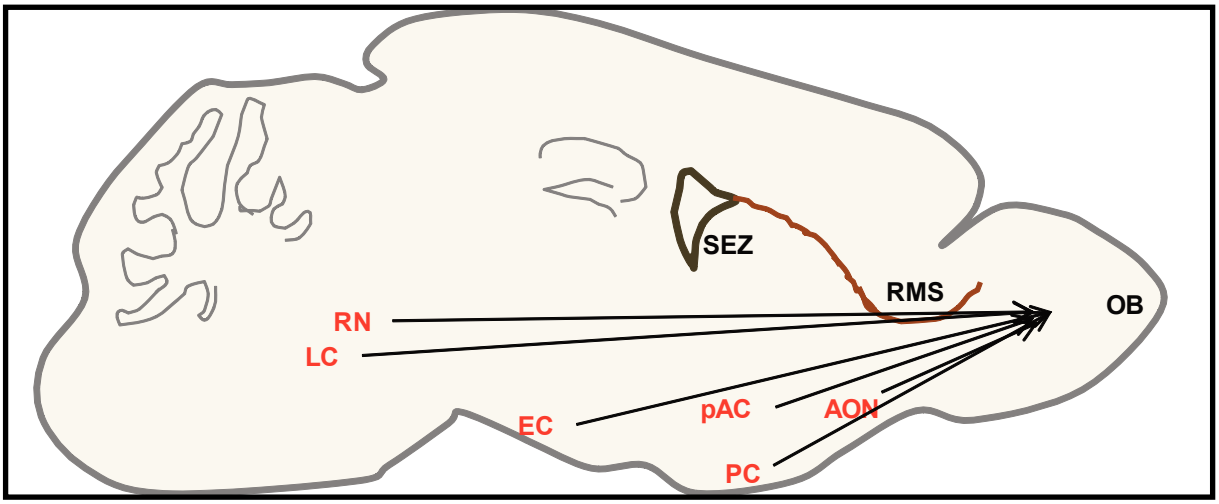

Fig. 1.6. Schematic of afferent inputs to the olfactory bulb.
Arrows extending to the OB originate from brain structures that have inputs to these areas. SEZ=subependymal zone; OB=olfactory bulb; AON=anterior olfactory nucleus; PC=piriform cortex; pAC=periamygdaloid cortex; EC=entorhinal cortex; RN=raphe nucleus; LC= locus coeruleus (adapted from Arenkiel, B., 2011).

1.3.3 Olfactory system: Overview of adult neurogenesis

The SEZ harbors radial glia-derived NSCs that exhibit typical astrocyte-like properties including expression of GFAP as well as morphological and ultrastructural properties of astrocytes (Doetsch et al., 1999). These slow dividing NSCs, designated as type B cells, are the primary precursors in the SEZ and give rise to Dlx2- or Mash1-expressing fast proliferating transit amplifying precursors (TAPs) or type C cells which in turn produce Dcx- and polysialic acid neural cell adhesion molecule (PSA-NCAM)-positive neuroblasts (Lledo et al., 2008), also known as type A cells (Doetsch et al., 1999). In addition, the adult SEZ also harbors TAPs expressing the oligodendrogenic transcription factor, Olig2, that migrate to the corpus callosum and differentiate into oligodendrocytes (Hack et al., 2005). The aNSCs in different regions of the SEZ give rise to progenitors that generate only a very specific subset of interneuron type in the olfactory bulb (**Fig. 1.7**). It has been demonstrated by viral labelling of radial glia and their progeny that the dorsal SEZ generates primarily superficial granule cells and tyrosine hydroxylase (TH)-positive PGCs and a small proportion of glutamatergic interneurons, the ventral SEZ produces mostly deep granule cells and calbindin-positive PGCs, while

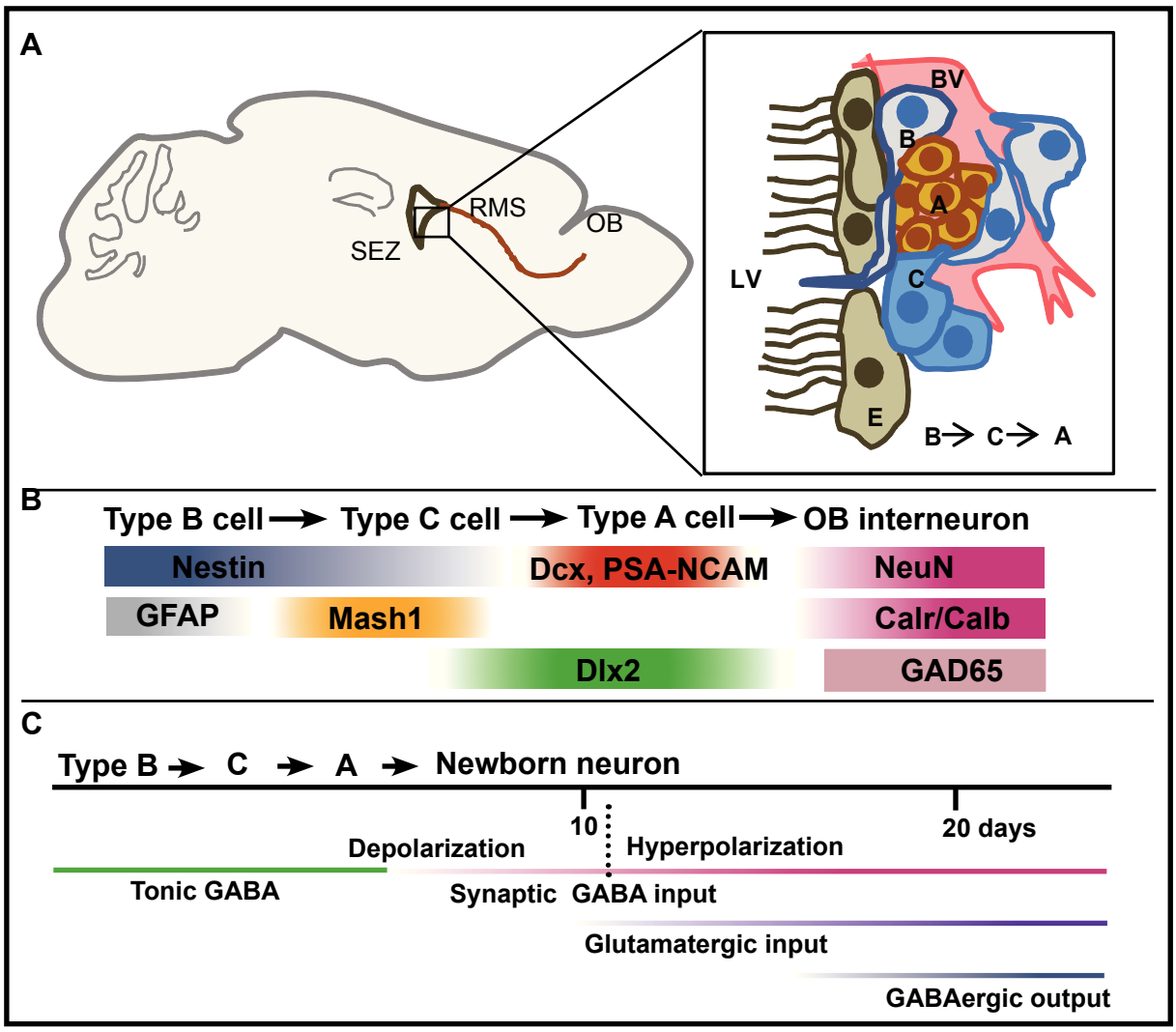

Fig. 1.7 Subependymal zone neurogenesis.
(A) Activation of radial glia-like stem cells, type B cells, in the SEZ of the lateral ventricle gives rise to rapidly dividing transit amplifying cells, type C cells, which produce neuroblasts, type A cells, that migrate in chains within the RMS and differentiate into granule cells and periglomerular cells in the OB. The slow dividing type B cells and other progenitors are in intimate contact with ependymal cells and blood microvessels. (B) Expression of markers in different cell types involved in adult neurogenesis. (C) Schematic for synaptic integration of newborn interneurons in the olfactory bulb. SEZ=subependymal zone; RMS=rostral migratory stream; OB=olfactory bulb; LV=lateral ventricle; BV=blood vessel; E=ependymal cells; B=radial glia-like stem cells; C=fast proliferating transit amplifying precursors; A=neuroblasts. (adapted from Ming and Song, 2011).

the medial SEZ and RMS give rise to calretinin-positive granule and PGCs (Brill et al., 2009; Merkle et al., 2007; Whitman and Greer, 2009). It has also been shown that different interneuron subtypes are preferentially generated at different ages that integrate into distinct circuits, suggesting that this temporal production of neuron types might control maturation of the olfactory bulb (Breton-Provencher and Saghatelyan, 2012). After their birth in the SEZ, chains of Dcx-positive neuroblasts exiting the SEZ migrate tangentially along the RMS ensheathed by a meshwork of astrocytes originating from

longitudinally oriented glial tubes that continue to the olfactory bulb (Lois et al., 1996). Once they reach the olfactory bulb, neuroblasts detach from the chains and migrate radially towards their final destination in the GCL or GL to complete their differentiation into different types of interneurons (Lledo et al., 2008). Recently it has been demonstrated that chains of neuroblasts are closely associated with blood vessels suggesting that these may use the blood vessels as a scaffold for tangential migration in the RMS as well as radial migration in the olfactory bulb (Bovetti et al., 2007; Whitman et al., 2009).

Adult-generated granule cells have been divided into five stages of differentiation - stage 1 cells migrate tangentially through the RMS with a prominent leading process and a small trailing process; stage 2 cells migrate radially through the GCL; stage 3 cells have stopped migrating and reached their final destination in the GCL, extending a dendrite towards the MCL; stage 4 cells have a highly branched dendritic arbor but no spines yet and stage 5 cells have a mature granule cell morphology with spiny dendrites. The entire process of granule cell maturation from stage 1 to stage 5 takes about 30 days (Petreanu and Alvarez-Buylla, 2002). Adult-generated PGCs undergo rapid maturation acquiring morphological and electrophysiological properties typical of mature PGCs by two weeks after their generation in the SEZ (Belluzzi et al., 2003).

1.3.4 Olfactory system: Synaptic integration and functional relevance of adult neurogenesis

Granule cells and PGCs are key players in processing odor stimuli in the olfactory bulb (Lledo et al., 2006). These are also the two major populations of interneurons generated during adulthood. Consequently, their functional integration into the pre-existing network in the olfactory bulb has been extensively investigated. Tangentially migrating neuroblasts first express functional GABA receptors, which likely respond to extrasynaptic GABA, and then AMPARs (Bolteus and Bordey, 2004; Carleton et al., 2003). Once they reach the olfactory bulb and start radial migration, some new neurons begin to express NMDARs. Newborn granule cells receive GABAergic and

glutamatergic synapses as soon as they reach the olfactory bulb (Nissant and Pallotto, 2011). Newborn granule cells have been proposed to receive axodendritic synapses from centrifugal fibres and/or from mitral cell axon collaterals (Whitman and Greer, 2007). These connections appear as early as 10 days post birth in the SEZ and form on proximal dendrites of newborn granule cells. At this stage, they are however unable to fire action potentials (Whitman and Greer, 2007). At about 21 days post birth begins the formation of the dendrodendritic synapses in the EPL between newborn granule cells and mitral cells. During dendrodendritic synaptogenesis, spine density on adult-born granule cells increases until 28 days after birth, remains stable till 42 days and decreases by 56 days (Whitman and Greer, 2007). This synaptic pruning suggests slow refinement of interneuron connectivity over the course of several weeks after their arrival in the olfactory bulb. The maturation of the GABAergic input has been suggested to be faster compared to the glutamatergic input (Nissant and Pallotto, 2011). Using channelrhodopsin-encoding lentiviruses, Bardy et al (2010) could demonstrate that newborn granule cells are able to inhibit mitral cells and modulate their activity about two weeks after lentiviral injection in the RMS. However, the probability of revealing a functional contact increases between 4 and 6 weeks after injection (Bardy et al., 2010). This suggests that although the GABAergic output synapses of newborn granule cells are formed quickly, functional maturation of these contacts takes several weeks. Thus, new neurons receive information about the network before contributing to it. This delay in generating output may have evolved to protect the existing circuitry from disruption due to uncontrolled transmitter release. Events occurring during developmental neurogenesis differ significantly where input/output synapses are formed simultaneously with the proximal excitatory input synapses (Kelsch et al., 2008; Lledo et al., 2004). Thus, synaptic integration of adult-generated cells in the olfactory bulb does not seem to recapitulate events occurring during embryonic and postnatal development.

Newborn PGCs, on the other hand, develop voltage-dependent sodium currents and the capacity to fire action potentials before the appearance of synaptic contacts

(Belluzzi et al., 2003). Periglomerular cells express elaborate dendritic arbors about 2 weeks after birth but mature pedunculated spines appear only at about 6 weeks (Whitman and Greer, 2007). Thus, periglomerular spines appear to mature slower than those of granule cells. This difference in maturation could stem from the intrinsic differences between these cells or the distinct neuronal networks into which they integrate. The PGCs integrate into circuits that undergo constant replacement of afferents (coming from sensory neurons) while newborn granule cells receive inputs from mitral and tufted cells that remain stable throughout the life of the organism (Mizrahi and Katz, 2003).

The functional role of adult neurogenesis in the olfactory bulb has been studied by ablating neurogenesis and its consequent effects at the cellular level as well as on olfactory behaviour. However, the results of these studies are contradictory probably because of the different experimental paradigms used. For example, after cytosine-b-D-arabinofuranoside (ARA-C) infusion for one month mitral cells received fewer inhibitory synapses, displayed reduced frequency of spontaneous inhibitory postsynaptic currents (IPSCs), experienced reduced dendrodendritic inhibition and exhibited decreased synchronized activity (Breton-Provencher et al., 2009). This, at the behavioural level manifested as an increased threshold for detecting odours and a reduction in short-term olfactory memory. However, long-term memory or the ability to discriminate between different odours was unaltered (Breton-Provencher et al., 2009). In contrast, studies have shown that irradiation of the SEZ or ARA-C treatment leads to impairment of long-term associative memory (Lazarini et al., 2009; Sultan et al., 2010). A third study involving genetic ablation of newborn neurons in the SEZ found that although numbers of newly generated granule cells decreased over time, there was no effect on olfactory discrimination in these mice (Imayoshi et al., 2008). However, an earlier study on neural cell adhesion molecule (NCAM)-deficient mice that display deficits in migration of neuroblasts to the olfactory bulb, showed a specific reduction in the turnover of granule cells which resulted in impairment of discrimination between odours while detection thresholds and short-term olfactory memory were not affected (Gheusi et al., 2000). A

recent study, using optogenetics-based methods, has suggested that adult-born but not postnatal-born granule cell-mediated inhibition of mitral cells is important for learning to discriminate similar odors and retaining the memory for it (Alonso et al., 2012).

Besides odour discrimination and olfactory learning and memory, olfactory neurogenesis has also been implicated in mating and maternal behaviour. Pheromones secreted by dominant males have been shown to increase neurogenesis in the female mice brain, suggesting female preference for dominant males over subordinate males (Mak et al., 2007). Neurogenesis is also markedly increased during pregnancy, stimulated by prolactin which is negated by blocking prolactin signalling. Loss of pup-induced maternal behaviour in prolactin receptor mutant females also suggests a role for neurogenesis in this behaviour (Shingo et al., 2003), although it is unclear if this effect is a direct consequence of new neurons or via another prolactin-mediated mechanism.

In conclusion, it is now clear that adult neurogenesis seems to have an impact on several aspects of olfactory function following sequential synaptic integration of newborn neurons. However, the connectivity of granule cells or PGCs with respect to the different pre- and postsynaptic partners and their location as well as the influence of sensory stimulation on newborn neuron connectivity remain unclear. For example, activity-dependent modifications have been shown to strongly influence the maturation and survival of new neurons. These manipulations are most effective during a critical time window of 2-4 weeks after generation (Nissant and Pallotto, 2011). This is the exact time during which these cells begin to receive glutamatergic synaptic inputs. Moreover, proximal glutamatergic inputs onto newborn granule cells are able to support LTP, which disappears as they mature and is no longer detectable 3 months after birth (Nissant and Pallotto, 2011). It would be interesting to know the identity of these inputs and the particular contribution of various synaptic inputs that regulate the addition of new neurons to the olfactory bulb and thereby its effect on olfaction.

1.4 Watching new neurons 'listen'

Becoming a neuron in the adult hippocampus or olfactory bulb requires it to undergo morphological as well as physiological changes and face the daunting task of competing with its contemporaries and older neurons for survival in order to stably integrate into a pre-existing network. Equallly challenging is the study of how a newborn neuron manages to overcome 'all odds' to incorporate into the neuronal circuitry in vivo and its functional correlation at the systemic level. Several decades after the discovery of adult neurogenesis, very little is known about the gradual temporal incorporation of adult-generated neurons into pre-existing networks and the cellular identity of their pre- and postsynaptic partners. Confocal and electron microscopy as well as electrophysiological techniques have adequately demonstrated the functional integration of these neurons but newer methods are required for mapping the connectome of newborn neurons and consequently, the effect of this connectome in regulating the functional integration.

1.5 Neuronal tracers

A classical technique of mapping neuronal circuits is through the use of substances called neuronal tracers that can be taken up by neurons and transported along their entire length to visualise their connections. Neuronal tracers such as Rhodamine isothiocyanate (RITC; Thanos et al., 1987),1,1'-dioctadecyl-3,3,3',3'-tetramethyl-indocarbocyanine perchlorate (DiI; Godement et al., 1987) or Evans Blue dye (EB) have been typically used to label populations of neurons in the brain and to identify the spread of their dendritic arbors and axonal projections (Huh et al., 2010). These tracers can be employed to visualize the projection fields of neurons by anterograde tracing where the tracers are taken up by neuronal cell bodies and transported via the axon tracts to the axon terminals. Alternatively, they can be used to identify the location of neuronal cell bodies of the labelled afferent nerve fibres by retrograde tracing where the tracer is taken up at the axon terminal and carried back to the cell soma (Huh et al., 2010). However, identification of connections between neurons requires the use of substances that can

be transferred between synaptically connected neurons, either anterogradely to trace postsynaptic targets or retrogradely to trace presynaptic partners. Several types of transneuronal tracers have been used to study neuronal circuits starting from a cell or population of cells and identifying its connectivity across several orders of neurons in different regions of the brain. These tracers can be broadly classified into two categories, non-viral or 'molecular' neuronal tracers and viral neuronal tracers.

1.5.1 Non-viral Transneuronal Tracers

Non-viral tracers are enzymes or other proteins that are used for neuroanatomical tracing. They are of plant origin or bacterial toxins that can act either anterogradely, retrogradely or bidirectionally. They bind to specific gylcoconjugates on neuronal membranes, get internalised and transported along the axon and/or dendrites to be released at the synaptic cleft (**Fig. 1.8**; Kobbert et al., 2000). The first plant lectin used

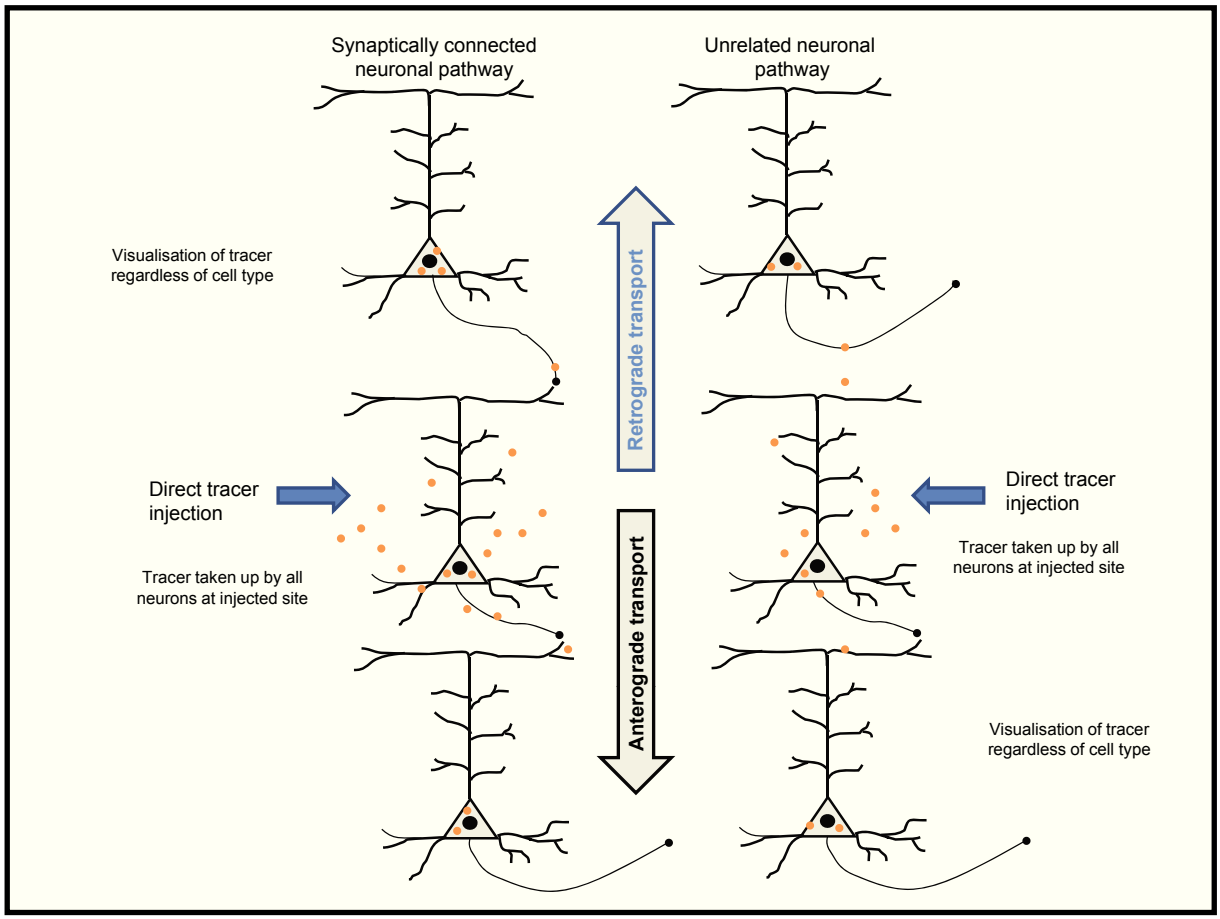

Fig. 1.8. Transneuronal transfer of tracer using conventional methods.
The tracer can be taken up by all the neurons at the injection site, leading to unspecific labelling of unrelated neuronal circuits (modified from Huh et al., 2010).

as a non-viral tracer for visualisation of neural circuits was Wheat germ agglutinin (WGA), a plant protein that can be transported along synaptically connected neurons (Ruda and Coulter, 1982). Examples of other non-viral tracers include fragment C of tetanus toxin (TTC; Evinger and Erichsen, 1986), Phaseolus vulgaris leucoagglutinin (PHA-L; Ruda and Coulter, 1982), horseradish peroxidase (HRP; Harrison et al., 1984) and their conjugates. They can be visualised either enzymatically or immunohistochemically. However, they all suffer from several disadvantages such as lack of specificity (Rhodes et al., 1987), bidirectional spread (Yoshihara et al., 1999) or inefficient synaptic transfer and dilution at every synaptic step (Sawachenko, 1985) resulting in weak labelling of synaptically connected neurons. Although novel genetic approaches such as expressing these tracers under the control of cell type-specific promoters (Yoshihara et al., 1999) or fusion with green fluorescent protein (GFP) or DsRed (Huh et al., 2010) eliminates some of the drawbacks, it still does not resolve the problem of weak labelling.

1.5.2 Viral Transneuronal Tracers

The limitations of non-viral transneuronal tracers were overcome after the discovery that certain neurotropic viruses can be used as neuroanatomical tracers by exploiting their ability to specifically infect neurons. These viral transneuronal tracers can be transported across the synaptic cleft between connected neurons and have the added advantage over non-viral tracers that they can replicate in the infected neurons, thus producing intense labelling by amplification of the tracer signal (Kuypers and Ugolini, 1990), that can be detected by immunohistochemistry (**Fig. 1.9**). The neurotropic viruses used for transneuronal (or transsynaptic) tracing include alpha-herpesviruses - Herpes Simplex Virus 1 (HSV-1) and pseudorabies virus (PrV) and the rhabdovirus, rabies virus (RABV) (Kuypers and Ugolini, 1990). Recently, the Vesicular stomatitis virus (VSV), also a rhabdovirus, has been used for tracing neuronal connections in vivo after pseudotyping it with glycoprotein from RABV or Lymphocytic choriomeningitis virus (Beier et al., 2011).

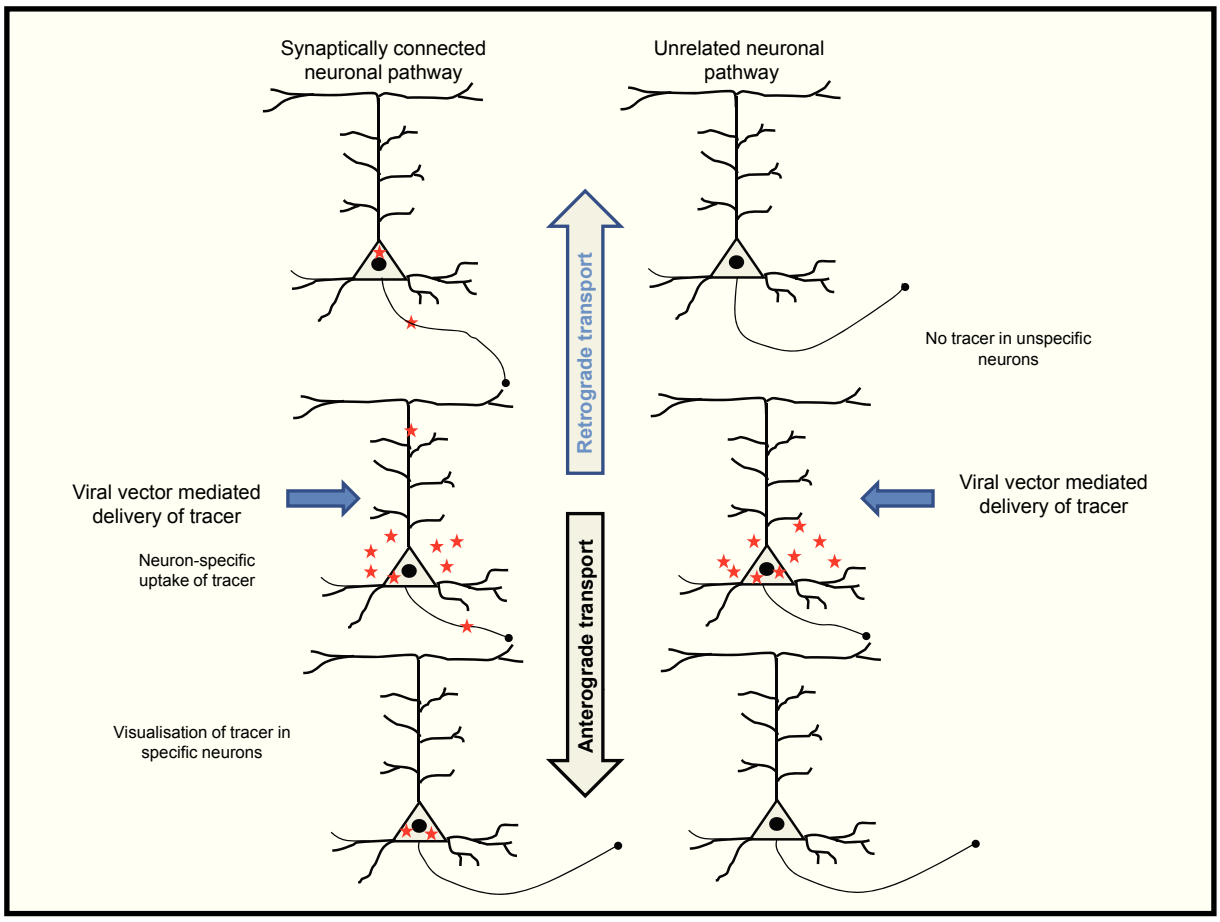

Fig. 1.9 Transneuronal transfer of tracer using viral tracers.
Tracers can be expressed selectively in specific neurons, leading to specific labelling of synaptically connected neuronal pathways (modified from Huh et al., 2010).

1.5.2.1 Herpes viruses

Herpes simplex virus 1, HSV-2 and PrV belong to the family of enveloped double-stranded, linear DNA genome viruses having icosahedral symmetry. The cellular receptor for HSV-1 and HSV-2 is heparan sulphate found on membranes of different cell types (Norgren and Lehman, 1998). Several strains of HSV-1 (Ugolini et al., 1989) and PrV (Card et al., 1990) have been used as transneuronal tracers. The spread of wild-type herpes viruses is bidirectional however certain strains have been shown to spread primarily if not exclusively in the anterograde or retrograde direction. For example, the H129 strain of HSV-1 has been identified to spread predominantly in the anterograde direction whereas the Bartha strain of PrV spreads exclusively via retrograde transsynaptic transport (Ugolini, 2010). However, herpes viruses have several disadvantages which might make them unfavorable as transneuronal tracers. Firstly, they are cytotoxic and

induce rapid neuronal degeneration of the infected neuron (Card et al., 1990; Ugolini et al., 1987). This could lead to local spread of the virus from the infected cell to surrounding cells which may be glia (Card et al., 1993) or spurious labelling of neurons that are not synaptically connected (Ugolini et al., 1987). The extent of local spread can be controlled in a dose- and time-dependent manner but this has a consequence of reduction in transneuronal tracing (Ugolini, 2008). For example, high doses of the virus are required to label second or third order neurons but this increases spurious labelling of neurons surrounding the primary infected neurons whereas low doses of virus used to reduce local spread may fail to label second or third order neurons entirely (Ugolini, 2010). Secondly, the transneuronal spread of HSV-1 and PrV is also dependent on the strain, titre of the virus and the cell type infected, making it critical to select the correct strain of herpes virus for tracing experiments (Norgren and Lehman, 1998).

1.5.2.2 Rabies virus

Besides being the causative agent of one of the most lethal zoonotic diseases, RABV has been successfully used as a neuronal tracer to map neuroanatomical connections for over two decades now (Kuypers and Ugolini, 1990). It is a small, neurotropic virus that belongs to the *Rhabdoviridae* family of viruses due to its characteristic 'bullet shape'. It has a relatively simple, negative strand RNA genome, about 12 kilobases (Kb) long, encoding five proteins (Conzelmann et al., 1990; Mebatsion et al., 1996; Schnell et al., 2010) (**Fig. 1.10**):

Nucleoprotein (N). The viral RNA is the template for viral replication and transcription. It is tightly associated with the nucleoprotein and together they form the ribonucleoprotein (RNP).

Polymerase (L) and Phosphoprotein (P). The RNA-dependent RNA polymerase is the enzyme catalysing the replication and transcription of the viral RNA and the phosphoprotein

is the non-catalytic subunit of the polymerase. They form part of the viral capsid which is surrounded by a host-cell membrane derived envelope.

Matrix protein (M). The matrix protein interacts and condenses the helical RNP and links it with the viral envelope. It also interacts with the cytoplasmic domain of the glycoprotein.

Glycoprotein (G). The G is the component responsible for the infectivity of the wild-type RABV. It is a 62-67 kDa type I glycoprotein with 2-4 glycosylation sites, existing as a trimer on the surface of the virus. The glycoprotein spikes play an important role in binding of the virion to the host cell membrane, receptor-mediated uptake and low pH-induced fusion of the viral envelope with the endosomal membrane. Similarly, it is also required for budding of rabies virions from the infected neuron membrane, specifically at synapses.

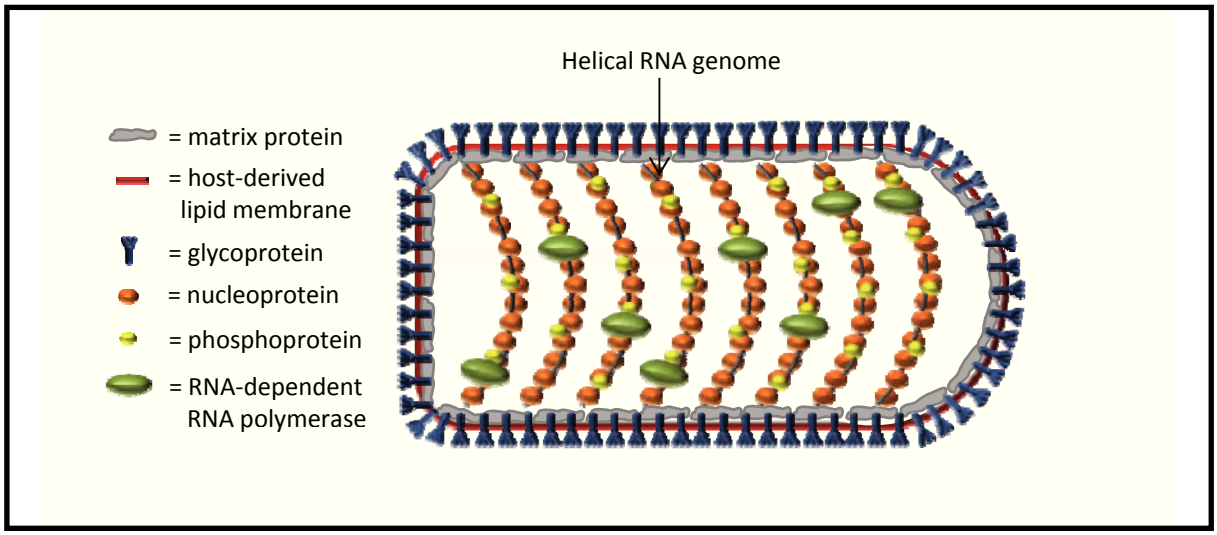

Fig.1.10. Rabies virion.
The rabies virion consists of a RNP core made up of the negative-strand RNA genome encoding five proteins and encapsidated by nucleoprotein, RNA polymerase and the polymerase cofactor phosphoprotein. The matrix protein links the RNP to the viral envelope derived from the host lipid membrane. The envelope is studded with glycoprotein spikes. RNP=ribonucleoprotein (adapted from Warrell et al, Lancet, 2004).

1.5.2.3 Lifecycle of the rabies virion.

The entry of RABV into the CNS from the periphery occurs at the neuromuscular junction, mediated by nicotinic acetylcholine receptors (AChR) present on the postsynaptic muscle membrane (Lentz et al., 1982). Binding of the RABV G to AChRs can be blocked

either with the nicotinic cholinergic antagonist, α-bungarotoxin, or with monoclonal antibodies against the glycoprotein (Jackson, 2002). Besides AChRs, other cellular receptors implicated in the infection by the RABV include NCAM, a cell surface glycoprotein localised on presynaptic membranes (Thoulouze et al., 1998) or the low-affinity p75 neurotrophin receptor (Tuffereau et al., 1998). However, blocking or eliminating these receptors in vivo does not prevent infection by RABV suggesting that they may act in combination with other cell surface molecules. Carbohydrates, gangliosides and lipids have also been implicated as RABV receptors but conclusive evidence for this is still lacking (Schnell et al., 2010). Binding of RABV to its receptor at the axon terminal initiates an internalisation process which involves receptor-mediated endocytosis and fusion of the viral membrane with an endosome at low pH. The virus is then carried to the cell body for replication and transcription in the endosomal vesicle by fast axonal transport (Klingen et al., 2008). It has been shown that retroviral vectors pseudotyped with G are transported similarly as RABV (Parveen et al., 2003), indicating that the G plays an important role in this transport, however, the exact mechanism is still unknown. Once at the cell soma, the helical RNP is released into the cytosol, decondensed and the negative strand RNA is transcribed by the RNA-dependent RNA polymerase. This is followed by translation of the 5' capped and polyadenylated viral mRNAs to produce viral proteins (Schnell et al., 2010). The RABV uses the host cell cytoplasmic machinery for protein synthesis. Once sufficient viral proteins are translated, there is assembly of the viral components and release of the virus at the cell membrane (budding). Electron microscopy studies have indicated that most viral budding occurs at the synaptic cleft or the adjacent cell membrane of dendrites, with very little budding at the cell soma (Charlton and Casey, 1979). Moreover, most virions were found to be engulfed by the membrane of an adjacent axon terminal, indicating transneuronal dendro-axonal viral transfer (Charlton and Casey, 1979). The RABV G and M have been implicated to play an important role in the budding process. Budding of RABV was found to be reduced by 30-fold in the absence of the G and viral titres reduced by 500,000 fold in the absence of

the M (Mebatsion et al., 1996; Mebatsion et al., 1999). In addition, studies have shown that stereotactiic injection of recombinant RABV lacking G limits infection to the injection site with no observable transsynaptic transport (Etessami et al., 2000).

Many characteristic features in the lifecycle of RABV make it an almost ideal transneuronal tracer. The main advantage over other viral tracers, namely the herpesviruses, is its relative lack of pathology. Rabies virus does not cause cell lysis which reduces the likelihood of random release and non-specific uptake of virus. It preferentially infects neurons and glial infection is thought to be rare. It is transported exclusively in the retrograde direction across neurons connected exclusively via chemical synapses and is not spread through gap junctions nor taken up by fibres in passage (Ugolini, 2010). There are several strains of RABV like SAD (Street Alabama Dufferin) B19 (SAD strain is attenuated and used as a vaccine), CVS (Challenged Virus Strain) or ERA that differ in their ability to infect neurons, cell to cell spread and rate of viral replication (Ugolini, 2010). "Street" RABV strains, directly isolated from the CNS of infected hosts (e.g. in the wild), like SAD, produce low amounts of G and do not induce apoptosis or necrosis in the infected cells. On the other hand, "fixed" strains, like CVS or ERA, have been adapted by passage in brains of animals or cells in culture and they produce higher amounts of the G and may induce apoptosis or necrosis in the host tissues. The key determinant in the virulence of these strains is the RABV G that mediates fast entry, fast transsynaptic spread and controlled synthesis of viral RNA (Dietzschold et al., 2008). Transneuronal transfer by conventional RABV tracers has been used to map polysynaptic neuronal afferent circuits controlling a particular function with great specificity (Salin et al., 2008; Ugolini, 1995). However, polysynaptic RABV tracers do not distinguish number of synaptic steps crossed as different synapses are crossed at different rates and strong polysynaptic inputs are labelled before weak monosynaptic ones (Ugolini, 1995). This hampers determining the nature of synaptic connectivity between traced neurons and primary infected neurons.

1.5.2.4 *Monosynaptic tracing using rabies virus*

Wickersham et al, in 2007, developed a transneuronal tracing technique that allows tracing of only monosynaptic connections of a target neuronal population (Wickersham et al., 2007b). First, they generated a *G*-deficient RABV (strain SAD B19) mutant by replacing the *glycoprotein* gene (*G*) with the coding sequence of *enhanced GFP* (*eGFP*) (Wickersham et al., 2007a) and termed it SADΔG-eGFP. This RABV variant could not spread beyond the initially infected cells and as G is not required for replication or

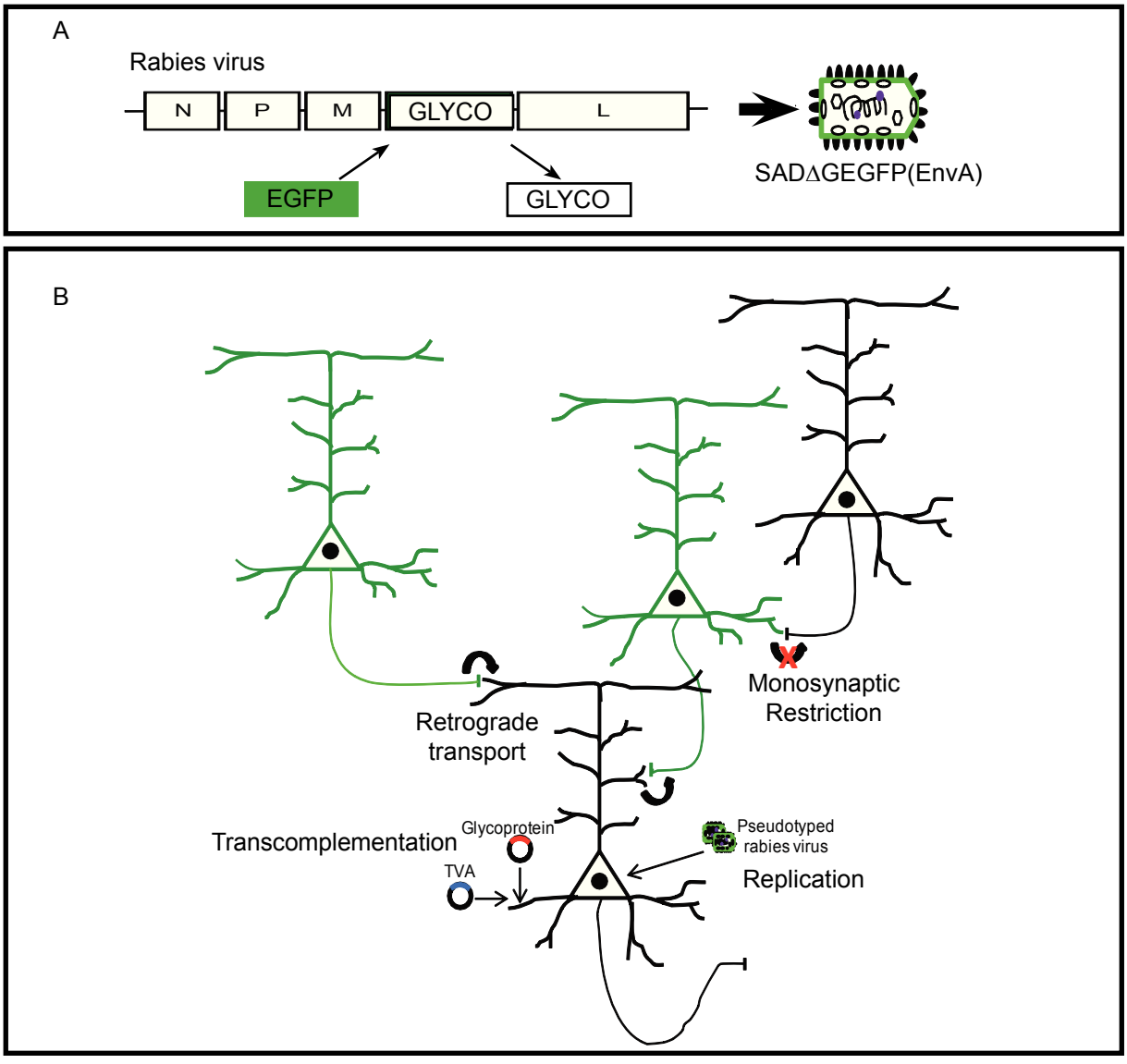

Fig. 1.11. Monosynaptic tracing technique.
(A) The RABV genome. The glycoprotein gene from the viral RNA genome is replaced by the coding sequence for *eGFP*. The viral envelope is pseudotyped for that of the ASLV-1 envelope, EnvA. (B) Monosynaptic restriction. The pseudotyped RABV, SADΔG-eGFP(EnvA), infects mammalian cells only when they express the cognate receptor for EnvA called TVA and they are able to retrogradely transport the virus to their presynaptic partners through transcomplementation by G. These neurons can be visualised by the presence of eGFP and since they lack the glycoprotein gene, cannot tranport the virus any further (modified from Wickersham et al., 2007).

transcription from the viral genome, it produced abundant eGFP to brightly label fine cellular details. Second, they altered the tropism of the *G*-deficient, replication-competent mutant virus by pseudotyping it with the envelope protein, EnvA, of the Avian Sarcoma and Leukosis Virus Type A (ASLV-A; Wickersham et al., 2007b). The receptor for EnvA is a cell surface protein called TVA (Tumor Virus A) which is found in birds but is not expressed by mammalian cells (Barnard et al., 2006; Elleder et al., 2004). In this way, they restricted the infection of SADΔG-eGFP(EnvA) or EnvA-pseudotyped RABV specifically to cells expressing the TVA receptor. By providing *TVA* and *G* in trans, they could achieve specific infection by EnvA-pseudotyped RABV of a subpopulation of neurons or "starter cells" which then could spread the virus to their immediate presynaptic partners after transcomplementation with the G. The *G* gene was not present in transsynaptically traced cells and hence the virus could not spread to the next order neurons (Wickersham et al., 2007b). This technique, therefore, allowed unambiguous labelling of neurons directly connected to the starter cells (**Fig. 1.12**). Using various strategies for the delivery of transgenes, *TVA* and *G*, such as single-cell electroporation, adenovirus associated virus-mediated transduction or Cre-mediated recombination in transgenic mice, studies have established the efficient expression of TVA and G in restricted populations of starter cells in vivo (Osakada et al., 2011; Wall et al., 2010; Weible et al., 2010). The delivery of EnvA-pseudotyped RABV to and subsequent transfer from these starter cells located in diverse neuroanatomical regions such as the cerebral cortex, the spinal cord and olfactory bulb, to name a few, has been successfully used for mapping the connections established by specific sets of short- and long-range presynaptic partners (Choi and Callaway, 2011; Miyamichi et al., 2011; Stepien et al., 2010).

In contrast to the above mentioned strategies in which the connectivity of already fully integrated neurons was assessed, a comprehensive description of the presynaptic partners of neurons in their process of maturation within an already pre-existing network, such as newly-generated neurons of the adult dentate gyrus and olfactory bulb, is still lacking. By adapting the approach of RABV-mediated monosynaptic labelling to

neurogenic systems in the adult murine brain, I have attempted to elucidate the presynaptic connectome of newborn neurons in vivo (Deshpande et al., in preparation).

Aim of the study

The aim of this thesis project was the development of a novel approach, based on a rabies virus (RABV)-mediated transsynaptic tracing technique (Wickersham et al., 2007b), to obtain a better understanding of the functional integration of adult-generated neurons in the dentate gyrus and olfactory bulb in the murine brain; the rationale behind this study being that to fully appreciate the functional role of newly generated neurons in the adult mammalian brain, it would be crucial to understand their gradual integration into the pre-existing neuronal circuitry and to determine the identity of their pre- and postsynaptic partners. In this approach, a previously described monosynaptic tracing technique (Wickersham et al., 2007b) was modified to specifically target the proliferating progeny of adult neural stem cells in the neurogenic niches by generating a retroviral system to provide the TVA receptor and RABV G, two proteins key to infection by (TVA) and transsynaptic transport of (G), respectively, the replication competent, deletion-mutant RABV pseudotyped with the envelope protein, EnvA.

Consequently, the primary infection of EnvA-pseudotyped RABV was restricted to a "starter population" comprising of proliferative transit amplifying progenitors and their neuronal progeny. On maturation of these neurons, RABV was retrogradely transported to their immediate presynaptic partners, which could be visualized owing to the *eGFP reporter* encoded by RABV. This strategy would thereby allow us to determine presynaptic partners of adult-generated neurons.

I employed the approach oulined above to address the following questions:

- What are the local and long-range projections received by newborn neurons in the dentate gyrus in vivo?
- What is the identity of the presynaptic partners of adult-generated neurons in the olfactory bulb in vivo?
- How do these presynaptic connectomes develop over time?

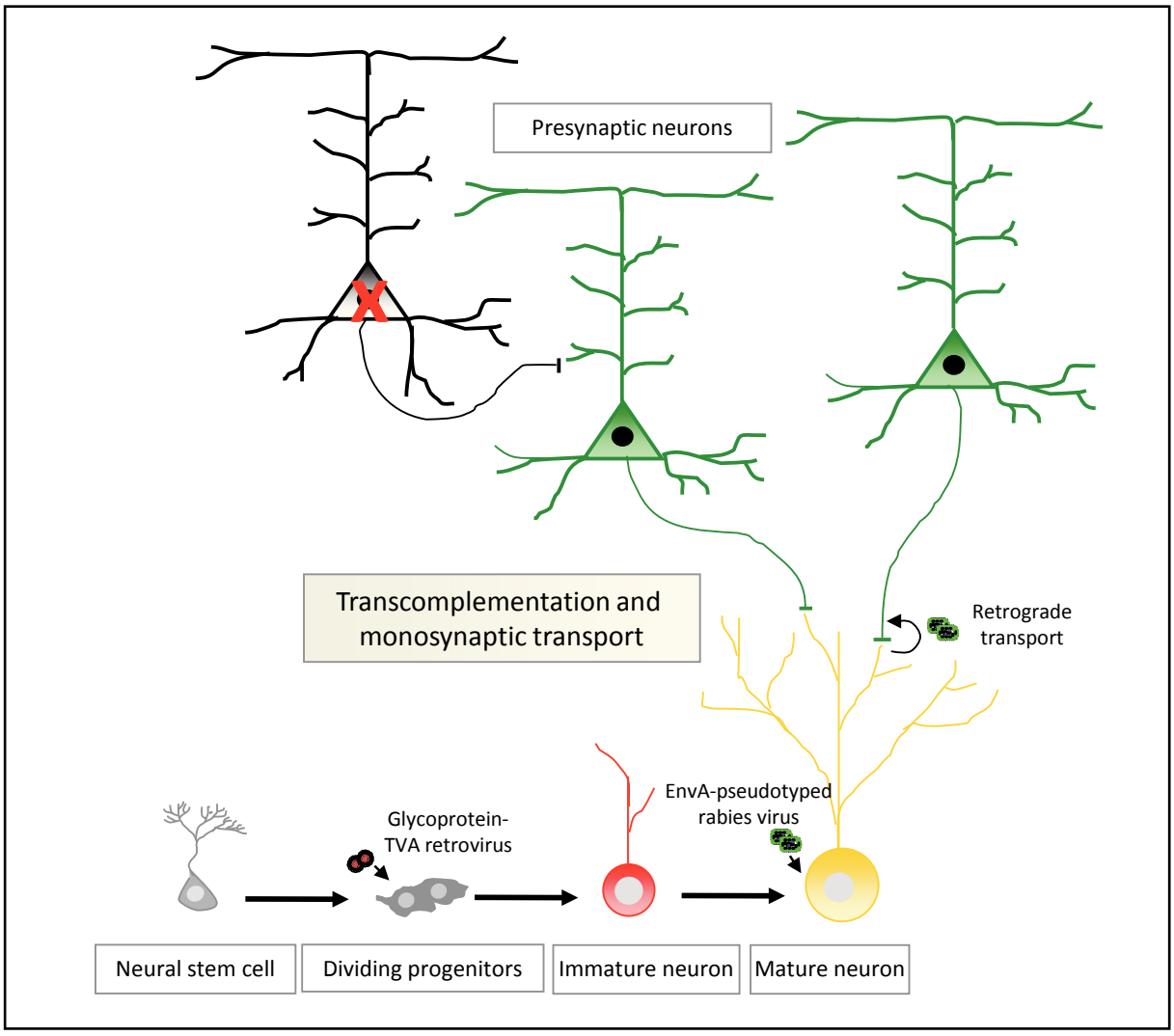

Fig. 2.1. Graphical abstract.
Schematic of the monosynaptic tracing technique adapted for studying the presynaptic connectome of adult-generated neurons.

2 Results

2.1 In vitro validation of the monosynaptic tracing technique

2.1.1 Embryonic cortical culture

The rabies virus (RABV)-mediated tracing technique outlined above was adapted to specifically assess the functional integration of adult generated neurons at the level of their presynaptic connectivity. Specificity for transduction of newborn neurons was intended through the use of Moloney murine leukemia virus (MMLV)-based retroviral vectors.Vesicular stomatitis virus glycoprotein (VSVG)-pseudotyped retroviral vectors that exclusively transduce proliferating cells, have been extensively used for exogenous gene expression. They have a broad host range and have been demonstrated to transduce cells derived from several lineages (Burns et al., 1993). However, once internalised, efficient over-expression of the transgenes is possible only if the viral RNA is reverse transcribed into DNA and integrated into the host cell genome. Since retroviruses lack a nuclear transport machinery, integration can occur only when the nuclear envelope is degraded, thereby providing the provirus access to chromosomal DNA, an opportunity that occurs during mitosis. This limits the transduction to proliferating cells, i.e., in this case, neural progenitors.

In order to assess the validity of this modified transsynaptic tracing method, I made use of mouse embryonic day 14 (E14) cortical cultures, as they still comprise of proliferating neuronal progenitors. Initially, neuronal progenitors in E14 cortical cultures were cotransduced with two retroviral vectors, pMX-Glyco-IRES-Tomato and

CMMP-TVA (kind gift from K. Conzelmann; **Fig.2.2**). The two vectors separately carry the transgenes, *TVA*, indispensable for infection by the EnvA-pseudotyped rabies virus (EnvA-pseudotyped RABV) encoding eGFP as a reporter and the *glycoprotein* (*G*) from the CVS strain of RABV, necessary for subsequent retrograde transport of EnvA-pseudotyped RABV to presynaptic partners via transcomplementation, respectively. After

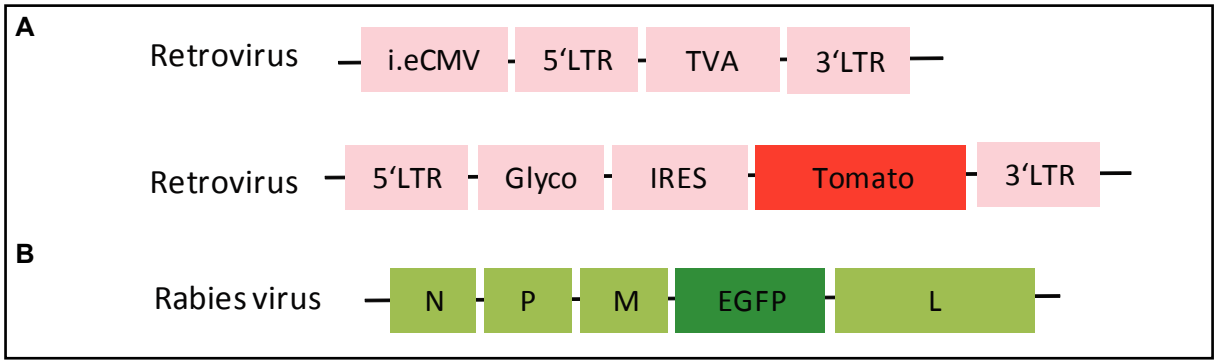

Fig. 2.2. First generation of retroviral constructs and RABV vector.
(A) Retroviral vectors separately encoding *TVA* and *glycoprotein* (*G*) from the CVS strain of RABV. TVA expression is driven by a retroviral long terminal repeat (LTR) and the immediate early enhancer of the cytomegalovirus (ieCMV). The *G* is also driven by a viral LTR and contains a Tomato fluorescent marker to monitor transduced cells. (B) *G*-deficient RABV vector.

allowing sufficient time for progenitors to differentiate into neurons and form synapses (2-3 weeks), the culture was infected with EnvA-pseudotyped RABV. Typically, neurons double transduced with *TVA* and *G* (yellow) were found to be surrounded by a cluster of neurons transduced with EnvA-pseudotyped RABV alone (green; **Fig.2.3**). This could be indicative of transcomplentation by G and eventual retrograde transport to presynaptic partners. However, co-transduction with two retroviruses was not efficient and since the CMMP-TVA retrovirus was lacking a reporter, it was unclear if the eGFP-only neurons were primarily or secondarily infected by EnvA-pseudotyped RABV. Nevertheless, when the E14 culture was transduced with CMMP-TVA alone followed by EnvA-pseudotyped RABV infection, there were only single eGFP-positive cells devoid of any surrounding clusters, suggesting a lack of retrograde transsynaptic transport in the absence of G expression (**Fig.2.3**).

In order to improve the efficiency of the system in vitro and for its implementation in vivo, retroviral vectors that expressed the two transgenes -*TVA* and *G* – in the same

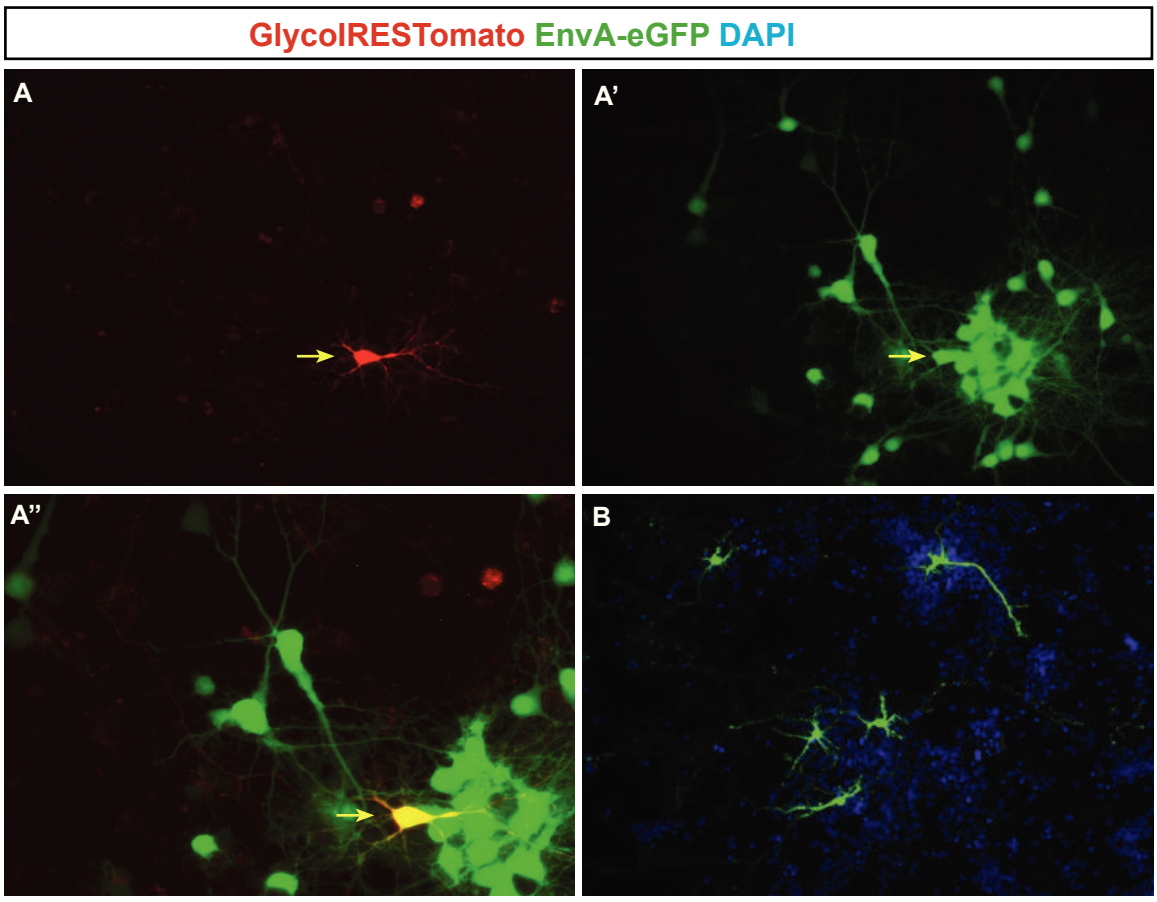

Fig. 2.3. Transduction of E14 cortical culture.
(A) Single and merged channel images of unstained live E14 cortical culture transduced with the two retroviral vectors, pMX-Glyco-IRES-Tomato and CMMP-TVA, 2h after plating and infected with RABV 2 weeks later. Double-transduced cells (yellow; yellow arrow) were typically found surrounded by clusters of eGFP-positive neurons (green). (B) E14 cortical culture transduced with CMMP-TVA followed by RABV infection 2 weeks later. Nuclei stained with DAPI.

construct were generated. This was achieved by using a short 2A peptide derived from the virus, *Thosea asgnia* (T2A; Donnelly et al., 2001a). The T2A is a short 18 amino acid peptide that serves as an alternative to the classical IRES (Internal Ribosomal Entry Site) used for expressing multiple proteins from a single mRNA. The T2A peptide mediates co-translational cleavage of the proteins flanking it by preventing the formation of a peptide bond between its penultimate amino acid, glycine (Gly) and the terminal proline (Pro). This results in the ribosome skipping to the next codon and cleavage of the nascent peptide between the Gly and Pro (Donnelly et al., 2001b). After cleavage, the short T2A peptide remains attached to the C-terminus of the protein upstream of it and the proline remains at the N-terminus of the downstream protein (**Fig.2.4**).

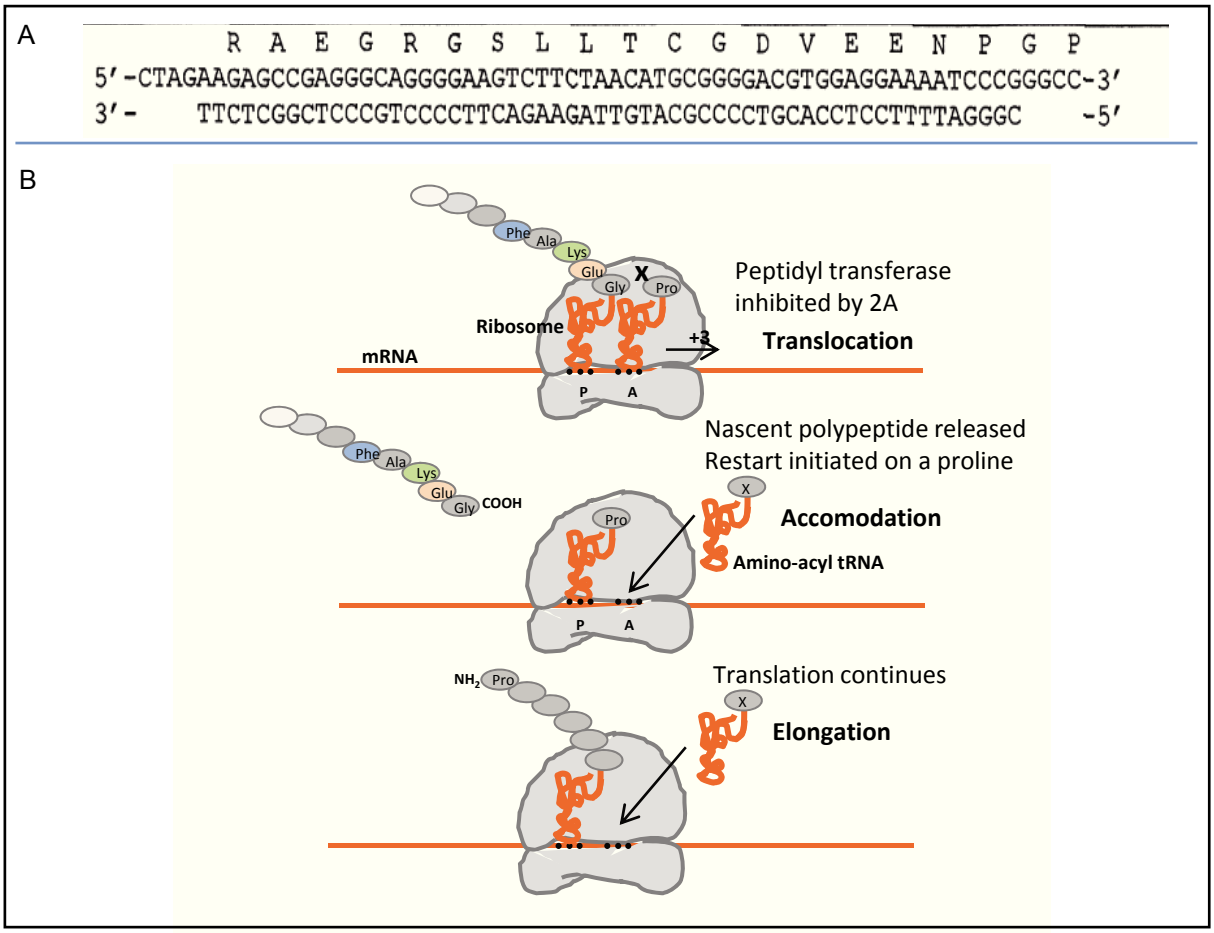

Fig. 2.4. Mechanism of 2A peptide co-translational cleavage.
(A) 2A peptide and DNA sequence from *Thosea asigna* (Donnelly et al, 2001a). (B) Cartoon depicting co-translational cleavage of the 2A peptide. After the Gly-Pro peptide bond is formed, the glycyl-tRNA translocates from the A site (the site mostly occupied by the amino-acyl tRNA) to P site (the site mostly occupied by the peptidyl tRNA) and the prolyl-tRNA moves to the A site. Peptide bond formation is prevented by 2A and the peptidyl(2A)-tRNAGly bond is hydrolyzed, releasing the nascent polypeptide from the ribosome. Prolyl-tRNA in the A site is then translocated to the P site and translation of the downstream polypeptide continues (Adapted from viralzone.expasy.org).

Polycistronic retroviral vectors encoding *G*, *TVA* and *DsRed* or *DsRedExpress2* fluorescent reporters to visualize the transduced cells were generated (**Fig.2.5**). The first retroviral construct encoding *DsRed* has the *G* and *TVA* flanking the T2A sequence and the fluorescent reporter, *DsRed* lies behind an IRES. This construct is denoted as **Glyco2ATVA**. The second retroviral construct has the *DsRedRExpress2* and *G* flanking the T2A and *TVA* behind the IRES. This construct is designated as **GlycoIRESTVA**. The **GlycoIRESTVA** construct was designed with *DsRedExpress2*, a more stable variant of DsRed, to improve detectability of transduced cells in unfixed brain slices.

The expression of transgenes from the retroviruses and specificity of expression was confirmed by immunocytochemistry using monoclonal antibodies against G and

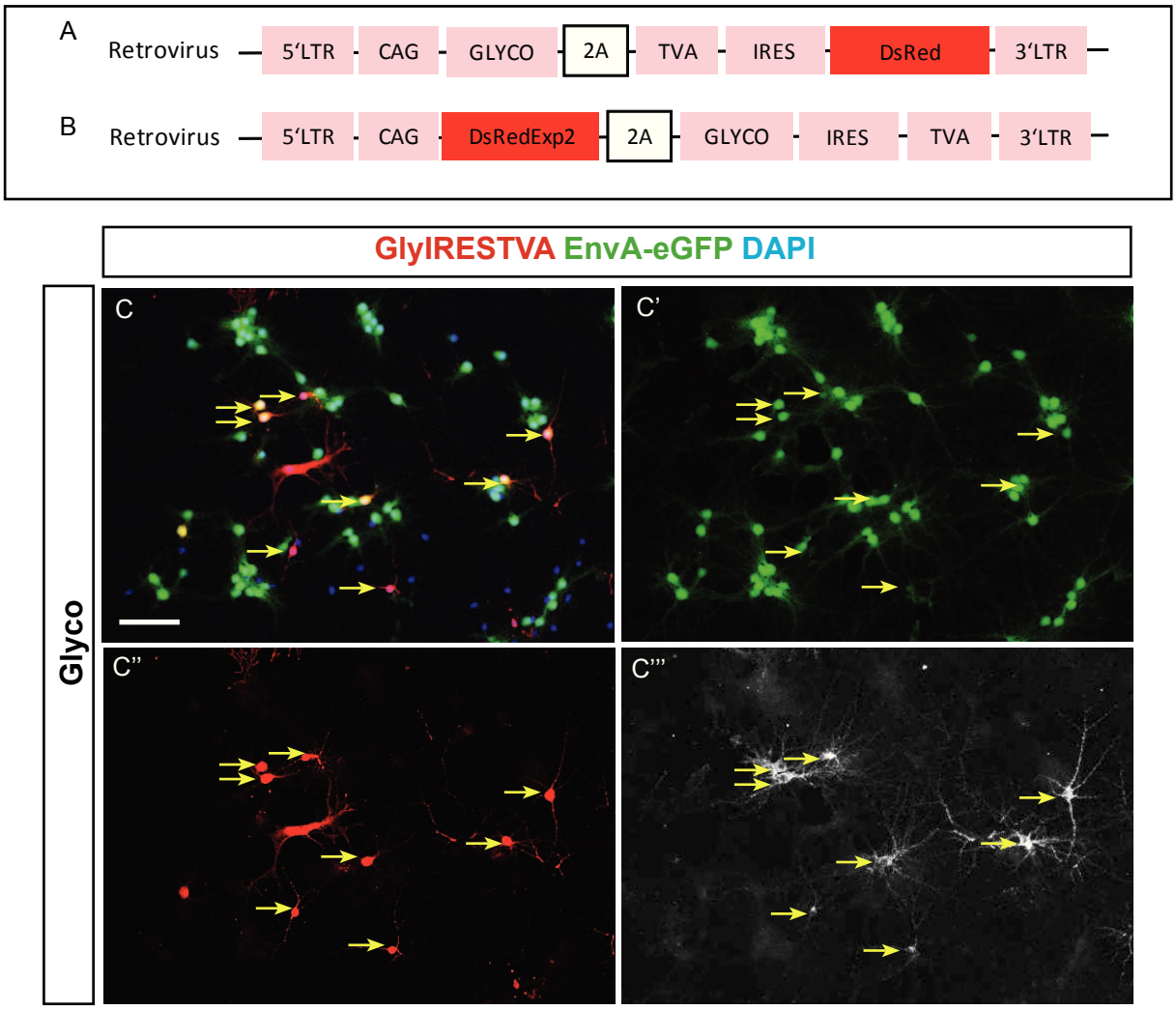

Fig. 2.5. Glycoprotein expression from retroviral constructs.
(A) Retroviral construct, **Gly2ATVA**, encoding *G* and *TVA*, separated by the T2A sequence and *DsRed* behind the IRES. (B) Retroviral construct, **GlyIRESTVA**, encoding G and TVA separated by an IRES. Transgenes are driven by the CAG promoter. (C) E14 cortical neurons transduced with *G*- and *TVA*-encoding retrovirus (red) followed by infection with EnvA-pseudotyped RABV (green) after two weeks in culture. Immunostaining for DsRedExpress2 (red), eGFP (green), G (white) and DAPI nuclear staining (blue). Nuclei stained for DAPI (blue). (C'-C''') Single channel images of C. Cells transduced with the retrovirus are also immunoreactive for RABV G (yellow arrows). Scale bar 100 µM.

TVA (**Fig.2.5-7**). The monoclonal antibody against TVA was generated by immunizing rats with a synthetic peptide conjugated to ovalbumin as a hapten, in the laboratory of Dr. Elizabeth Kremmer at the Monoclonal Antibodies Service Unit of the Helmholtz Zentrum Neuherberg. This synthetic peptide corresponds to amino acids 55-69 of the chicken TVA800 receptor and was selected as a potential immunogen based on its hydrophobicity index. The antibody, labelled 5H9, specifically recognized the HEK293 cells over-expressing the TVA receptor when transduced with the **Glyco2ATVA** retrovirus (**Fig.2.7**).

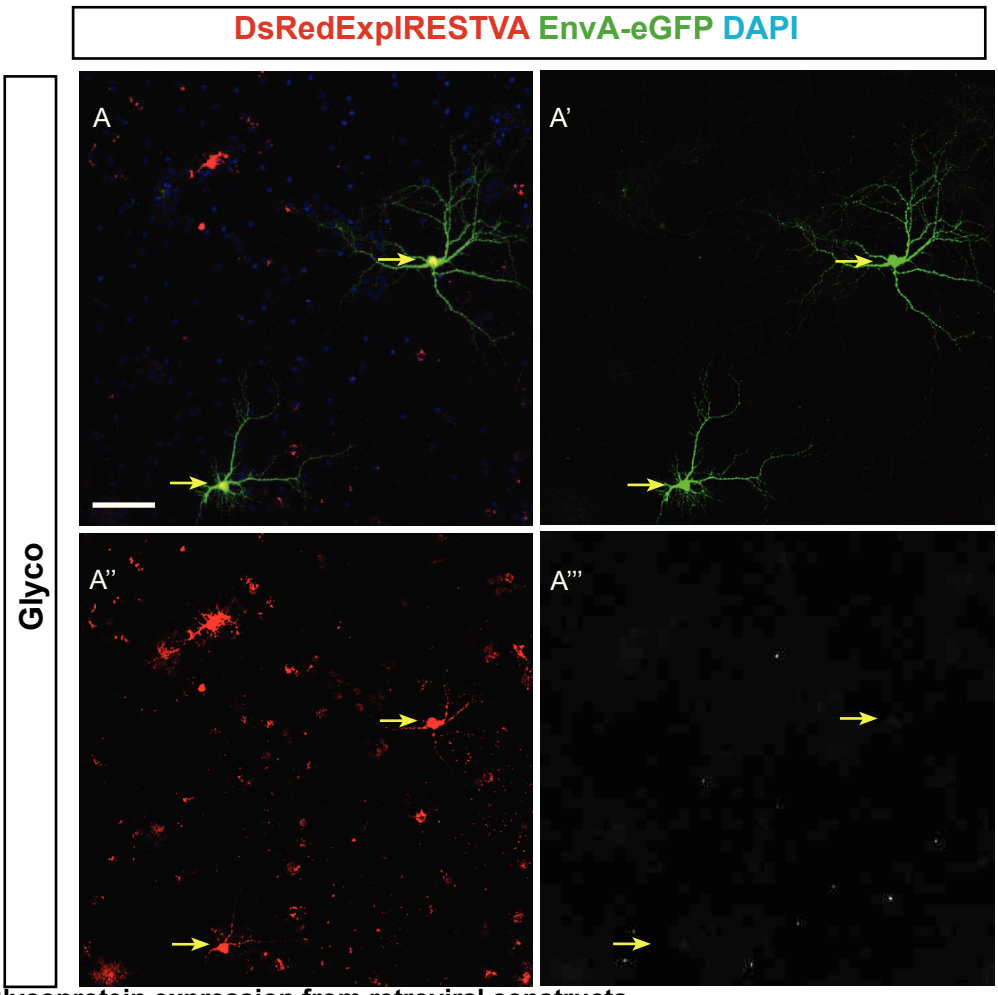

Fig. 2.6. Glycoprotein expression from retroviral constructs.
(A) E14 cortical neurons transduced with *TVA*-encoding (lacking *G*) retrovirus followed by infection with EnvA-pseudotyped RABV after two weeks in culture. Immunostaining for DsRedExpress2 (red), eGFP (green), G (white) and DAPI nuclear staining (blue). (C'-C''') Single channel images of C. Cells transduced with the *TVA only*-encoding retrovirus are not immunoreactive for RABV G (yellow arrows). Scale bar 100 µM (*TVA only*-encoding retrovirus constructed in collaboration with Francesca Vigano).

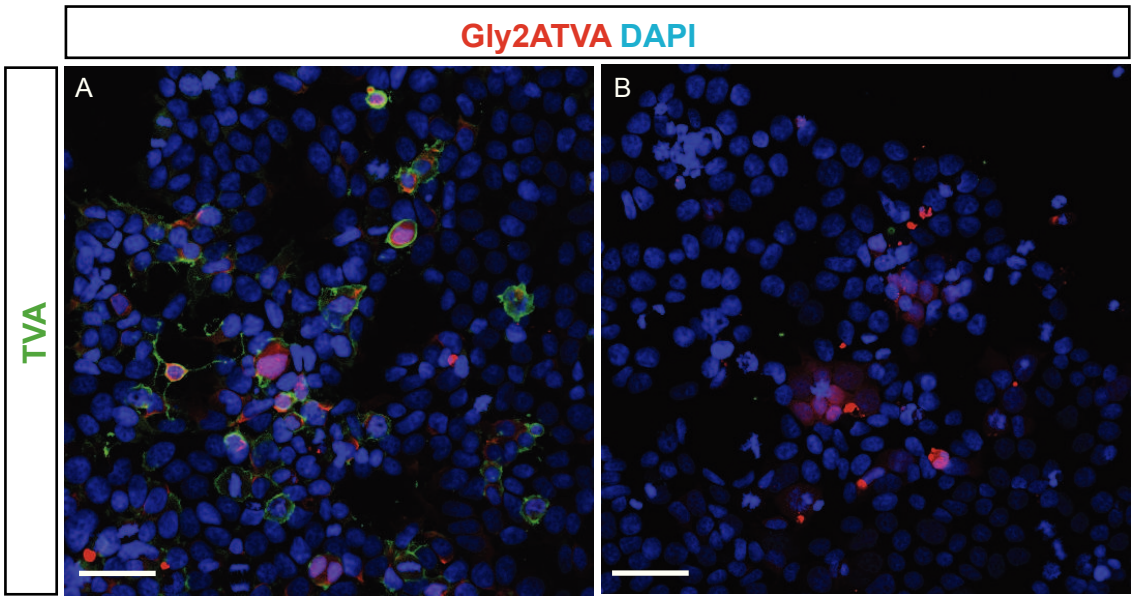

Fig. 2.7. Monoclonal antibody against TVA.
(A) HEK293 cells tranduced with **Gly2ATVA** retrovirus for 5 days and immunostained for TVA (green) using the monoclonal antibody against TVA. (B) No immunoreactivity against TVA was detected in the absence of the primary antibody. Scale bar 50 µM (Monoclonal antibody generated in the laboratory of Dr. Elizabeth Kremmer at the Helmholtz Zentrum Neuherberg).

On transduction of E14 cortical cultures with *G*- and *TVA*-encoding retrovirus and subsequent infection by EnvA-pseudotyped RABV 2-3 weeks later, neurons double transduced with retrovirus and EnvA-pseudotyped RABV, co-labelled with eGFP and DsRed/DsRedExpress2, were observed. These were typically surrounded by several EnvA-pseudotyped RABV-only transduced neurons, labelled with eGFP alone (**Fig.2.8**). Transduction of E14 cultures with EnvA-pseudotyped RABV alone resulted in no infected (green) cells, underscoring the importance of TVA for infection by EnvA-pseudotyped RABV infection. Synaptic connectivity between double (postsynaptic) and single (presynaptic) transduced cells was demonstrated by paired recordings (**Fig.2.8,** courtesy of Benedikt Berninger).

These data suggest that the *G*- and *TVA*-encoding retrovirus infects proliferating neuronal progenitors in E14 cortical cultures, rendering them susceptible to infection

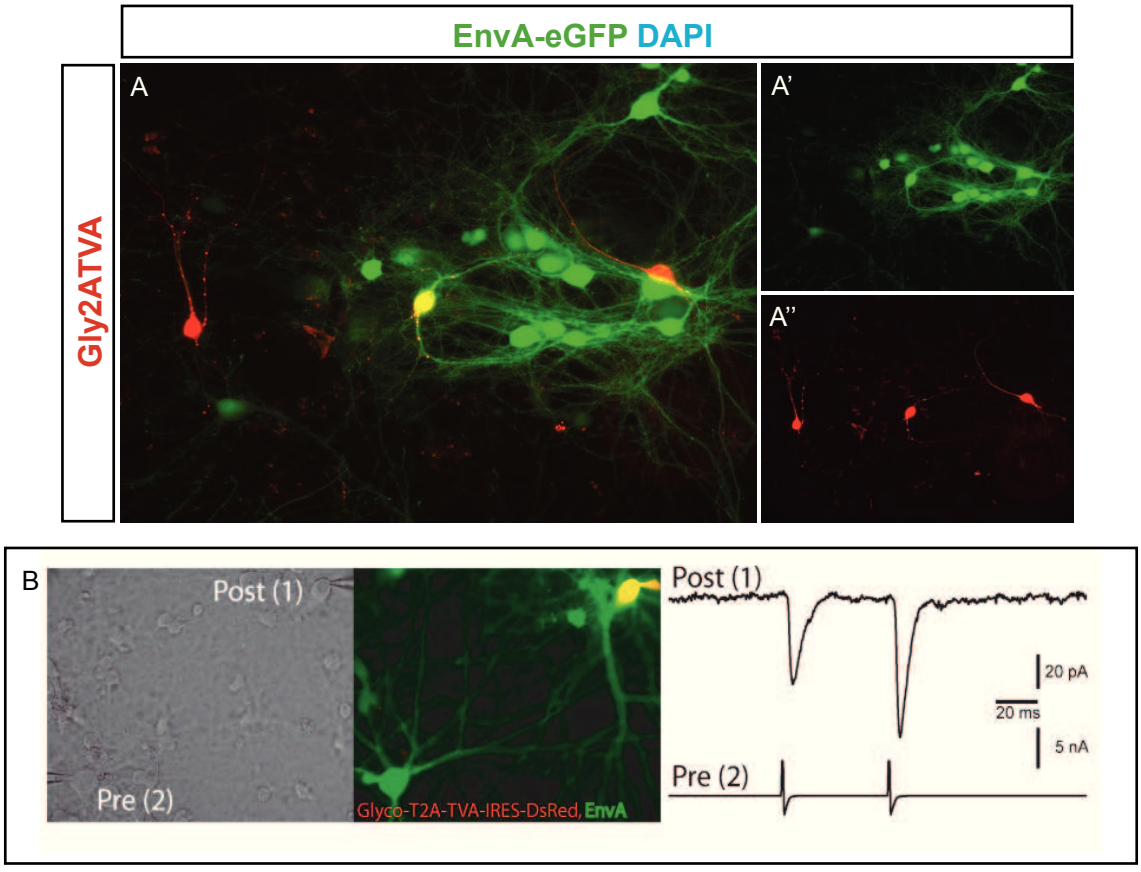

Fig. 2.8. Transduction of E14 cortical culture and synaptic connectivity.
(A) Unstained live E14 cortical cultures transduced with **Gly2ATVA** retroviral vector 2h after plating and infected with EnvA-pseudotyped RABV 2 weeks later. Double-transduced cells (yellow) were typically found surrounded by clusters of eGFP only-positive neurons (green). Panels A'-A'' show single channel images of A. (B) Example of pair recording in which a supra-threshold current injection (1 ms) in a presynaptic EnvA-pseudotyped RABV-transduced neuron (Pre 2) induced a synaptic inward current in a nearby double-transduced neuron (Post 1) (Eletrophysiology results courtesy of Benedikt Berninger).

by EnvA-pseudotyped RABV and on their subsequent maturation into neurons, allows for retrograde transport of EnvA-pseudotyped RABV to presynaptic partners owing to transcomplementation by the glycoprotein.

2.1.2 Postnatal astroglial culture

The “fixed” strains of RABV (such as CVS) have been adapted by passage in brains of animals or cells in culture and are supposed to not infect glial cells even when injected directly into the CNS (Prevosto et al., 2009). However, in culture, different cell types have the capacity to be infected by RABV and support its replication (Ugolini, 2010). Indeed, E14 cortical cultures transduced with a G-pseudotyped RABV includes among eGFP-labelled neurons, also some eGFP-labelled astrocytes (**Fig.2.9**). The G-pseudotyped RABV is a G-deficient mutant encoding eGFP and has the tropism of the wild-type RABV.

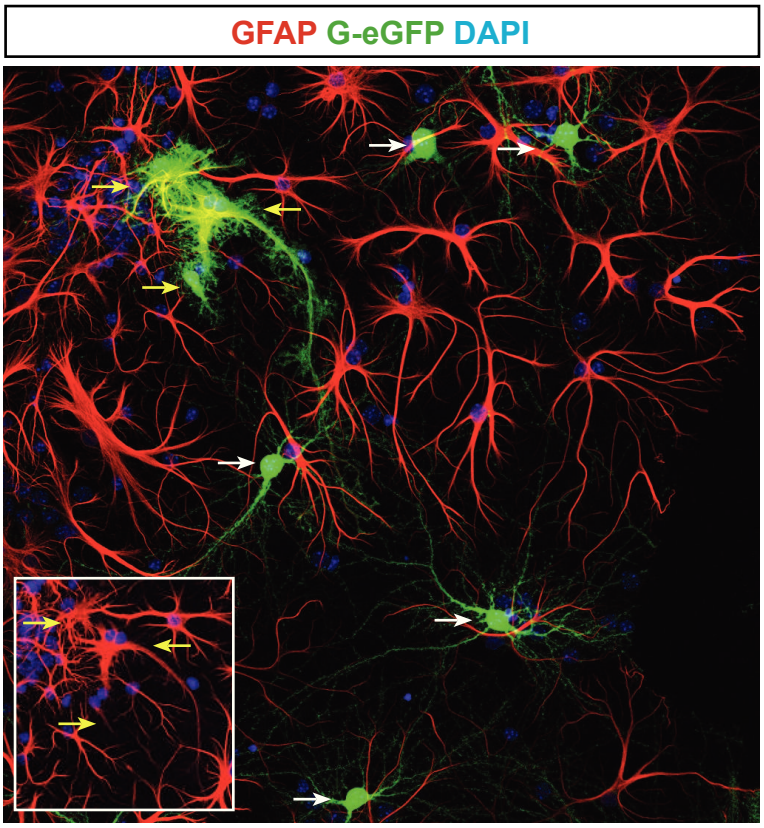

Fig. 2.9. Transduction of E14 cortical culture with G-pseudotyped RABV.
E14 cortical culture transduced with a G-pseudotyped RABV. This virus has the tropism of a wild-type RABV owing to G in its envelope, however it lacks the gene for *G* and therefore cannot be transsynaptically transported. It can infect neurons (white arrows) as well as astrocytes (yellow arrows) in the culture. Inset shows single channel image for GFAP. Scale bar 50 μM.

Moreover, postnatal astrocyte cultures transduced with the *G*- and *TVA*-encoding retrovirus followed by infection with EnvA-pseudotyped RABV (lacking *G*) resulted in the appearance of double-transduced astrocytes already at 24 hours after RABV infection. At 72 hours post EnvA-pseudotyped RABV infection, more eGFP-only positive cells were observed compared to double-transduced cells (**Fig.2.10**). This could either be due to RABV sequestering the host machinery for its own replication and translation, resulting

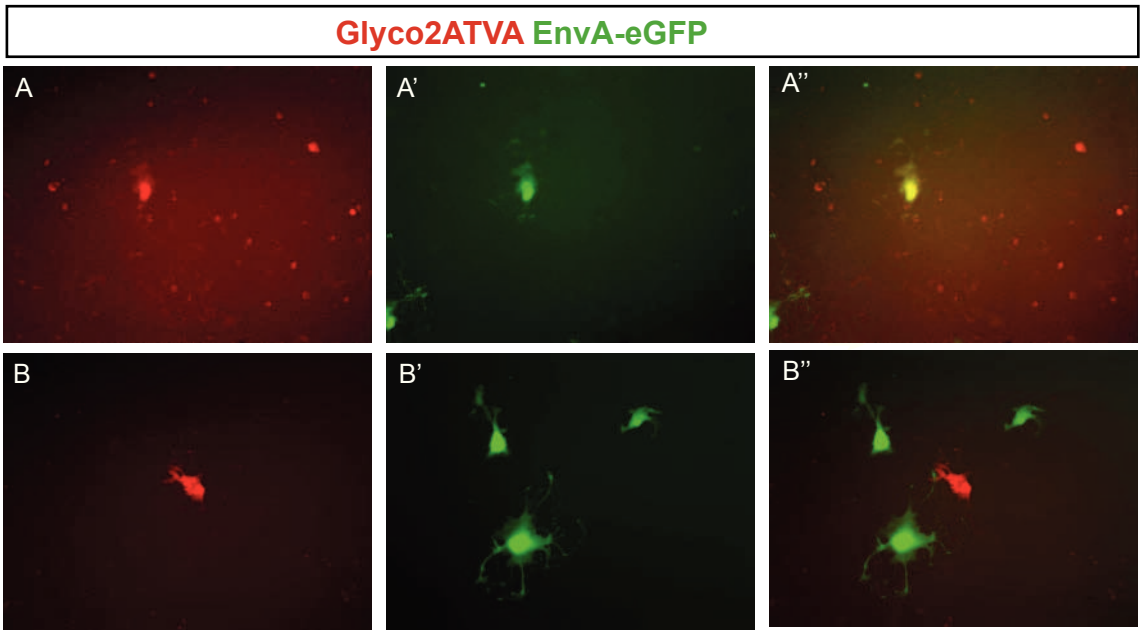

Fig. 2.10. Transduction of postnatal astrocytes with RABV.
(A-A'') Single and merged channel images of postnatal astrocyte cultures transduced with retrovirus encoding *G* and *TVA* 2h after plating and infected with RABV 2 weeks later. Double-transduced astrocytes (yellow arrow) were typically observed. (B-B'') Postnatal astrocytes expressing eGFP but not DsRed 72h after RABV infection (Results courtesy of N. Hagendorf and Prof. K. Conzelmann).

in down-regulation of DsRed protein expression or due to the budding of rabies virions into the astrocyte culture medium by double-transduced astrocytes, which would lead to infection by EnvA-pseudotyped RABV of other astrocytes in the culture. However, the latter explanation could be ruled out by the fact that there was no significant increase in virus titres in the astrocyte culture medium collected at 24, 48 or 72 hours post infection with the non-deficient SAD L16 strain of RABV (encoding the autologous SAD *G*), even at high doses, indicating that astrocytes do not bud out rabies virions into the surrounding medium (**Fig.2.11**).

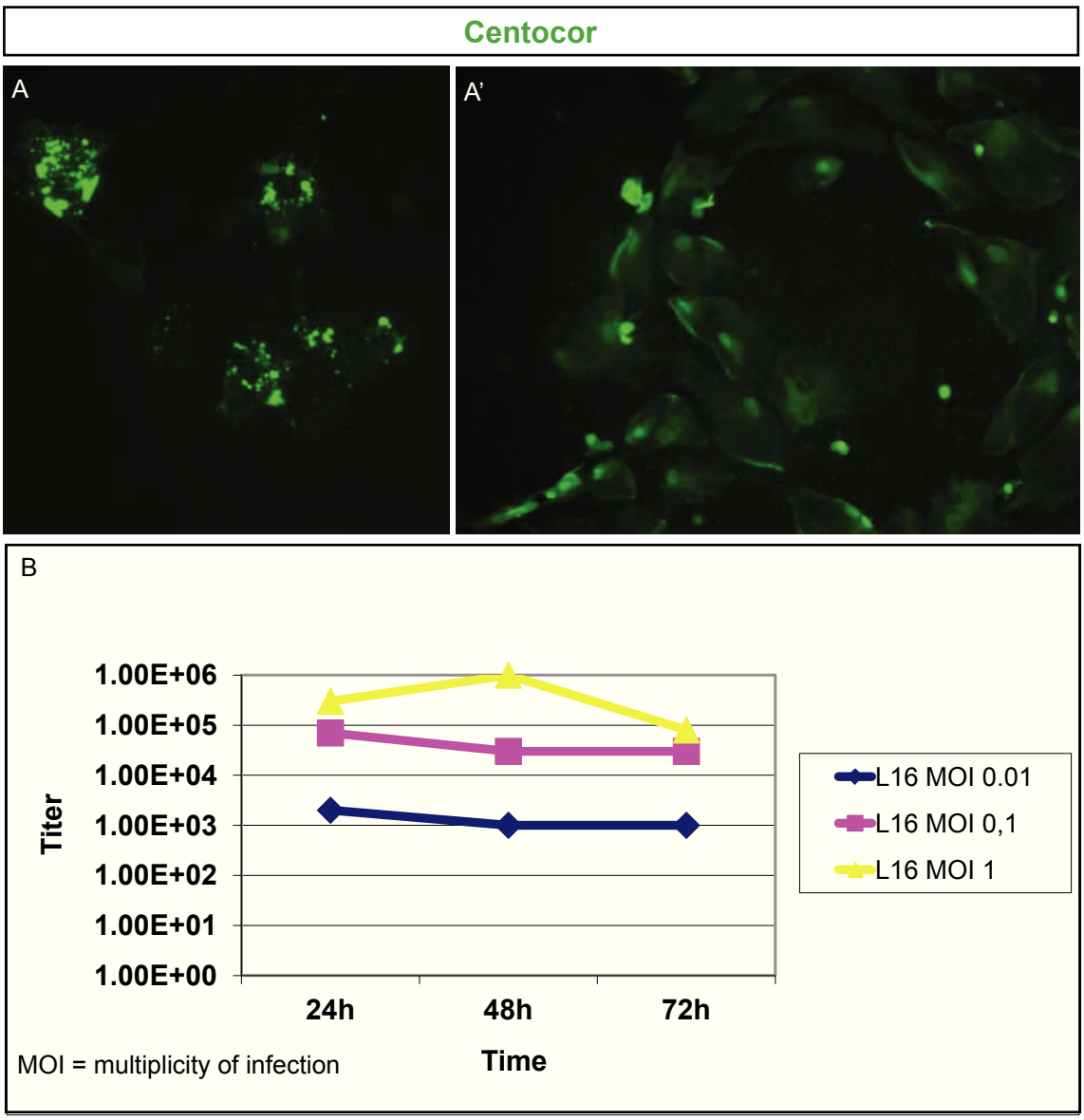

Fig. 2.11. Transduction of postnatal astrocytes with SAD L16 RABV.
Postnatal astrocyte culture transduced with SAD L16 strain of RABV at (A) MOI 0.01. (A') MOI 1. Cells were fixed 96h after infection and stained for antibody against RABV nucleoprotein (Centocor). Single cells were infected at lower MOI while most cells were infected by SAD L16 at higher MOI. (B) SAD L16 titer in postnatal astrocyte culture transduced with increasing virus dose. Astrocyte culture medium was collected at 24, 48 and 72h post infection and transfered on BSR cells for titering the virus. Note that the titer did not increase even at high doses and later time points after infection. MOI=multiplicity of infection. (Results courtesy of N. Hagendorf and Prof. K. Conzelmann).

These data suggest that the *G*- and *TVA*-encoding retrovirus transduced glial cells are susceptible to EnvA-pseudotyped RABV infection and support RABV replication although they may not produce spurious labelling by releasing infectious virions, regardless of dose or time after infection.

2.2 In vivo implementation of the monosynaptic tracing technique

2.2.1 Tracing the connectivity of adult-generated neurons in the dentate gyrus in C57Bl6 mice

After in vitro validation, I stereotactically injected the *G*- and *TVA*-encoding retrovirus in the two neurogenic niches, i.e., the dentate gyrus of the hippocampus and the subependymal zone (SEZ) lining the lateral ventricle of 8-10 week old C57Bl/6 mice in order transduce progenitors derived from adult neural stem cells (aNSCs) that eventually give rise to neurons. I then performed a second injection of EnvA-pseudotyped RABV at different time intervals to identify presynaptic partners of adult-generated neurons (**Fig.2.12**).

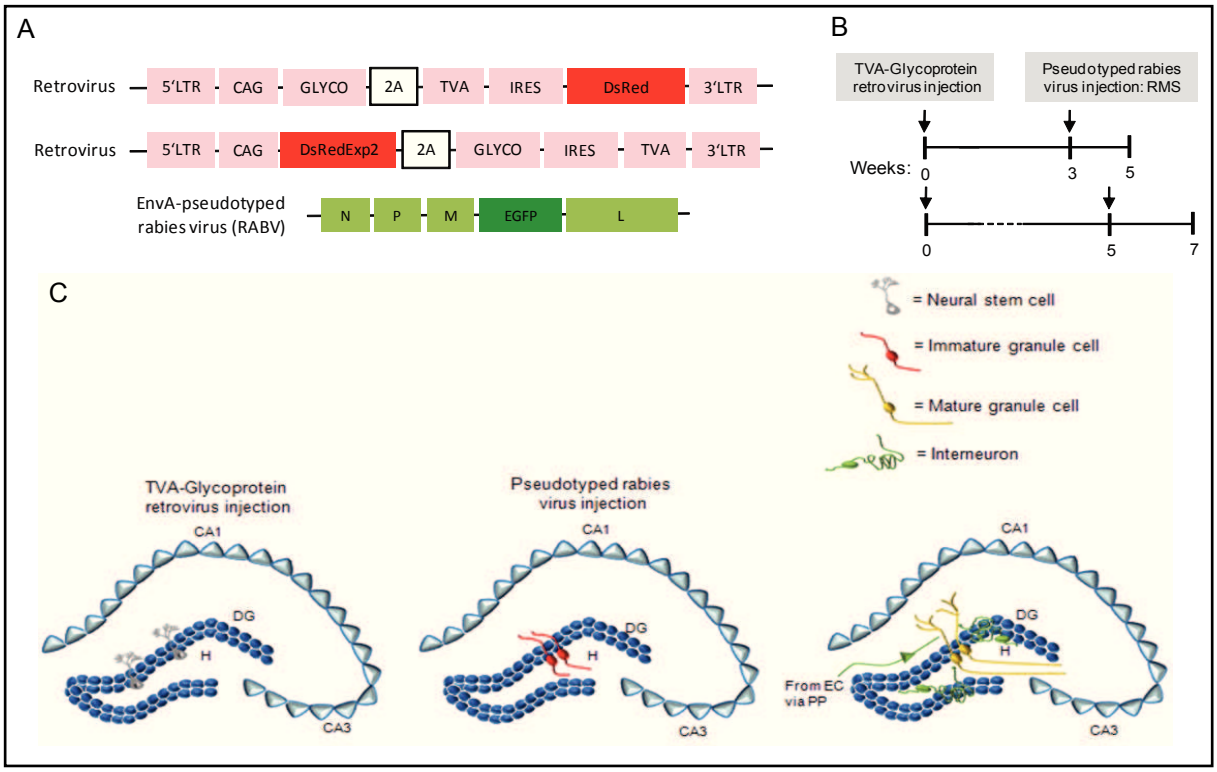

Fig. 2.12. Implementation of the tracing technique in the adult dentate gyrus. (A) Viral constructs. (B) Injection schemes 1 and 2 employed in the adult hippocampus. (C) Schematic of the transsynaptic tracing technique by stereotaxic injection of the *G*- and *TVA*-encoding retrovirus and EnvA-pseudotyped RABV into the dentate gyrus of adult mice. DG=dentate gyrus; H=hilus; EC=entorhinal cortex; PP=perforant path.

In preliminary experiments, injection of the *G*- and *TVA*-encoding retrovirus into the dentate gyrus led to transduction of newborn granule neurons with a very poor efficiency. Very few granule neurons were infected with the retrovirus which could be a

consequence of suboptimal injection. This resulted in reduced probability of subsequent infection with EnvA-pseudotyped RABV which in turn affected visualizing neurons labelled by retrograde transsynaptic transport. It is well known that voluntary exercise increases cell proliferation and survival of newborn granule neurons in the adult dentate gyrus (van Praag et al., 1999). Taking advantage of this to improve the infection efficiencies, adult mice were housed in cages with running wheels prior to retrovirus and EnvA-pseudotyped RABV injections. Indeed, there was a substantial increase in retroviral transduction efficiency in running animals (**Fig.2.13**). Concomitantly, there was also an increase in the proportion of cells infected with EnvA-pseudotyped RABV and its transsynaptic spread. Further injections into the dentate gyrus were therefore performed in mice

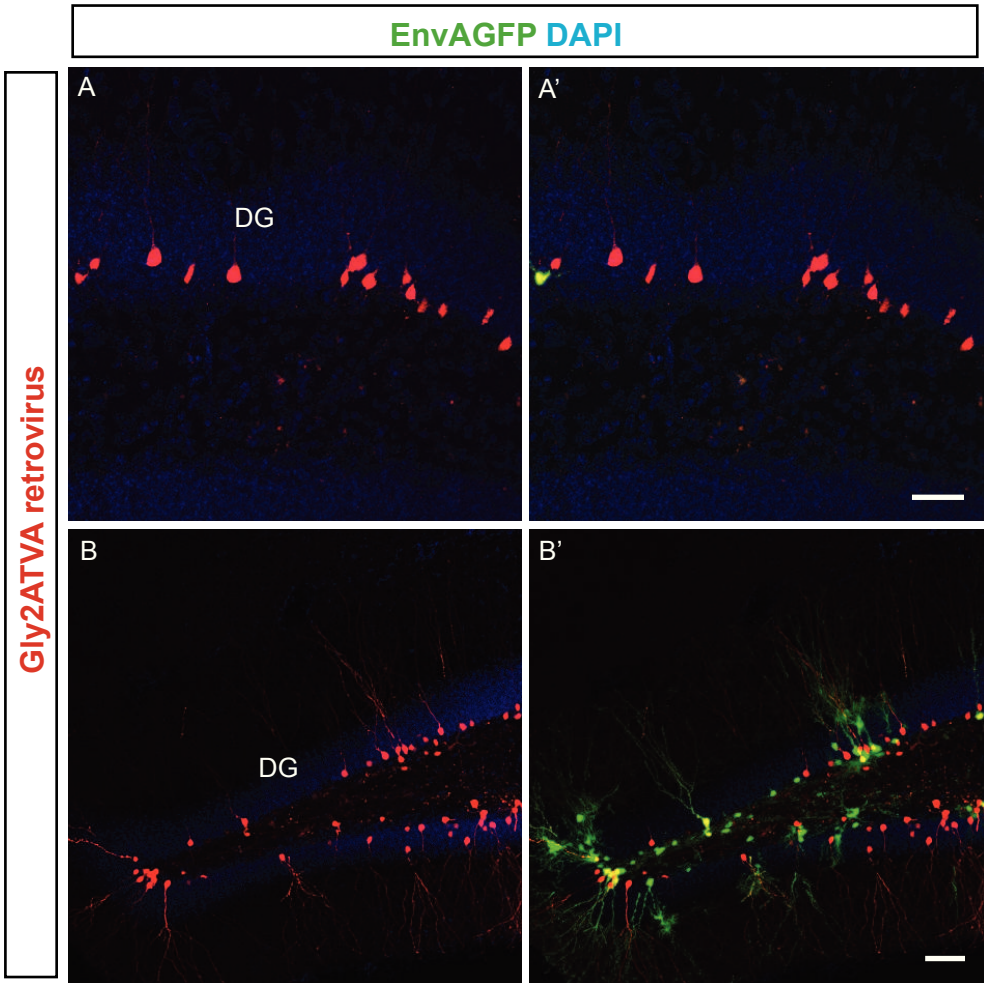

Fig. 2.13. Voluntary exercise increases neurogenesis.
(A-A') Injection of retrovirus into the dentate gyrus of non-runners, followed by EnvA-pseudotyped RABV injection 3 weeks later. (B-B') Injection of the same retrovirus into the dentate gyrus of mice subjected to voluntary running. Increase in proliferation due to running leads to higher number of granule neurons being infected by the retrovirus, resulting in greater infection by the EnvA-pseudotyped RABV and increased subsequent transsynaptic spread. Scale bar 50 μM. DG=dentate gyrus.

subjected to voluntary wheel running paradigm. In order to test whether different time intervals between retroviral and EnvA-pseudotyped RABV injection would reveal different populations of presynaptic neurons, I performed EnvA-pseudotyped RABV injections into the dentate gyrus at different time points after retrovirus injection (**Fig.2.12**). Stereotactic delivery of *G*- and *TVA*-encoding retrovirus and EnvA-pseudotyped RABV resulted in the appearance of double reporter-positive granule neurons, indicating they had undergone double transduction (**Fig.2.14,15**; Deshpande et al., in preparation). Electrophysiological

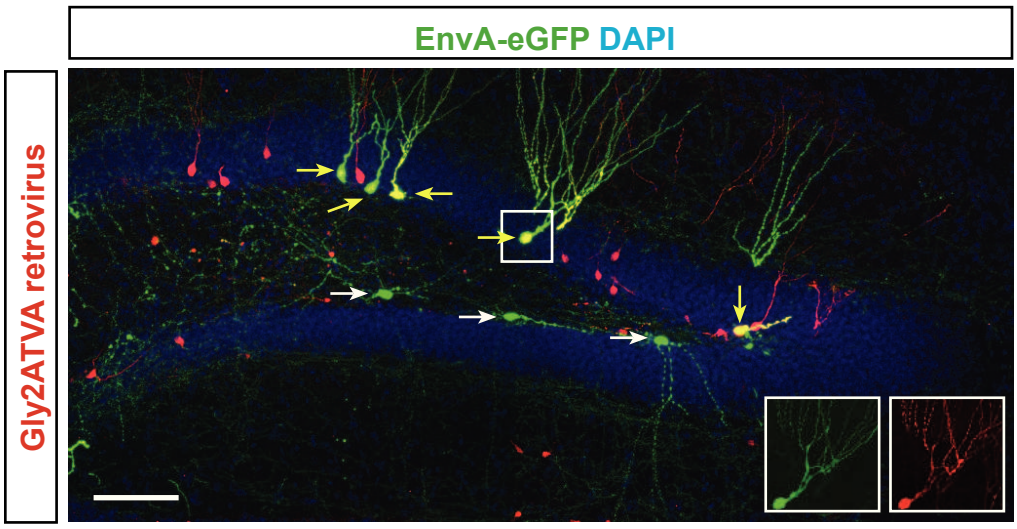

Fig.2.14. Transsynaptic tracing in the adult dentate gyrus.
Example of transsynaptic tracing, 7 weeks after retrovirus injection. Double-transduced adult-generated granule neurons (yellow arrows) and putative presynaptic neurons (white arrows) are indicated. Insets show single channel images of the boxed cell. Scale bar 50 µM (Deshpande et al., in preparation).

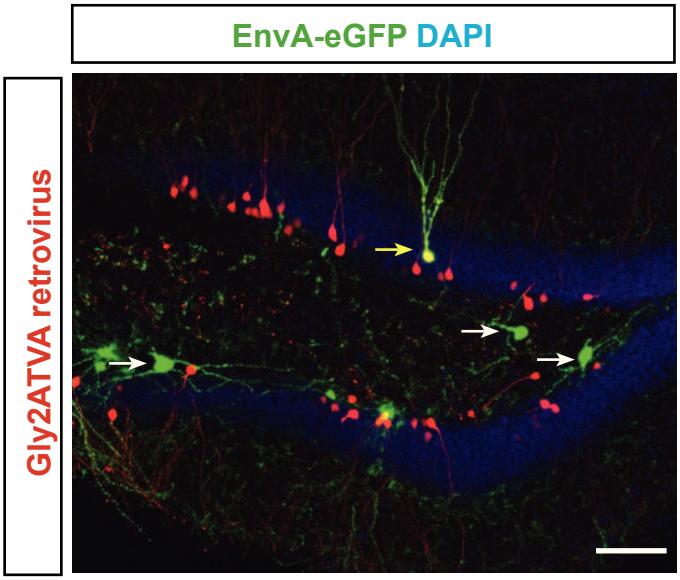

Fig.2.15. Transsynaptic tracing in the adult dentate gyrus.
Another example of transsynaptic tracing, 7 weeks after retrovirus injection. Double-transduced adult-generated granule neurons (yellow arrows) and putative presynaptic neurons (white arrows) are indicated. Scale bar 100 µM.

recordings from double-transduced granule neurons revealed that these had properties similar to non-transduced control granule neurons indicating that transduction with these two viruses does not have an adverse effect on the physiology of the double-transduced newborn neurons within a time window of 7 weeks (Deshpande et al., in preparation). These injections also revealed a population of cells in the hilus and molecular layer (ML) of the dentate gyrus that was positive for eGFP alone (**Fig.2.14,15**; Deshpande et al., in preparation). The location, morphology and profuse axonal arborisation within the hilus, granule cell layer (GCL) or ML indicated that these are local interneurons (**Fig.2.16**;

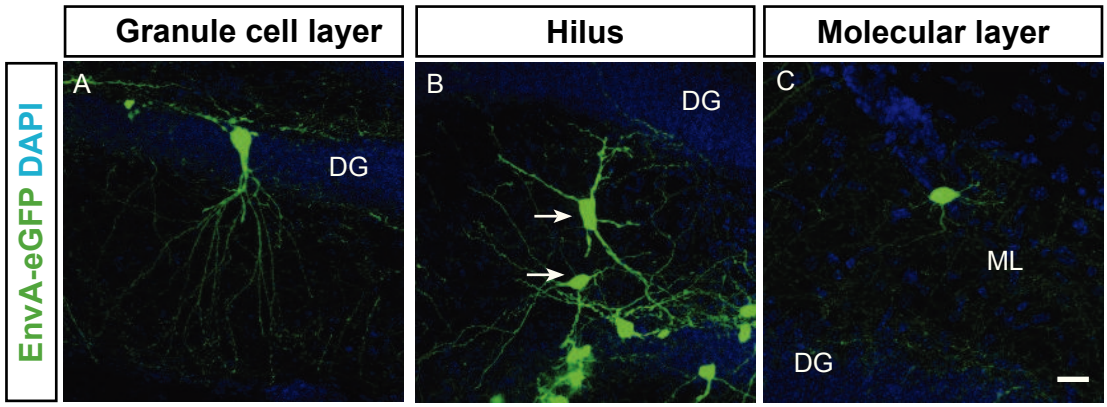

Fig. 2.16. Location of transsynaptically labelled neurons.
(A) Local interneuron in the granule cell layer labelled with EnvA-pseudotyped RABV. (B) Interneurons in the hilus labelled with EnvA-pseudotyped RABV (white arrows). (C) Transsynaptically labelled molecular layer interneuron. Scale bar 20 µM. DG=dentate gyrus; ML=molecular layer (Deshpande et al., in preparation).

Deshpande et al., in preparation**)**. These interneurons had extensive axonal arborizations extending across several slices along the septotemporal length of the dentate gyrus (**Fig.2.17**; Deshpande et al., in preparation). The identity of eGFP only-labelled neurons was confirmed by immunostaining for neurochemical markers of interneurons such as γ-aminobutyric acid (GABA), parvalbumin, or somatostatin and by electrophysiological recordings (**Fig.2.18**; Deshpande et al., in preparation). A population of the eGFP-positive neurons was found to be immunoreactive for the calcium-binding protein, parvalbumin (**Fig.2.18**). Cell bodies of parvalbumin-positive neurons were located at the base of the GCL and rarely in the hilus. Based on their morphology, location and immunoreactivity for parvalbumin, they could be classified as basket cells (Freund and Buzsaki, 1996). Some of the other interneurons labelled with the EnvA-pseudotyped RABV were found

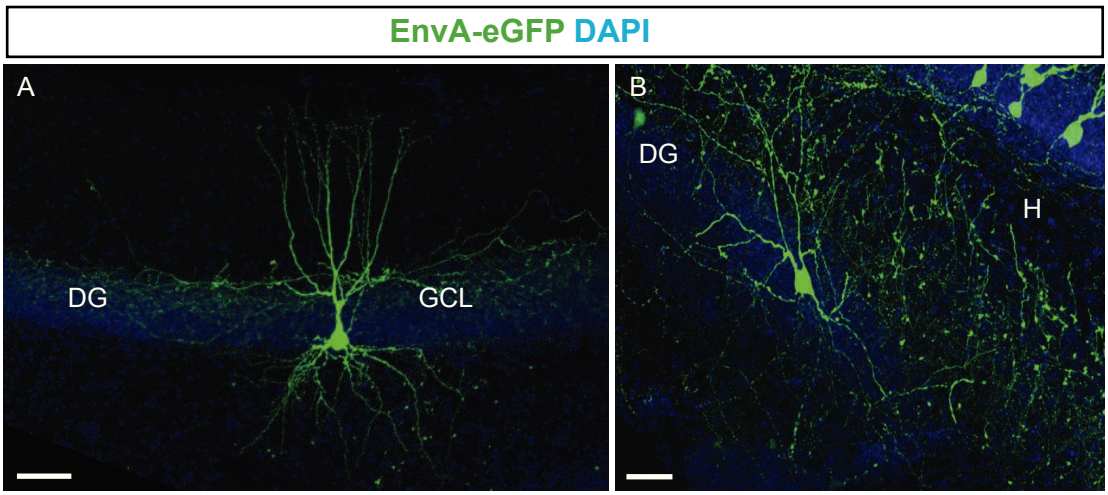

Fig. 2.17.Axonal arborisation of EnvA-pseudotyped RABV-traced dentate interneurons.
(A) Example of a reconstructed EnvA-pseudotyped RABV-traced interneuron profusely innervating the granule cell layer. (B) Example of a reconstructed EnvA-pseudotyped RABV-traced interneuron in the GCL with its axon branching in the hilus. Scale bar 50 μM. DG=dentate gyrus; H=hilus; GCL=granule cell layer (Deshpande et al., in preparation).

to be immunopositive for somatostatin (**Fig.2.18**). Judging by their dendritic arbors and location, the eGFP only-labelled neurons in the ML may be Molecular layer Perforant Path-associared (MOPP) cells whose axons arborise profusely in the ML and make synapses with distal dendrites of granule neurons (Han et al.,1993; **Fig.2.16**). These data are consistent with the notion that GABAergic interneurons are amongst the first to form synapses onto adult-generated granule neurons (Esposito et al., 2005).

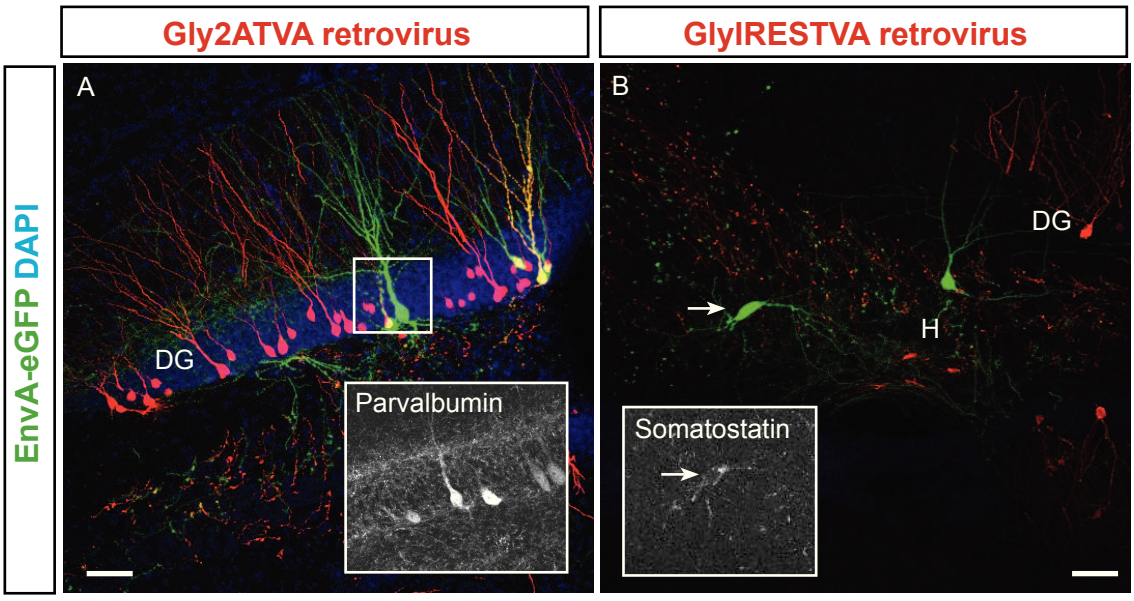

Fig. 2.18. Phenotypic characterisation of EnvA-pseudotyped RABV-traced interneurons.
(A) Parvalbumin-positive interneuron in the GCL. Inset shows parvalbumin staining of the boxed neuron. (B) Somatostatin-positive interneuron (white arrow) in the dentate gyrus labelled with EnvA-pseudotyped RABV alone. Inset shows somatostatin staining of the interneuron. Scale bar 50 μM. DG=dentate gyrus; H=hilus; granule cell layer.

Importantly, no eGFP-positive cells were observed upon EnvA-pseudotyped RABV injection without prior retroviral transduction or following transduction with a retrovirus encoding *DsRed* only as control (**Fig. 2.19**; Deshpande et al., in preparation).

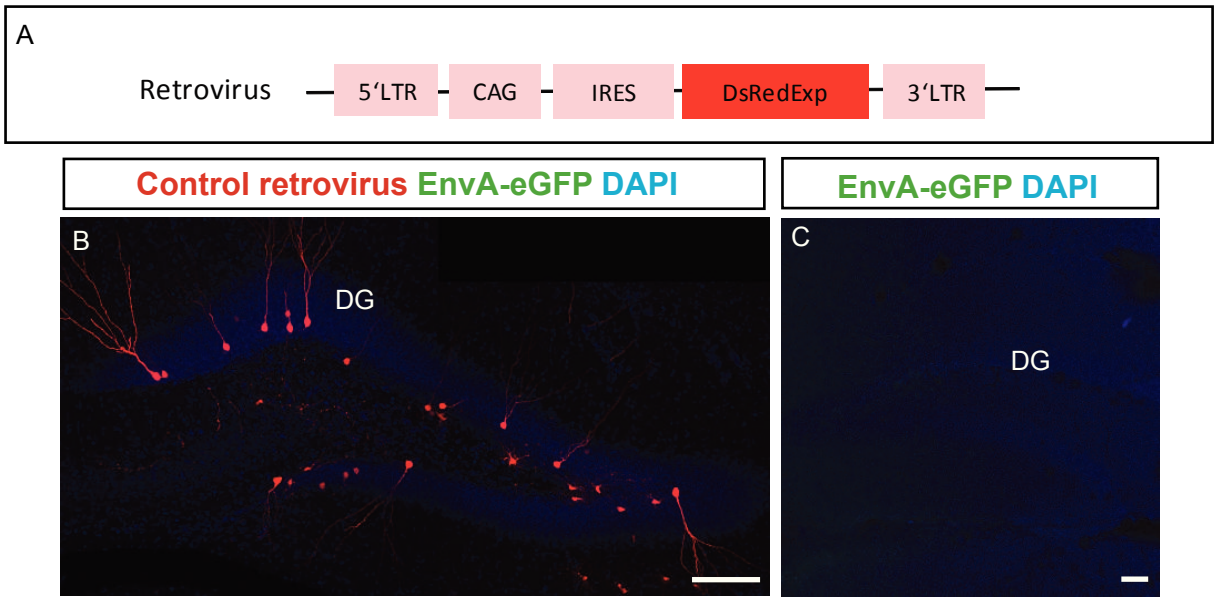

Fig. 2.19. Dependence of EnvA-pseudotyped RABV infection on TVA expression.
(A) Control retroviral construct. (B) Injection of control retrovirus lacking TVA or G in the dentate gyrus followed by EnvA-pseudotyped RABV injection. No eGFP-positive cells were observed in the absence of TVA. (C) Injection of EnvA-pseudotyped RABV into the dentate gyrus without prior retrovirus injection also results in no eGFP-positive cells being labelled. Scale bar 100 µM. DG=dentate gyrus (Deshpande et al., in preparation).

This indicates that the EnvA-pseudotyped RABV infection is strictly dependent on TVA expression and transcomplementation by G is necessary for transsynaptic spread to putative presynaptic partners. Therefore, eGFP-only labelled neurons may have received the EnvA-pseudotyped RABV via retrograde transsynaptic transport from adult-generated granule neurons.

On the other hand, injection of a deletion mutant RABV pseudotyped for *G* into the adult dentate gyrus resulted in the infection of a wide variety of cell types in the hippocampus such as CA3 neurons, CA1 neurons, hilar interneurons and granule neurons besides a few glial cells as well as EC neurons (**Fig. 2.20**). This is consistent with previous reports that the G-pseudotyped RABV can infect cells at axon terminals, travel retrogradely along the axon and express eGFP once it reaches the cell body (Kelly and Strick, 2000; Nassi and Callaway, 2007).

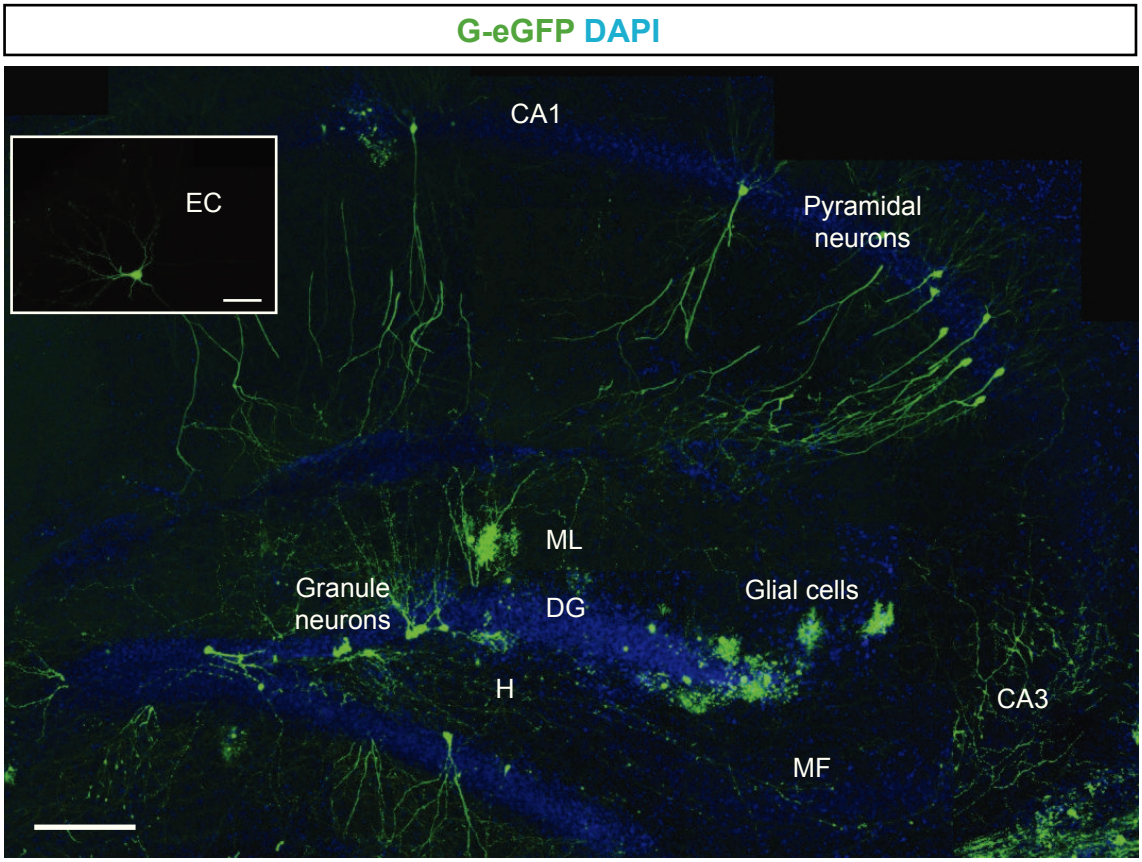

Fig. 2.20. Cell poplulations infected with G-pseudotyped RABV.
Overview in a sagittal section of different cell types transduced with the G-pseudotyped RABV after injection into the DG. Inset shows a neuron in the EC labelled with eGFP. The G-pseudotyped RABV can be taken up by axon terminals of projection neurons. Scale bar 50 µM. DG=dentate gyrus; H=hilus; MF=mossy fibres; ML=molecular layer; EC=entorhinal cortex.

Among the eGFP-labelled cells on injection of the *G*- and *TVA*-encoding retrovirus and EnvA-pseudotyped RABV, I also observed mossy cells in the hilus, the local excitatory input to granule neurons in the dentate gyrus (**Fig.2.21**; Deshpande et al., in preparation). These were readily distinguishable by the characteristic thorny excrescences on their somata and proximal dendrites. Mossy cells are mostly known to project to granule neurons in the distant ipsilateral dentate gyrus and the contralateral hippocampus via the associational/commisural projections (Amaral et al., 2007). Partially in line with this, I observed eGFP-labelled mossy cells in the ipsilateral dentate gyrus however none in the contralateral dentate gyrus. Although there were no eGFP labelled cell bodies in the contralateral dentate gyrus, I could often detect eGFP-postive fibres in the ML originating presumably from eGFP-labelled cells in the ipsilateral dentate gyrus. These could potentially be the axonal projections of mossy cells labelled with eGFP.

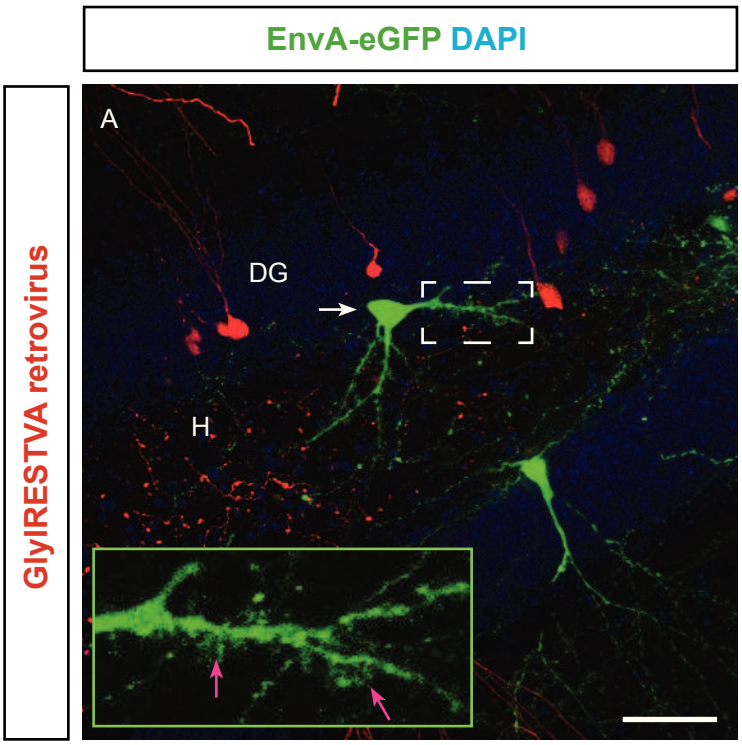

Fig. 2.21. Transsynaptically traced putative mossy cells.
(A) Labelling of a putative mossy cell (white arrow) in the hilus following retrovirus and EnvA-pseudotyped RABV injection in the dentate gyrus. Inset shows the enlarged image of the boxed area. Magenta arrows indicate the thorny excrescences typically found on mossy cells. Scale bar 50 μM. DG=dentate gyrus; H=hilus (Deshpande et al., in preparation).

Two interesting observations in the dentate gyrus following *G*- and *TVA*-encoding retrovirus and EnvA-pseudotyped RABV were: (i) the regular appearance of eGFP-positive astrocytes especially surrounding the dendrites of retrovirus and EnvA-pseudotyped RABV double-labelled newborn granule neurons and (ii) EnvA-pseudotyped RABV only-labelled myelinating oligodendrocytes along axonal tracts in the fimbria fornix of the hippocampus (**Fig.2.22**). Since astrocytes are known to be closely associated with synapses via perisynaptic processes and myelinating oligodendrocytes are closely associated with myelinated axons, it would seem that they are taking up either EnvA-pseudotypted RABV or eGFP by a process that is not entirely clear.

Injection of *G*- and *TVA*-encoding retrovirus followed by EnvA-pseudotyped RABV also revealed long-distance projections to dentate granule neurons. Delivery of EnvA-pseudotyped RABV at different time points following retrovirus transduction (2, 3 or 5 weeks) resulted in eGFP labelling of different types of afferents. These long-distance connections included presynaptic inputs originating from the entorhinal cortex (EC) as

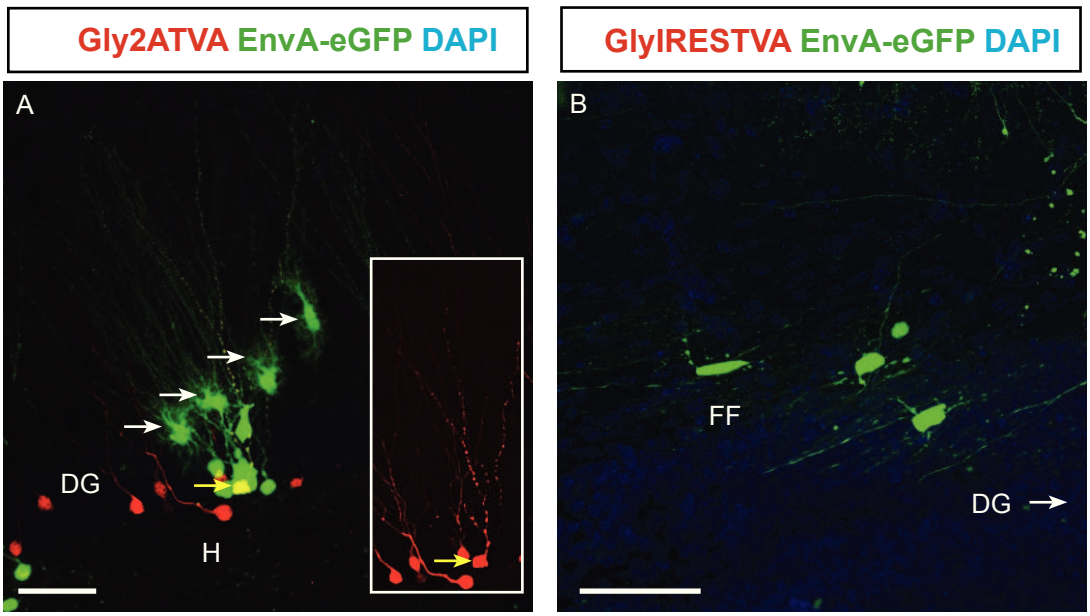

Fig. 2.22. EnvA-pseudotyped RABV-labelled glial cells.
(A) eGFP-labelled astrocytes closely associated with the dendrites of a newborn granule neuron transduced with *G*- and *TVA*-encoding retrovirus and RABV. Inset shows newborn granule neuron (yellow arrow). (B) RABV-transduced myelinating oligodendrocytes in the fimbria fornix of the hippocampus. Scale bar 50 μM. DG=dentate gyrus; H=hilus; FF=fimbria fornix.

well as cholinergic inputs arising from the medial septal nucleus and the nucleus of the diagonal band of Broca (MS-NDB) (**Fig.2.23,24**; Deshpande et al., in preparation). The eGFP signal profusely labelled the dendrites and axons of the projection neurons. Surprisingly, there were eGFP-positive neurons located in the subiculum, a cortical structure adjacent to the hippocampus proper (**Fig.2.25**). The subiculum is known to be the main output of the hippocampus but its projection to the dentate gyrus has not been well studied.

Altogether, these results indicate that adult-generated granule neurons receive input from local as well as long-distance presynaptic partners and that innervation from local sources precedes that arising from long-range projections.

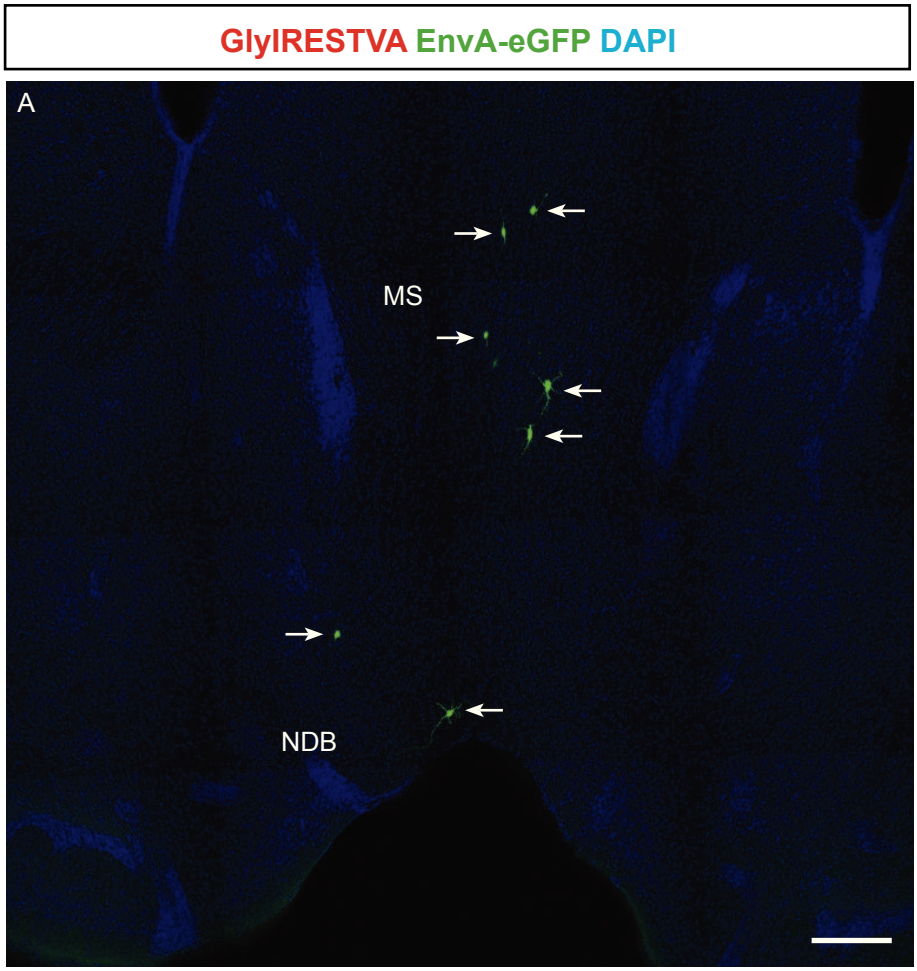

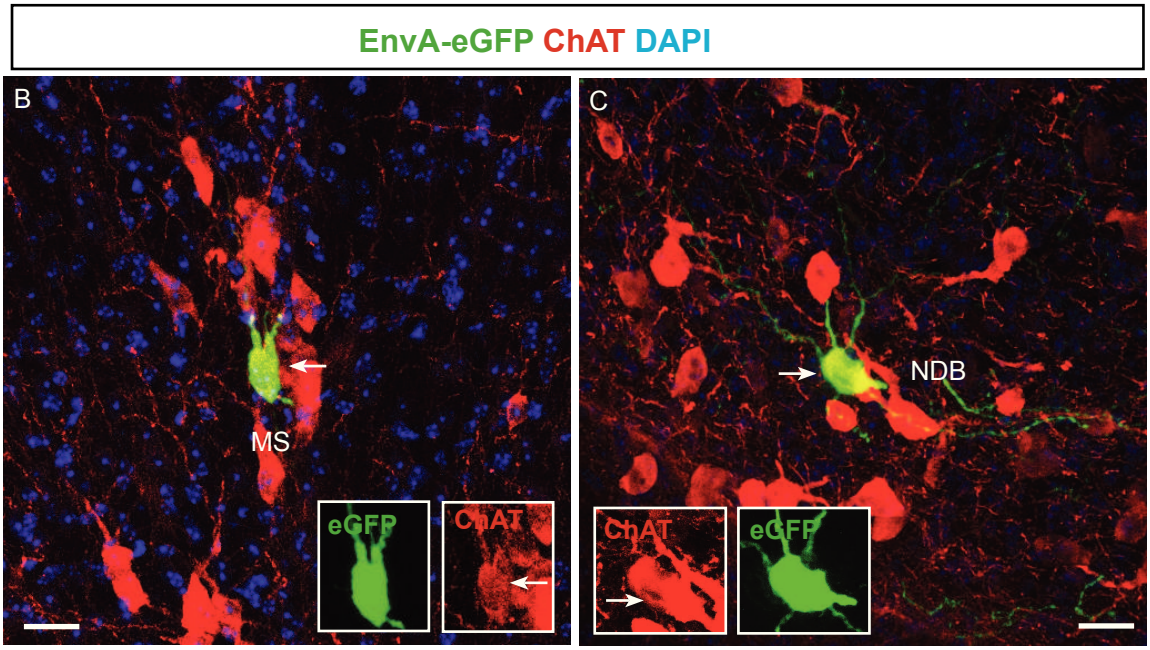

Fig. 2.23. Monosynaptically traced neurons in the basal forebrain.
(A) Overview of eGFP-labelled neurons in the medial septum and the diagonal band of Broca (white arrow). Scale bar 50 µM. (B) High magnification image of an EnvA-pseudotyped RABV-traced neuron immunopositive for choline acetyltransferase (ChAT) in the MS (white arrow). (C) High magnification image of an EnvA-pseudotyped RABV-traced cholinergic neuron in the NDB (white arrow). Insets show single channel images of ChAT-positive neurons. Scale bar 20 µM. MS=medial septum; NDB=nucleus of the diagonal band of Broca (Deshpande et al., in preparation).

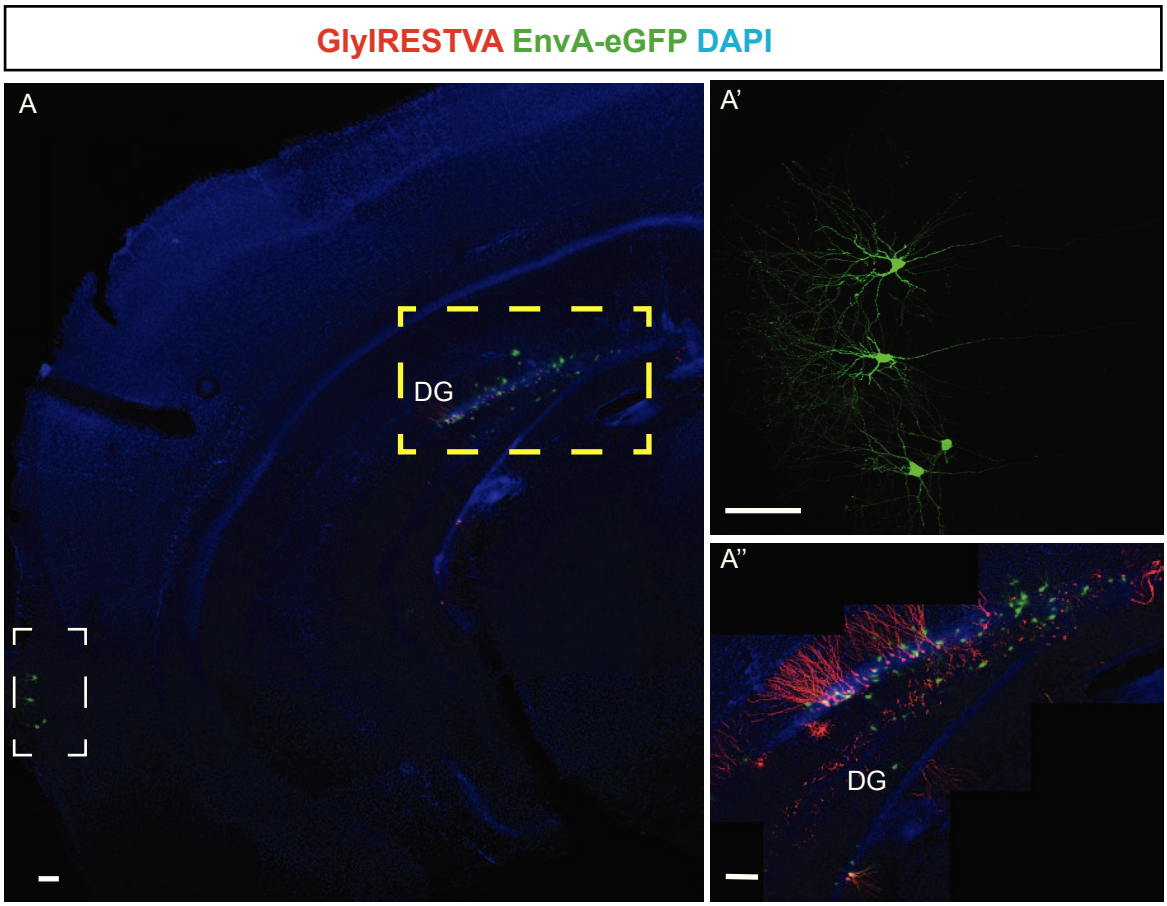

Fig. 2.24. Monosynaptically traced cortical projections.
(A) Overview of entorhinal cortex neurons labelled with eGFP following injection of EnvA-pseudotpyed RABV 5 weeks post *G*- and *TVA*-encoding retrovirus retrovirus injection. Enlarged image of the entorhinal cortex pyramidal neurons (white boxed area) is shown in A'. Enlargement of the dentate gyrus (yellow boxed area) is shown in A''. Scale bar 100 µM. DG=dentate gyrus (Deshpande et al., in preparation).

2.2.2 Tracing the connectivity of adult-generated neurons in the dentate gyrus in hGFAP-TVA transgenic mice

Control injections of EnvA-pseudotyped RABV alone into the dentate gyrus of adult mice or injection of a retrovirus encoding *DsRed*, but not *TVA* or *G*, followed by EnvA-pseudotyped RABV injection resulted in labelling by eGFP of neither granule neurons nor their local or long-distance projections, highlighting the specificity of EnvA for the TVA receptor (**Fig.2.19**). The RABV *G* has been extensively studied and its importance in the retrograde transport of the virus has been unequivocally demonstrated (Etessami et al., 2000). In order to demonstrate the specificity of the RABV *G* for transsynaptic transport via transcomplementation in our system, I designed a control retrovirus encoding *TVA* and *DsRedExpress2* but no *G* (denoted as **DsRedExpIRESTVA**; **Fig.2.26**; Deshpande et al., in preparation, in collaboration with Francesca Vigano. The

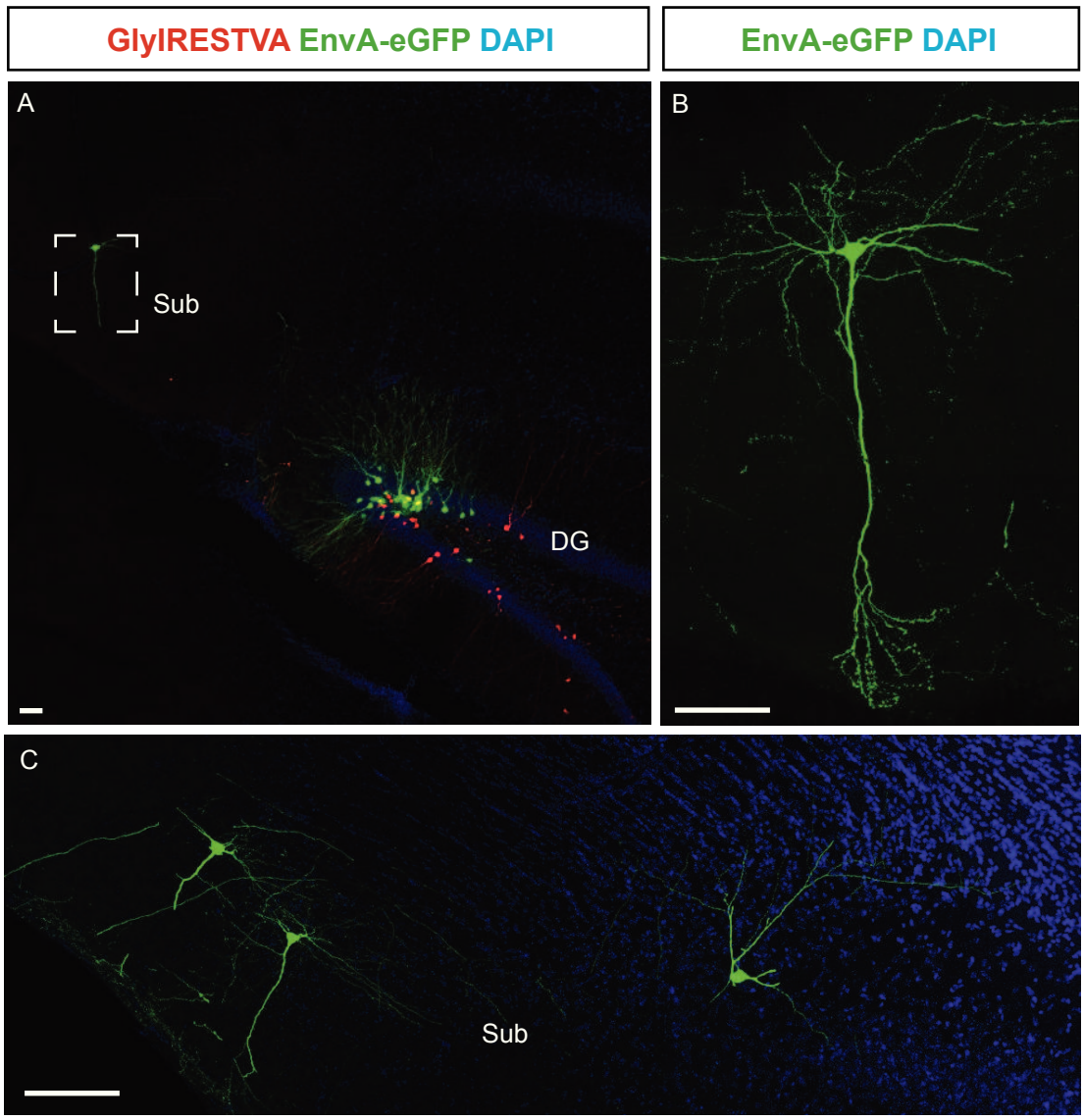

Fig. 2.25. Transsynaptically traced neurons in the subiculum.
(A) Overview of the location of subicular neuron in relation to the dentate gyrus in a single optical section. (B) Magnified and maximum intensity projection image of the boxed area in (A). (C) Example of EnvA-pseudotyped RABV-traced neurons in the subiculum. Note that these these neurons were observed at the latest time point analysed (i.e., 7 weeks after injection of *G*- and *TVA*-encoding retrovirus in the DG). Scale bar=50 μM. DG=dentate gyrus; Sub=subiculum.

expected result was that newborn granule

neurons transduced with the **DsRedExpIRESTVA** control retrovirus would be infected with EnvA-pseudotyped RABV but no transsynaptic transport to putative presynaptic partners would occur from these neurons in the absence of *G*. Stereotactic injections of the **DsRedExpIRESTVA** control retrovirus into the dentate gyrus of adult mice followed by the second injection with RABV 3 weeks later resulted in double transduced newborn granule neurons in the SGZ (**Fig.2.26**; Deshpande et al., in preparation), as

predicted. Surprisingly, there were also a few eGFP-only labelled cells having interneuron morphology restricted to the site of injection. These interneurons could not have been labelled transsynaptically since the presence of the glycoprotein on the surface of the rabies virion is imperative for its release at the synapse from the postsynaptic cell

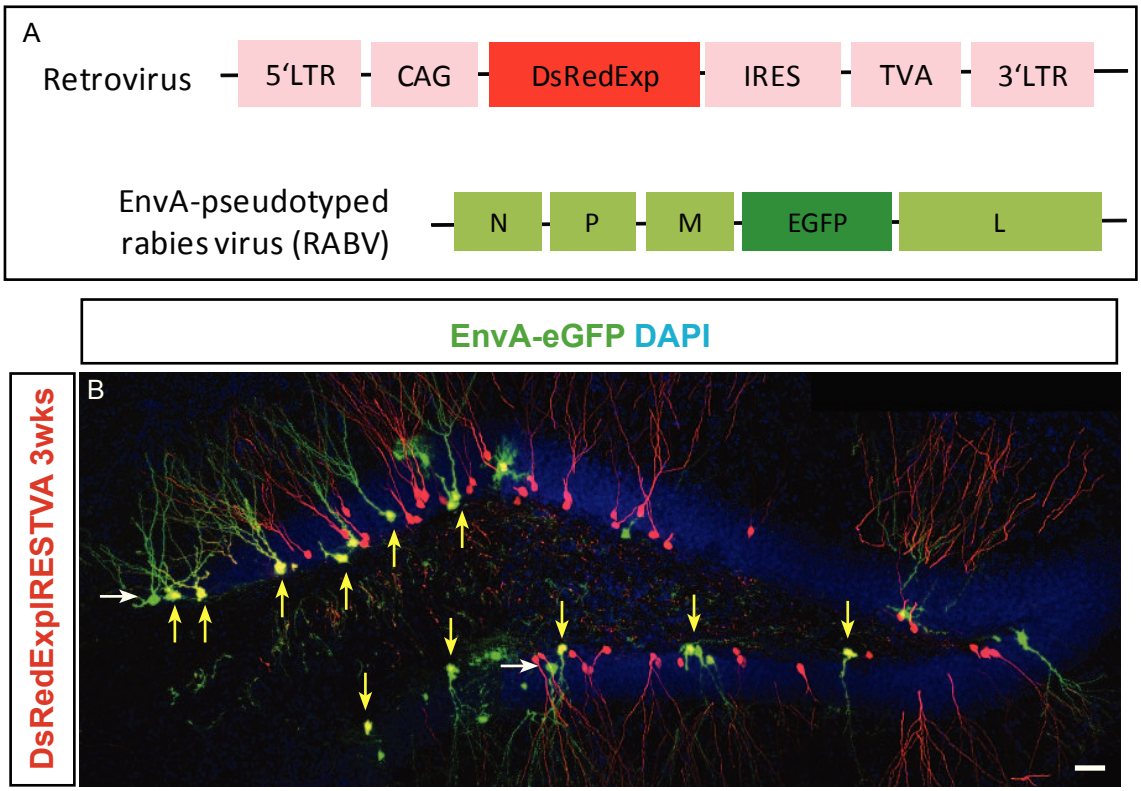

Fig. 2.26. Pseudotransduction of TVA.
(A) Retroviral construct encoding *TVA* but lacking *G*. (B) Injection of the *TVA* control retrovirus followed by EnvA-pseudotyped RABV, 3 weeks later led to labelling of granule neurons with both viruses (yellow arrows). It also resulted in labelling of some neurons with eGFP alone, probably due to expression of TVA on their cell membrane by pseudotransduction (white arrows). Scale bar 20 μM (Deshpande et al., in preparation).

(Etessami et al., 2000). The rabies virus has been shown not to produce spurious labelling by passive diffusion (Ugolini, 2008). Hence, this unexpected result indicates direct infection of the small number of neurons in the dentate gyrus by EnvA-pseudotyped RABV. This primary infection must be due to the presence of TVA on the surface of these neurons. One explanation for this could be a retrovirus-associated phenomenon called pseudotransduction. On entering a cell, the retroviral RNA genome must be reverse transcribed into DNA and eventually stably integrated into the host genome in order to over-express the transgene(s) it carries. However, a non-integrating retroviral infection could result in low to medium level transgene expression (Haas et al., 2000).

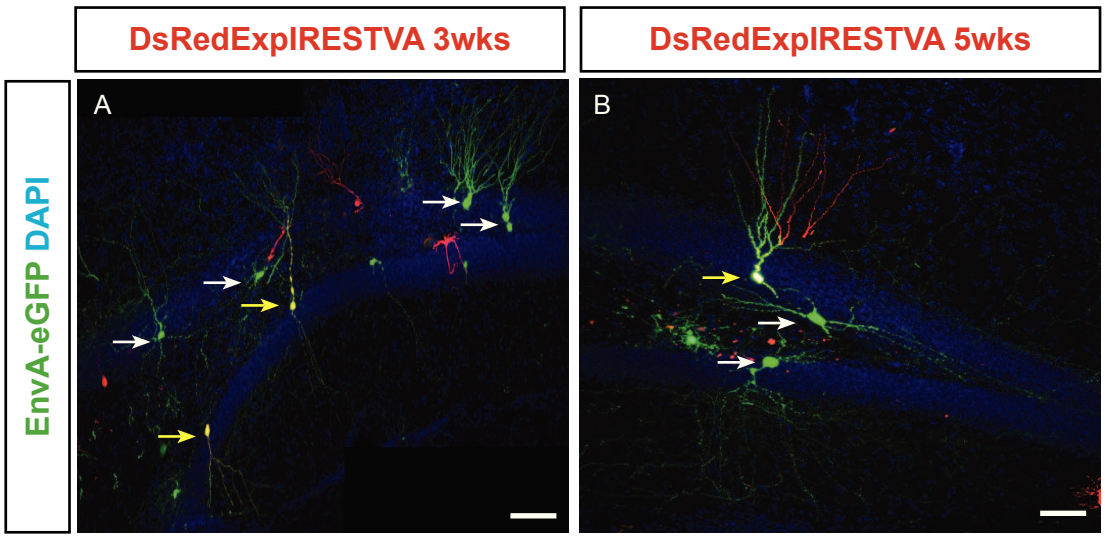

Fig. 2.27. Pseudotransduction of TVA.
(A) Direct labelling of hilar interneurons with eGFP after injection of EnvA-pseudotyped RABV 3 weeks post *G*- and *TVA*-encoding retrovirus injection, probably due to pseudotransduction (white arrows). (B) Direct labelling of hilar interneurons on injecting EnvA-pseudotyped RABV 5 weeks after retroviral injection indicates low turnover of TVA on the cell membrane. Note that the labelling is restricted to the site of injection. Scale bar 50 µM.

This is termed pseudotransduction. Moreover, it is known that small amounts of TVA on the plasma membrane is sufficient to render cells susceptible to infection by EnvA-pseudotyped viruses (Bates et al., 1993). The time interval between retrovirus and

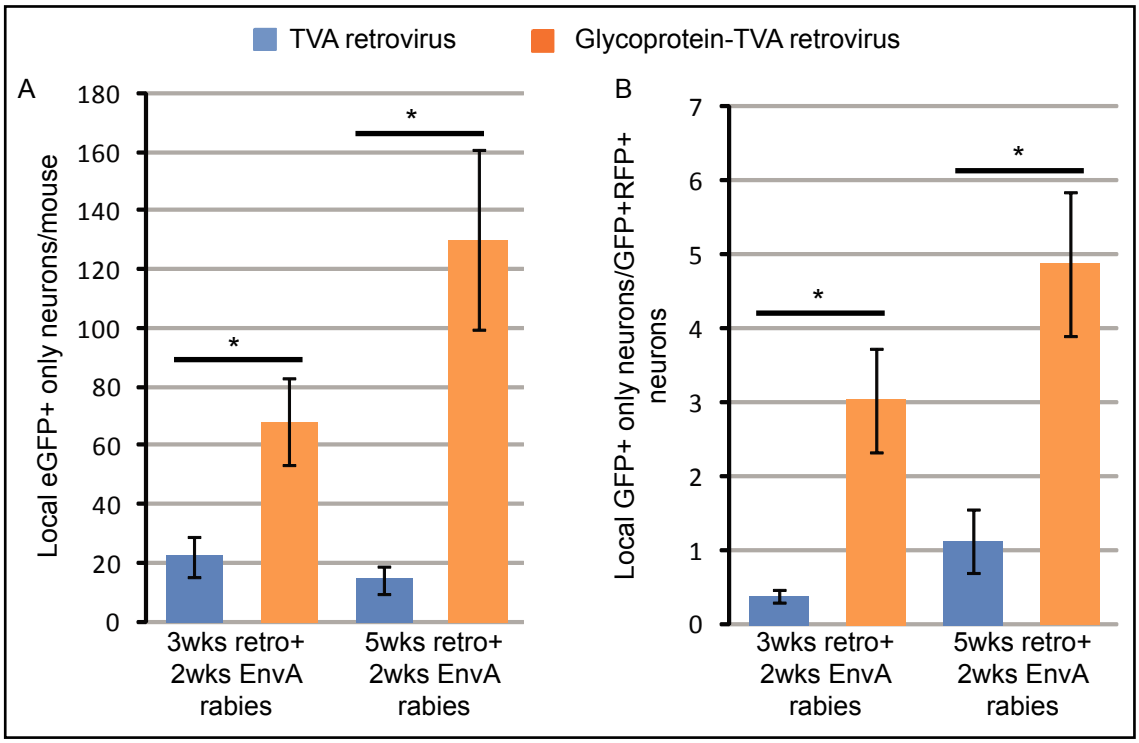

Fig. 2.28. Pseudotransduction of TVA.
(A) Quantification of the absolute number of EnvA-pseudotyped RABV-only transduced local neurons. (B) Their relative proportion compared to double-transduced neurons (n=3-5 mice per experimental condition; *p<0.05) (Deshpande et al., in preparation).

EnvA-pseudotyped RABV injections was then increased to 5 weeks, assuming that there must be a turnover of TVA on the cell membrane. Once again, this also resulted in the primary labelling of hilar interneurons restricted to the site of injection (**Fig.2.27**). Importantly, however, the proportion of interneurons infected by RABV following injection of the *TVA*-encoding control retrovirus was much lower as compared to that obtained when a *G*- and *TVA*-encoding retrovirus was used (**Fig.2.28**; Deshpande et al., in preparation). Notably, no mossy cells or long-distance projections were labelled using the **DsRedExpIRESTVA** control retrovirus at shorter or longer time intervals between retrovirus and EnvA-pseudotyped RABV injections.

Taken together, this data suggests that the hilar neurons directly infected with EnvA-pseudotyped RABV may be pseudotransduced causing them to express minute quantities of the TVA receptor on their surface which remains stable enough to allow infection by EnvA-pseudotyped RABV 3 or 5 weeks later but no transsynaptic transport occurs in the absence of rabies virus glycoprotein.

We speculated that the confounding results obtained due to TVA-mediated pseudotransduction could be circumvented if we avoid introducing the TVA receptor into the system via a retrovirus. Therefore, a transgenic mouse line that expresses *TVA* under the human glial fibrillary acidic protein (GFAP) promoter was used (hGFAP-TVA; **Fig.2.29**; Holland et al., 1998; Holland and Varmus, 1998). The hGFAP promoter is active in parenchymal astrocytes and aNSCs residing in the SGZ of the dentate gyrus that eventually give rise to granule neurons. Therefore, in the hGFAP-TVA mice, cell types having an active hGFAP promoter would be susceptible to EnvA-pseudotyped RABV infection. We further hypothesized that TVA protein expression may persist long enough to allow EnvA-pseudotyped RABV infection in the progeny of aNSCs and when combined with a *G*-encoding retrovirus, may allow for transsynaptic tracing of their putative presynaptic partners. Before using this mouse line for transsynaptic tracing experiments, different cell types in the dentate gyrus that are transduced by EnvA-pseudotyped RABV were determined. At 2 days post EnvA-pseudotyped RABV infection,

more than 65% of the cells labelled with eGFP were GFAP-positive radial glia-like or horizontal astrocytes in the subgranular zone, 25% were positive for Doublecortin (Dcx), a marker for immature neurons and 5% were mature granule neurons (Deshpande et al., in preparation). At 12 days post infection, majority of the cells labelled with eGFP were immunopositive for GFAP or Dcx (Deshpande et al., in preparation). However, no local interneurons, mossy cells or long-distance projection neurons were found to be

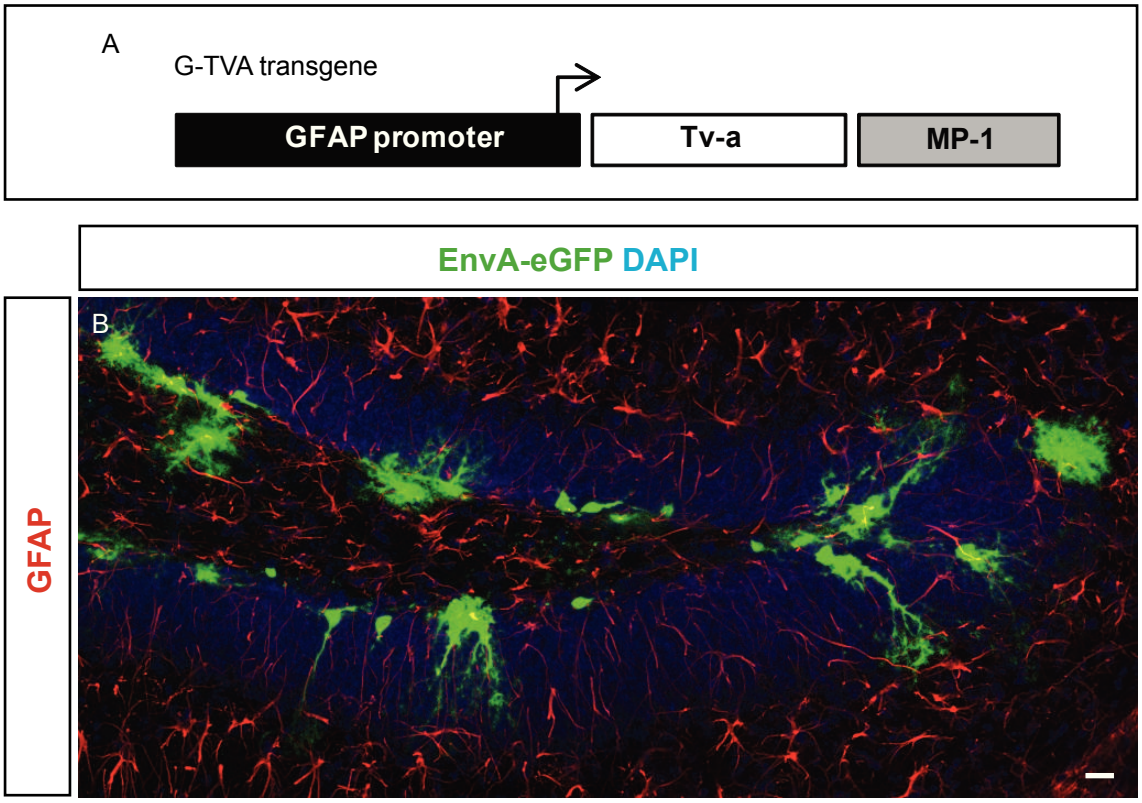

Fig. 2.29. Cell types labelled with EnvA-pseudotyped RABV in hGFAP-TVA mice.
(A) The quail *TVA* gene driven under the human GFAP promoter with part of the mouse protamine gene supplying an intron and polyadenylation site (Holland et al, 1998; Holland and Varmus, 1998). (B) Representative example of EnvA-pseudotyped RABV-infected cells in hGFAP-TVA mice 4 days after injeciton. Most of the cells labelled are in the glial lineage or young neurons. Scale bar 20 μM.

labelled with eGFP. This result indicates that expression of TVA is restricted to aNSCs and does persist in their progeny including adult-generated granule neurons (**Fig.2.29-31**).

For labelling presynaptic partners of newborn neurons, a retrovirus encoding *G* and *DsRed* reporter was injected into the dentate gyrus of 8-week old hGFAP-TVA mice (**Fig.2.32**). When this was followed by EnvA-pseudotyped RABV injection 5 days later (sacrifice at day 10), double labelled granule neurons and very few local interneurons

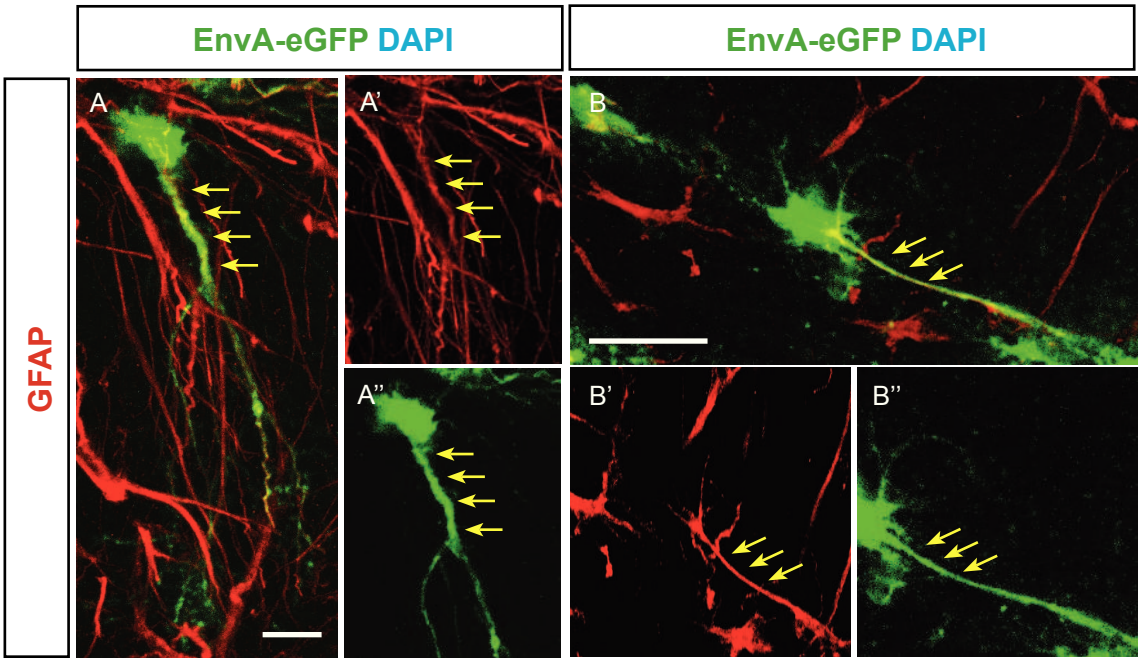

Fig. 2.30. Cell types labelled with EnvA-pseudotyped RABV only in the hGFAP-TVA mice.
(A) A GFAP-positive EnvA-pseudotyped RABV-labelled cell. Yellow arrows point to the colocalization of the immunoreactive signal. A' and A'' show single channel images of the colocalization. (B) Example depicting GFAP-positive horizontal astrocyte targeted by EnvA-pseudotyped RABV. B' and B'' show single channel images of the colocalized area in D (yellow arrows). Scale bar 20 μM.

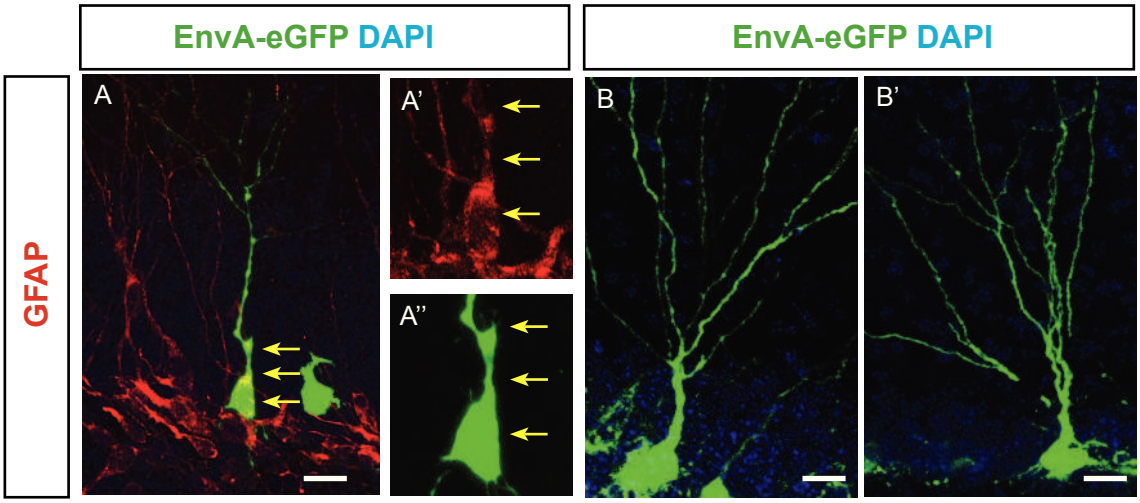

Fig. 2.31. Cell types labelled with pseudotyped RABV alone in the hGFAP-TVA mice.
(A) Example of an EnvA-pseudotyped RABV-labelled cell Dcx-postiive newborn neuron. Yellow arrows point to the colocalization of the immunoreactive signal. A' and A'' show enlarged single channel images of the colocalization. (B-B') Two examples depicting mature neurons targeted by EnvA-pseudotyped RABV. Scale bar 20 μM.

was observed. On injection of EnvA-pseudotyped RABV 10 days after retrovirus injection and allowing longer intervals between EnvA-pseudotyped RABV injection and sacrifice, there was a substantial increase in the number of local interneurons labelled with eGFP (Deshpande et al., in preparation; **Fig.2.33**). A population of these interneurons was also found to be immunoreactive for parvalbumin (**Fig.2.33**). This labelling pattern is

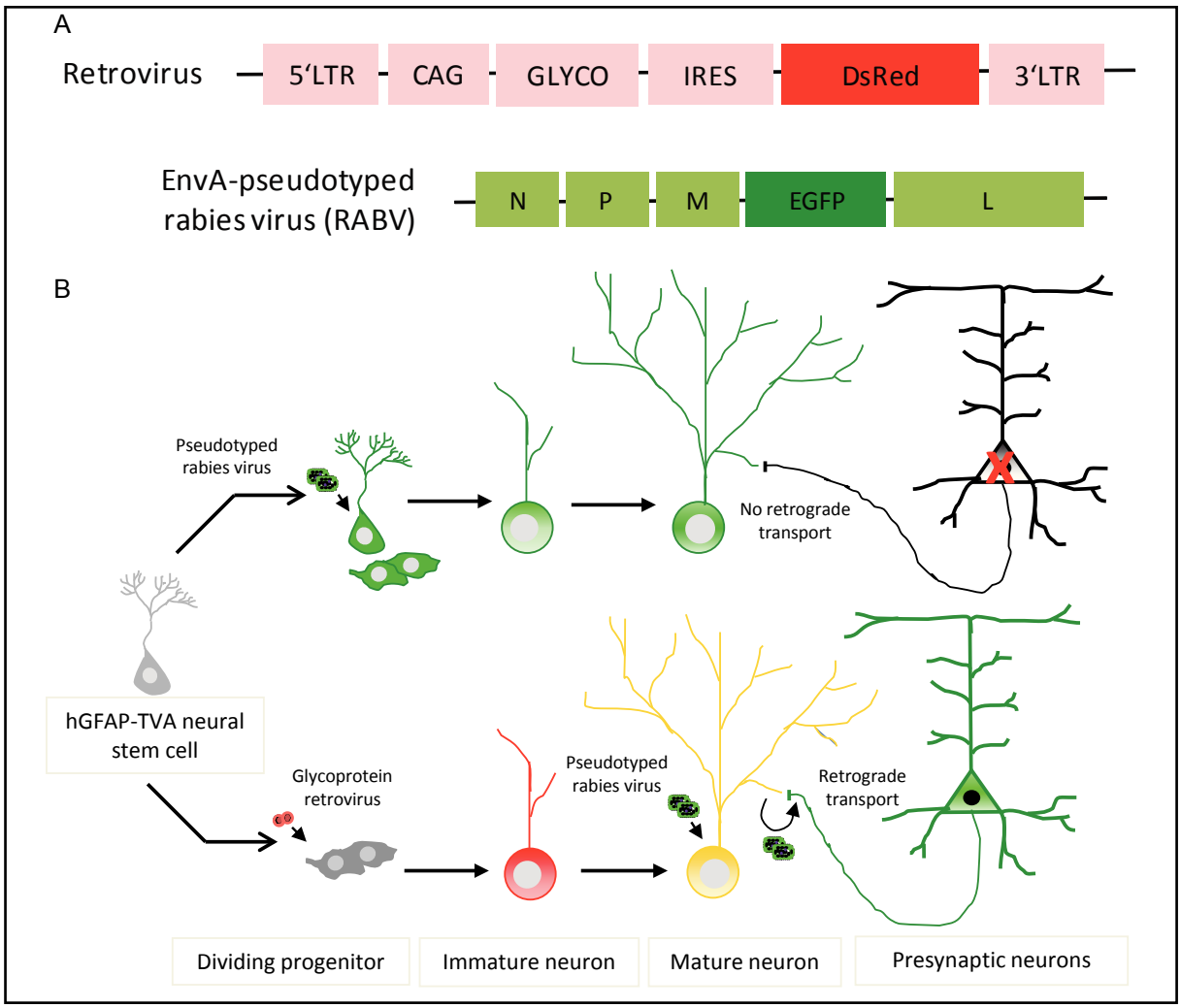

Fig. 2.32. Schematic of monosynaptic tracing in hGFAP-TVA mice.
(A) Retrovirus and RABV constructs. (B) Scheme of transsynaptic tracing in the hGFAP-TVA mice. Injection with EnvA-pseudotyped RABV alone leads to infection of cells in the glial lineage and a small number of newborn neurons. Injection with EnvA-pseudotyped RABV following the *G*-encoding retrovirus results in infection of aNSCs and their progeny including newborn neurons and subsequent transsynaptic transport to presynaptic neurons.

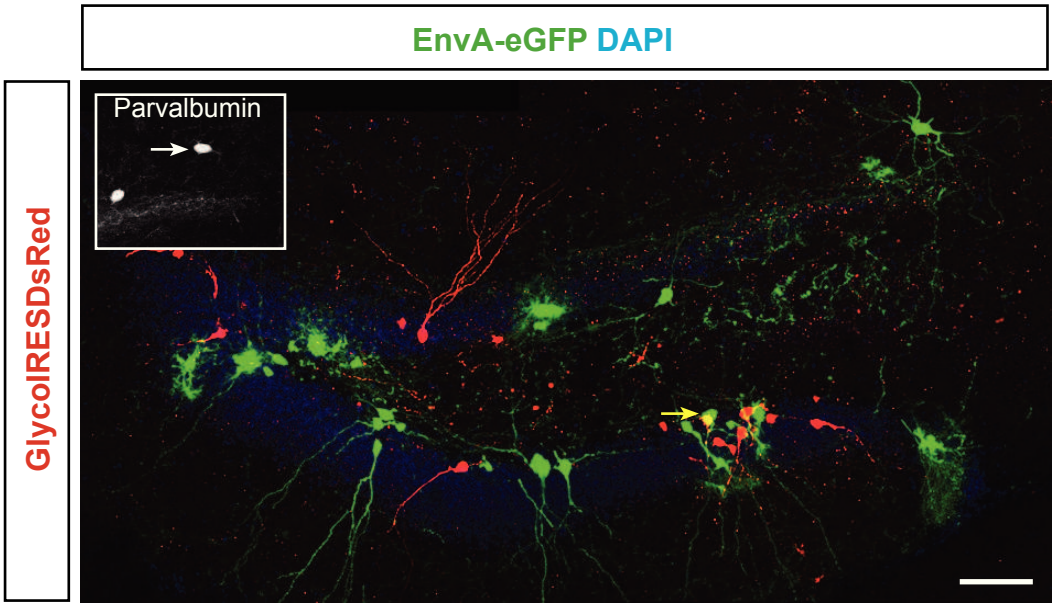

Fig. 2.33. EnvA-pseudotyped RABV-traced neurons in the dentate gyrus of hGFAP-TVA mice.
(A) Newly generated neuron transduced with *G*-encoding retrovirus and EnvA-pseudotyped RABV (yellow arrow). White arrow indicates an interneuron in the MLalso immunoreactive for parvalbumin (inset). Scale bar 50 µM. ML=molecular layer.

reminiscent of that observed in the dentate gyrus of adult C57Bl6 mice after injection of the *G*- and *TVA*-encoding retrovirus and EnvA-pseudotyped RABV (**Fig.2.14-15,18**) as well as the location, morphology and axonal arborisations of eGFP-only labelled cells suggest that they are local interneurons.

Additionally, I also observed labelling of mossy cells in the hilus (**Fig.2.34**) and eventually long-distance projections from the MS-NDB with eGFP, which were confirmed to be cholinergic in nature by immunoreactivity for ChAT(**Fig.2.35**; Deshpande et al., in preparation). These data indicate that following transcomplementation by G, transsynaptic labelling of local interneurons and long-distance projections by RABV can be clearly demonstrated in the hGFAP-TVA mice.

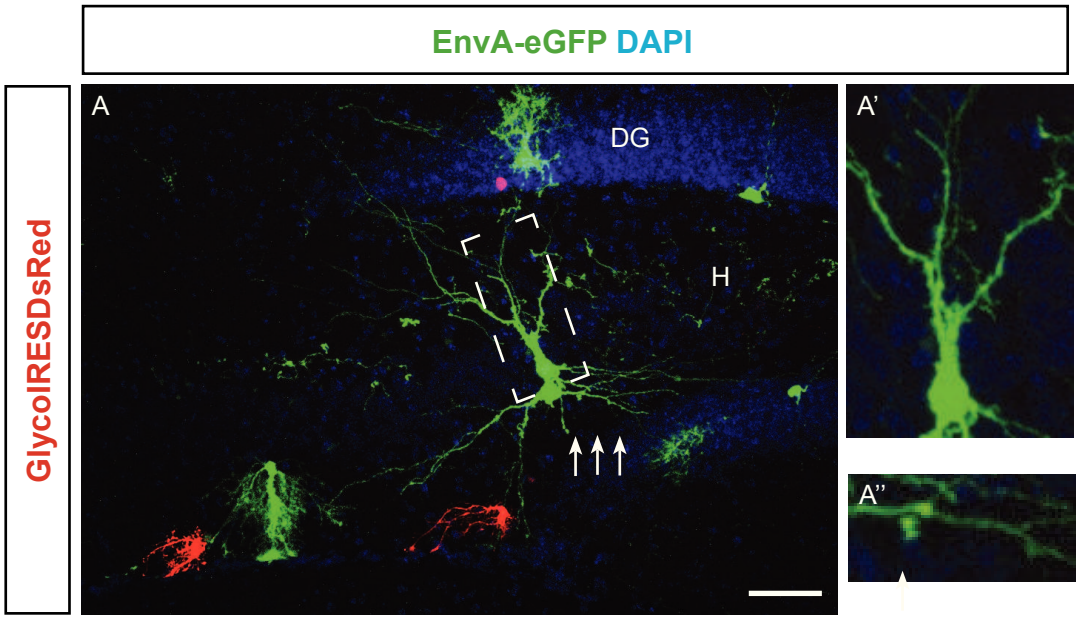

Fig. 2.34. EnvA-pseudotyped RABV-traced neurons in the dentate gyrus of hGFAP-TVA mice. (A) Two putative mossy cells labelled with eGFP alone, 3.5 weeks after G-encoding retrovirus injection and 1 week after EnvA-pseudotyped RABV injection. Magnification of the boxed area in A is shown in A'. Thorny excrescences of the putative mossy cell in A (white arrows) are enlarged in A''. Scale bar 50 µM. DG=dentate gyrus; H=hilus.

These mice can therefore be an alternative approach to study the presynaptic connectome of adult-generated granule neurons originating from aNSCs, with the added advantage of avoiding the confounding effect of pseudotransduction.

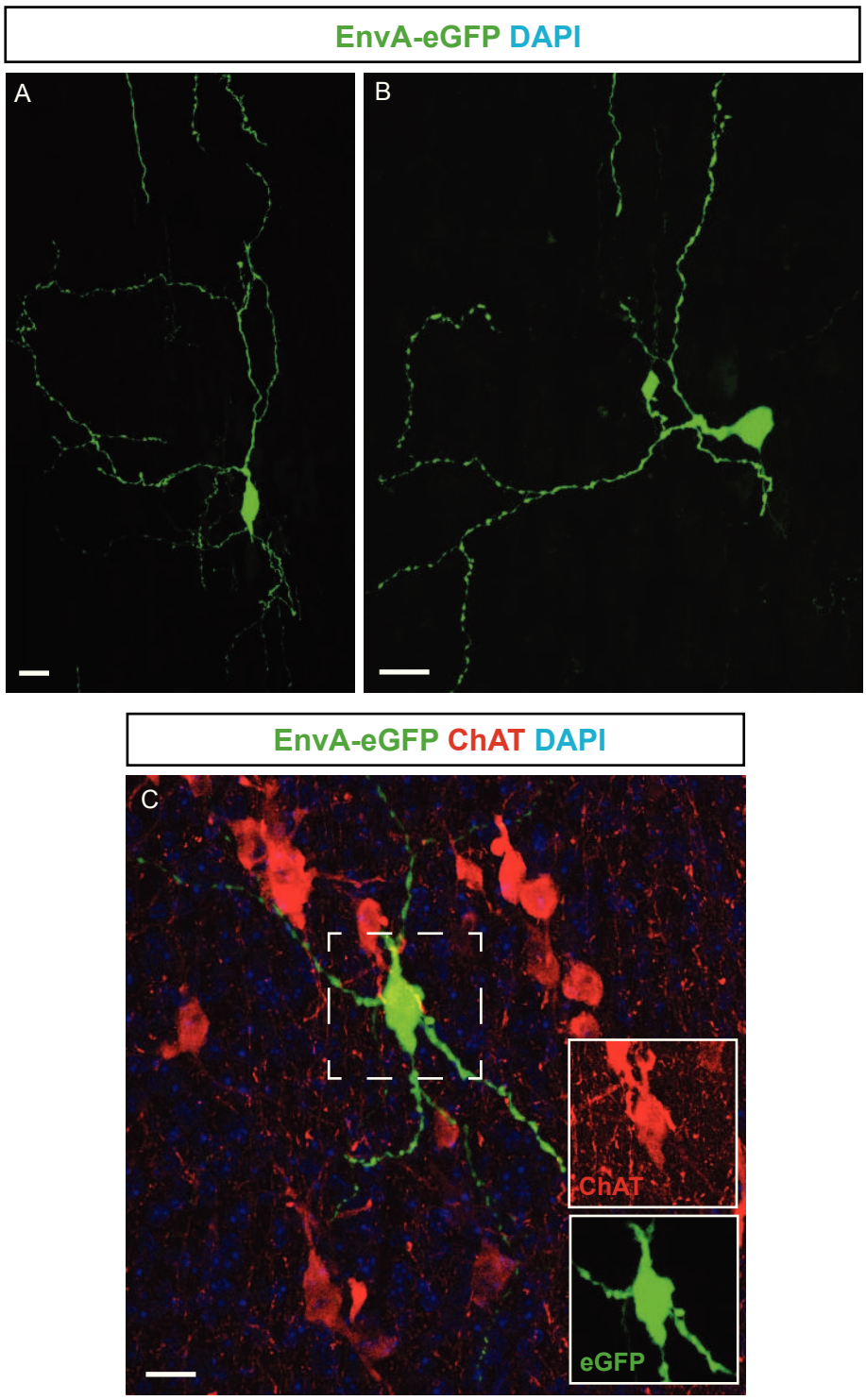

Fig. 2.35. Cholinergic projections to adult-generated neurons in hGFAP-TVA mice.
(A) Neuron in the medial septum labelled with eGFP 3.5 weeks after *G*-encoding retrovirus injection and 1 week after EnvA-pseudotyped RABV injection. (B) EnvA-pseudotyped RABV-traced neuron in the nucleus of the diagonal band of Broca. (C) Colocalization of choline acetyltransferase (ChAT) and eGFP in EnvA-pseudotyped RABV-traced neurons in the medial septum. Insets show magnified images of single channels. Scale bar 20 μM.

2.3 In vivo implementation of the monosynaptic tracing technique

2.3.1 Tracing of presynaptic partners of adult-generated neurons in the olfactory bulb

To assess the connectivity of adult-generated neurons in the olfactory bulb, I stereotaxically injected the *G*- and *TVA*-encoding retrovirus into the SEZ of the lateral ventricle of adult C57Bl6 mice (**Fig.2.36**). Progenitors in the SEZ give rise to neuroblasts that tangentially migrate along the rostral migratory stream (RMS) and ultimately differentiate into specific subtypes of interneurons in the granule cell layer (GCL) or glomerular layer (GL) of the adult olfactory bulb. After their generation in the SEZ, it takes about 6 days for the neuroblasts migrating along the RMS to reach the olfactory bulb. Taking advantage of this fact, the RABV was injected into the RMS 4 days after retrovirus injection in the SEZ (**Fig.2.36**). The objective was to target the retrovirus-infected neuroblasts, expressing TVA and G, with EnvA-pseudotyped RABV

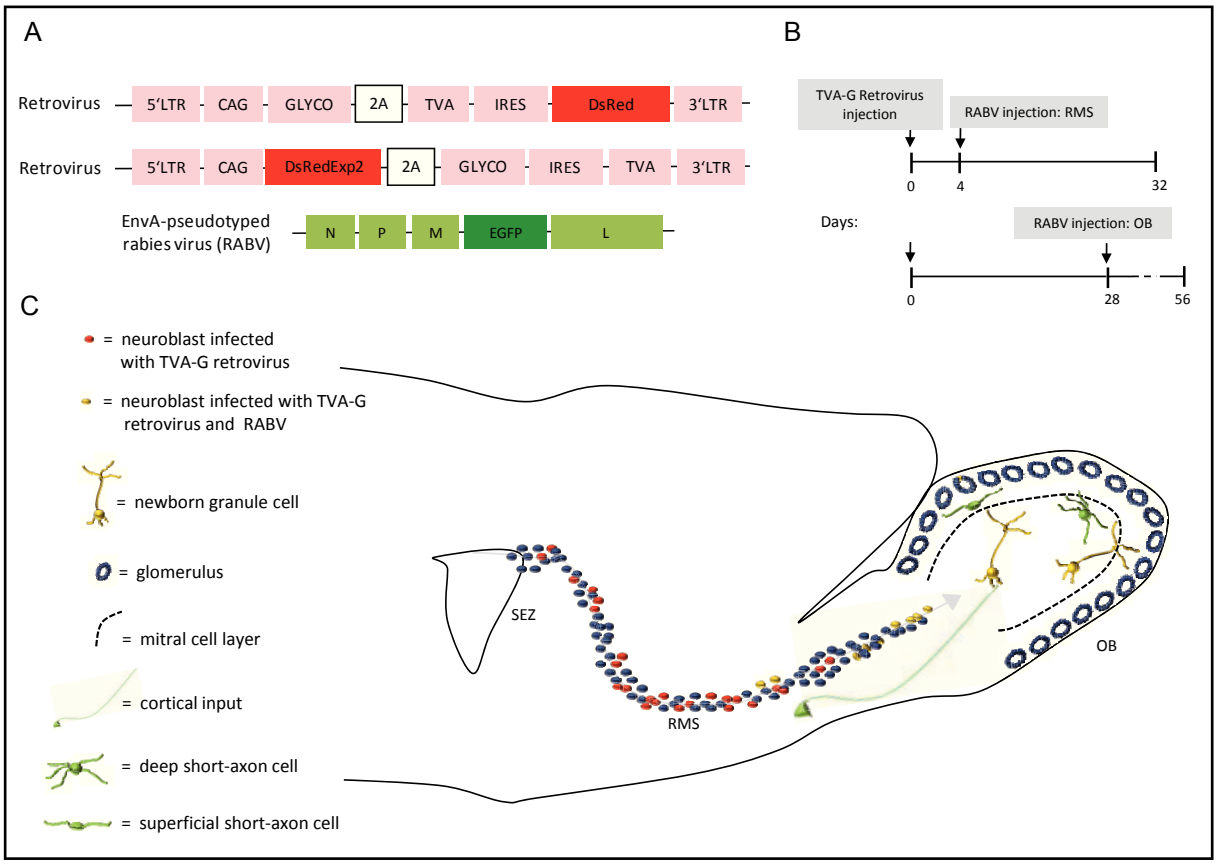

Fig. 2.36. Implementation of the tracing technique in the adult olfactory bulb.
(A) Viral constructs. (B) Injection time points employed in the adult olfactory system. (C) Scheme of sequential virus delivery: (1) Injection of retrovirus into the SEZ, followed by EnvA-pseudotyped RABV infection of migrating neuroblasts in the RMS; (2) Injection of retrovirus into the SEZ, followed by EnvA-pseudotyped RABV injection in the OB. SEZ=subependymal zone; RMS=rostral migratory stream; OB=olfactory bulb.

as they migrated along the RMS. On reaching the olfactory bulb and differentiating into either granule cells or periglomerular cells (PGC), the EnvA-pseudotyped RABV would be transported to presynaptic partners of these neurons via transcomplementation of G (**Fig.2.36**). In a second injection paradigm, the *G*- and *TVA*-encoding retrovirus was stereotactically injected into the SEZ and EnvA-pseudotyped RABV was delivered directly into the olfactory bulb, at 28 or 56 days after retroviral injection, aiming at EnvA-pseudotyped RABV infection of presynaptic partners of adult-generated neurons upon their integration in the olfactory bulb (Deshpande et al., in preparation; **Fig.2.36**).

In both injection paradigms, granule cells in the olfactory bulb transduced with *G*- and *TVA*-encoding retrovirus and EnvA-pseudotyped RABV were observed (**Fig.2.37**). Occasionally, double-transduced neurons in the GL were also observed (**Fig.2.38**).

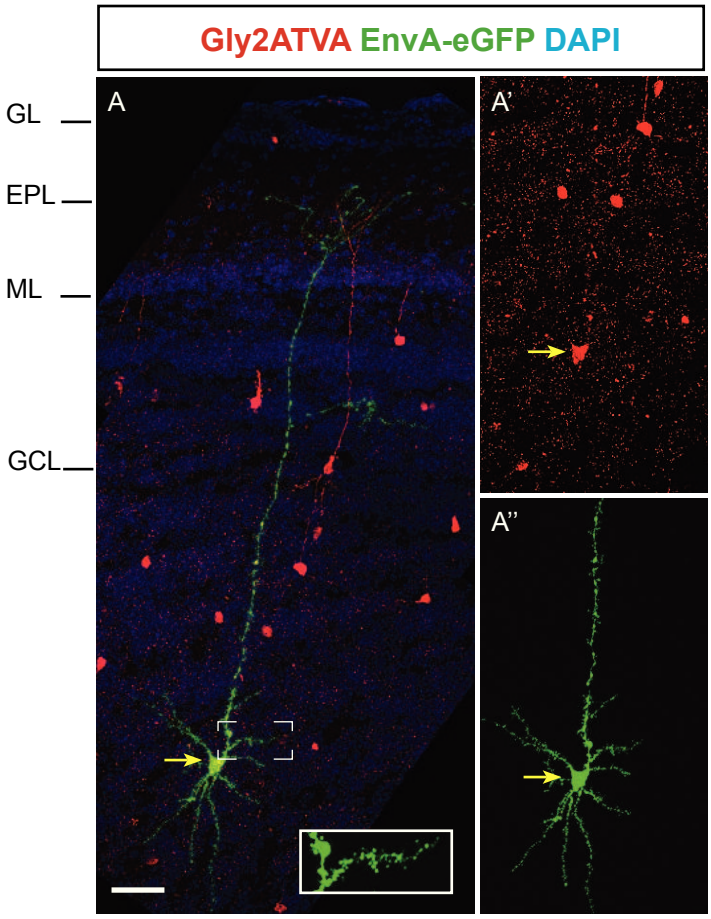

Fig. 2.37. Adult-generated granule cells in the olfactory bulb.
(A) Example of a newborn granule cell (yellow arrow) in the GCL, transduced with the *G*- and *TVA*-encoding retrovirus and EnvA-pseudotyped RABV. Inset shows the magnified image of the spiny basal dendrite of the newborn cell (boxed area). Panels A' and A'' show single channel images of the granule neuron in A. Scale bar 50 μM. GL=glomerular layer; EPL=external plexiform layer; ML=mitral cell layer; GCL=granule cell layer.

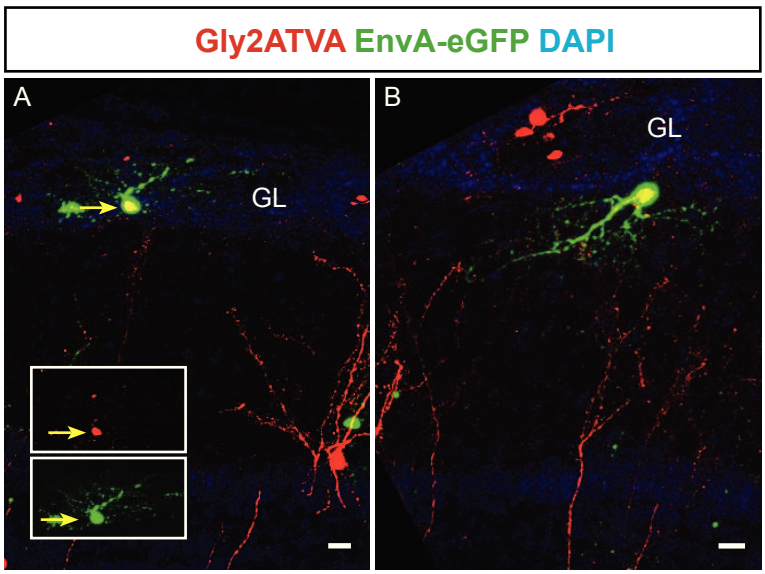

Fig.. 2.38. Adult-generated periglomerular cells in the olfactory bulb.
(A) Example of a newborn periglomerular cell (yellow arrow) in the GL, transduced with the *G*- and *TVA*-encoding retrovirus and EnvA-pseudotyped RABV. Insets show the enlargements of single channel images of the newborn neuron. (B) Another example of a newborn periglomerular cell in the GL. Scale bar 20 μM. GL=glomerular layer.

Notably, eGFP-only labelled neurons both in the GCL and the GL exhibiting an interneuron morphology were observed, suggesting transsynaptic spread from adult-generated granule cells or PGCs to their respective presynaptic partners (**Fig.2.39**). The morphplogy of these eGFP only-labelled local neurons is similar to that of short-axon cells which form a major population of inhibitory interneurons in the olfactory bulb. For example, the large, stellate cell bodies and multipolar dendrites of some eGFP-labelled cells bear a striking resemblance to deep short-axon cells such as Blanes cells that are known to innervate granule cells (**Fig.2.39,40**). Besides these, there were different types of eGFP only-labelled neurons in the GCL, internal plexiform layer, external plexiform layer and even GL (**Fig.2.41**). Their morphology was markedly different from mitral or tufted cells indicating that they probably belong as well to the rather heterogeneous category of short-axon cells.

However, conspicuous by the absence of their labelling were the principle neurons of the olfactory bulb, mitral and tufted cells. Granule cells and PGCs form dendrodendritic reciprocal synapses in the external plexiform layer with the lateral dendrites of mitral cells and tufted cells in the olfactory bulb (Shepherd, 2003). There were no EnvA-

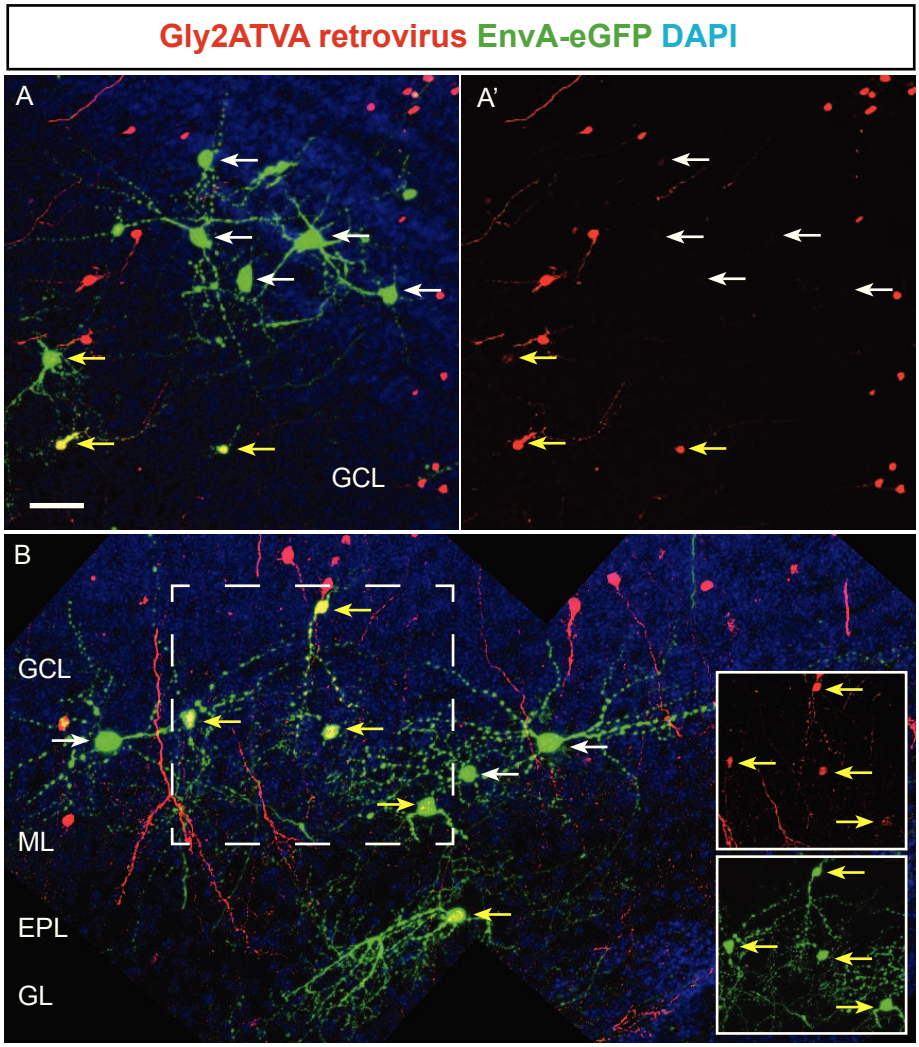

Fig. 2.39. EnvA-pseudotyped RABV-traced neurons in the olfactory bulb.
(A) Example of EnvA-pseudotyped RABV-traced neurons (white arrows) in the GCL. Several newborn neurons double transduced with retrovirus and RABV can also be seen in the same field (A'; yellow arrows). (B) Examples of EnvA-pseudotyped RABV-traced (white arrows) and newly generated neurons (yellow arrows) in the olfactory bulb. Insets show single channel images of the newborn neurons (boxed area). Scale bar 50 μM. GL=glomerular layer; EPL=external plexiform layer; ML=mitral cell layer; GCL=granule cell layer.

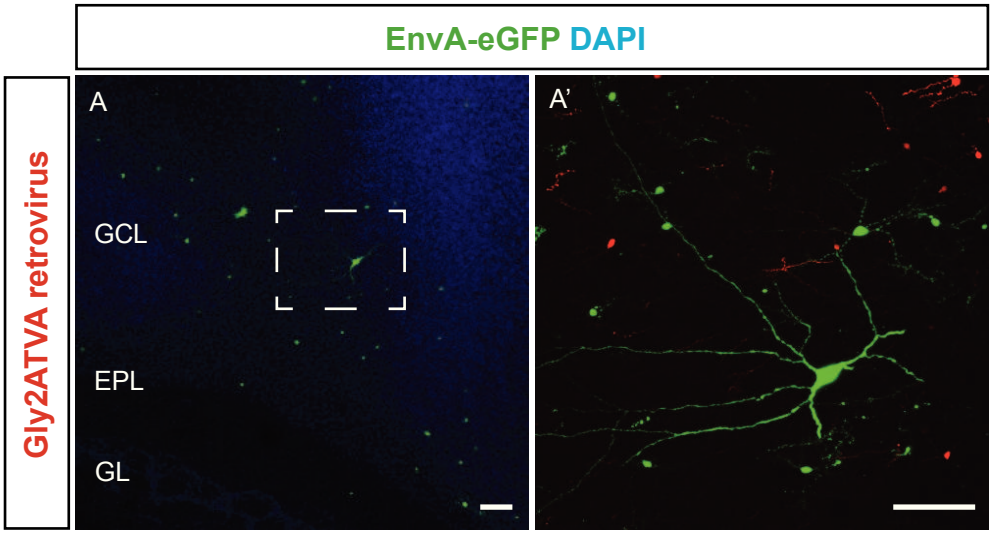

Fig. 2.40. EnvA-pseudotyped RABV-traced neurons in the olfactory bulb.
(A) Overview of transsynaptic tracing in the GCL. Magnification of the boxed area in A is shown in A'. The eGFP only-labelled neuron with a large cell body and multiple dendrites closely resembles a deep short-axon cell in morphology. Scale bar 100 μM. GL=glomerular layer; EPL=external plexiform layer; ML=mitral cell layer; GCL=granule cell layer.

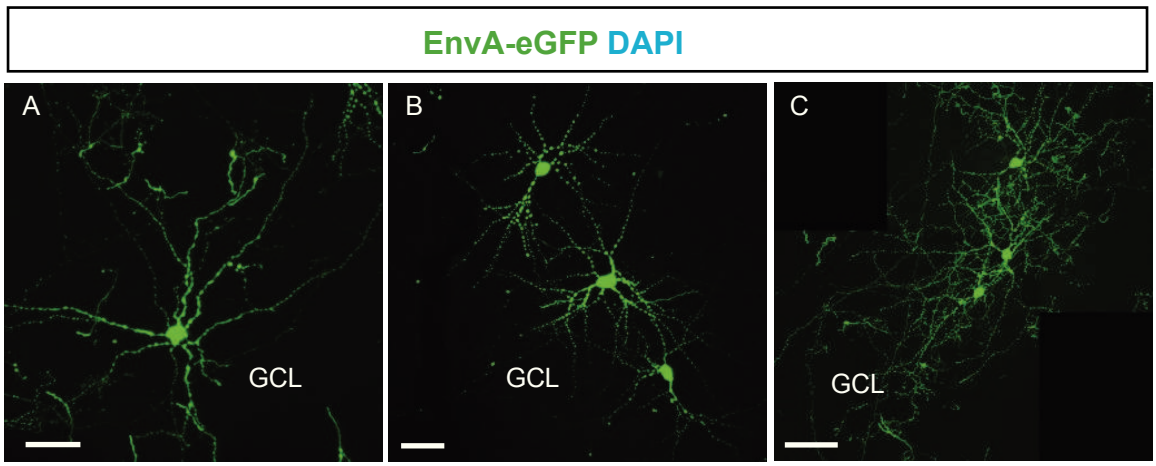

Fig. 2.41. EnvA-pseudotyped RABV-traced neurons in the olfactory bulb.
(A-C) Examples of EnvA-pseudotyped RABV-traced neurons in the GCL. Morphologically they look similar to short-axon cells. Scale bar 50 μM. GCL=granule cell layer.

pseudotyped RABV-labelled mitral cells or tufted cells even after extended periods following EnvA-pseudotyped RABV injection into the RMS or olfactory bulb (**Fig.2.42**).

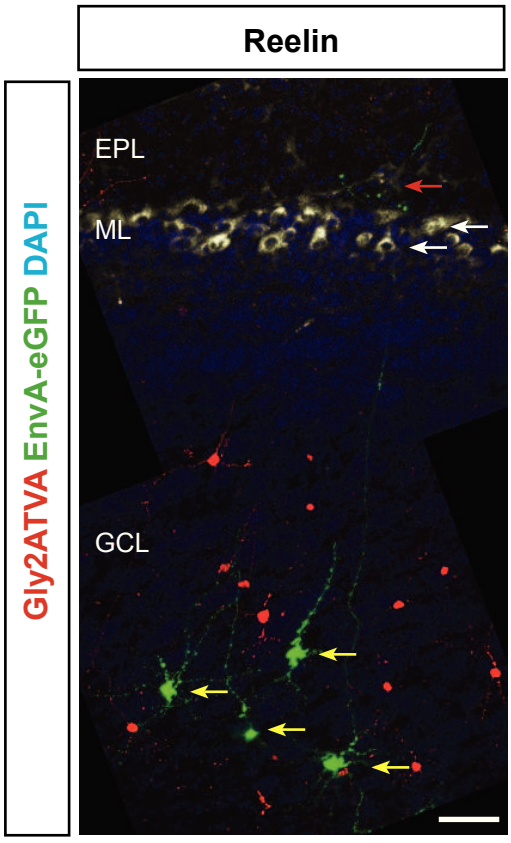

Fig. 2.42. Absence of mitral cell labelling by RABV.
Newly generated granule neurons in the olfactory bulb labelled with *G*- and *TVA*-encoding retrovirus and EnvA-pseudotyped RABV (yellow arrows) extending their dendrites to the EPL (red arrow) where they form dendrodendritic synapses with mitral cells. Mitral cells (white arrows) are labelled with specific marker Reelin. Scale bar 50 μM. GCL=granule cell layer; ML=mitral cell layer; EPL=external plexiform layer.

It has been suggested that new granule cells receive glutamatergic input either from the axon collaterals of mitral/tufted cells or from centrifugal fibres. Moreover, immunohistochemical and electron microscopical studies showing centrifugal fibres synapsing onto newborn granule cells in the olfactory bulb suggest that centrifugal inputs to the olfactory bulb form the first synapses onto newborn granule cells (Whitman and Greer, 2007). But the origin of these fibres remains unclear. Both injection paradigms in the olfactory bulb resulted in labelling of neurons ,with eGFP, in the anterior olfactory nucleus (AON) and the piriform cortex which are known to innervate granule cells via axodendritic synapses (**Fig.2.43**). These results confirm that newborn bulbar interneurons are targets for corticofugal control by neurons in the AON and piriform cortex.

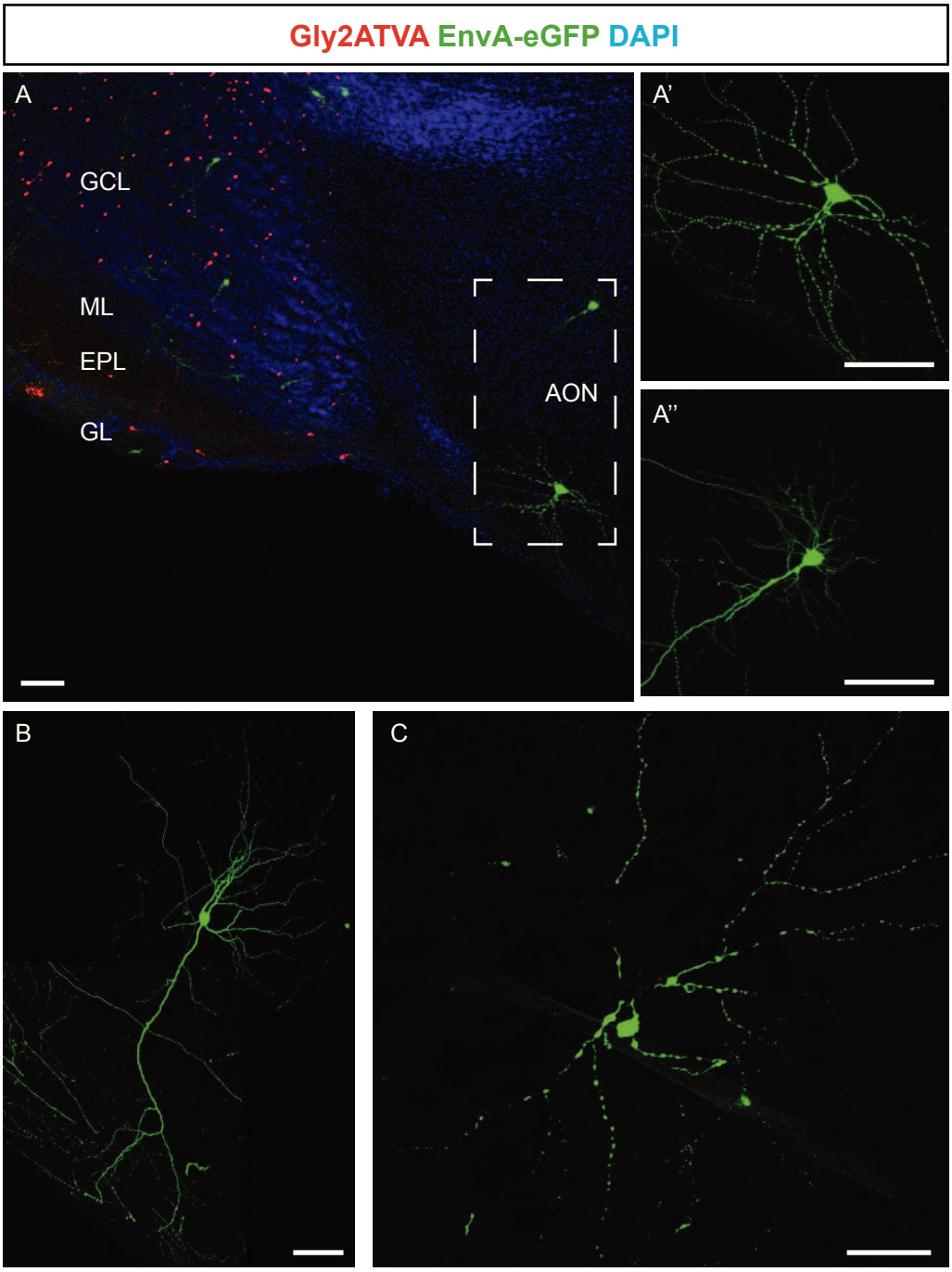

Fig. 2.43. Monosynaptically traced long-distance projections to adult-generated neurons in the olfactory system.
(A) Overview of *G*- and *TVA*-encoding retrovirus and EnvA-pseudotyped RABV injection in the olfactory system. Boxed area depicts neurons in the anterior olfactory nucleus (AON) transsynaptically labelled with EnvA-pseudotyped RABV. A'-A'' show magnified images of the boxed area in A. Scale bar 100 µM. (B) High power magnification of an EnvA-pseudotyped RABV-traced neuron in the AON. (C) Example of an EnvA-pseudotyped RABV-traced neuron in the piriform cortex. Scale bar 50 µM. GL=glomerular layer; EPL=external plexiform layer; ML=mitral cell layer; GCL=granule cell layer.

3 Discussion

The above work describes a novel retrovirus-based approach to target adult-generated neurons for primary RABV infection and retrograde transfer to study the presynaptic connectome of newborn neurons in the adult dentate gyrus and olfactory bulb in vivo. Establishing this seemingly straightforward technique presented with several challenges and tested the effectiveness of RABV as a transneuronal tracer as well as provided some useful insights into the integration of newborn neurons into the adult neuronal circuits.

3.1 Rabies virus to reveal the presynaptic connectome of adult-generated neurons

The main advantage of this monosynaptic tracing technique is the specificity of the EnvA-pseudotyped RABV for infecting not only the targeted cell population but also for retrogradely spreading exclusively to synaptically connected neurons. Furthermore, retrovirus mediated-delivery of *TVA* and *G* ensures stable transduction specifically of adult-born neurons and retains their expression throughout maturation. This permits tracing of presynaptic partners of newborn neurons at any time during their maturation by introducing the EnvA-pseudotyped RABV. In this regard, injecting the EnvA-pseudotyped RABV into neural progenitors or neurons at different stages following their birth revealed increasingly diverse populations of presynaptic partners suggestive of the gradual incorporation of adult-generated neurons into functional neural circuits.

However, this technique, robust and reliable as it is, has its limitations which to a certain extent can be overcome by tweaking the experimental design. Firstly, very few transsynaptically labelled neurons were observed in both systems indicating an

undersampling of presynaptic neurons, as was observed also in other monosynaptic tracing studies (Callaway, 2008; Marshel et al., 2010). One explanation for this could be the level of activity in neuronal networks. It is currently not known if the EnvA-pseudotyped RABV has a greater competence for propagating across active synapses compared to inactive ones. This caveat makes the monosynaptic tracing technique a qualitative rather than quantitative method. Increasing sensory stimulation by enriched environments may increase the basal level of neuronal activity and it would be interesting to apply this technique in this context to increase the number of presynaptic inputs labelled. Even so, it should be noted that sparse projections had strongly eGFP-positive cells due to the replication competence of EnvA-pseudotyped RABV. Secondly, there seems to be a clear bias in the transsynaptic transfer of RABV with respect to the type of synapse involved as demonstrated by the absence of eGFP-labelling of mitral or tufted cells (discussed later). Transfer across axodendritic synapses, however, was found to occur specifically, regardless of the GABAergic or glutamatergic nature of their neurotransmitters.

3.1.1 Specificity of retrovirus and RABV-based monosynaptic tracing: the pseudotransduction conundrum

Construction of a retrovirus encoding *TVA* but lacking *G* and stereoractically injecting it into the dentate gyrus of 8-10 week old C57Bl/6 mice, followed by a second injection with EnvA-pseudotyped RABV resulted in the labelling of local interneurons (as assessed by their morphology, location and axonal distribution) with eGFP which was unexpected because retrograde transsynaptic transport of RABV is strictly dependent on G. Further investigation into this perplexing result led back to the VSVG-coated retrovirus that had been used to introduce TVA into newborn neurons. Pseudotyping a retrovirus (or lentivirus) with VSVG renders it pantropic, resistant to ultracentrifugation and freezing (Lever et al., 2004). However, using a VSVG-pseudotyped virus also results in substantial occurrence of pseudotransduction which may be due to translation from the unintegrated viral mRNA or due to protein transfer, i.e., proteins produced from the transgenes in the packaging cells that are delivered via retroviral particles to the infected cell (Haas et al., 2000). The duration of protein expression depends on the stability of

the transduced mRNA (or protein) and on the infected cell type (Haas et al., 2000), although it has been speculated in one study on neutrophils that the pseudotransduced proteins may be non-functional (Geering et al., 2011). This was not the case in the present study as it led to the appearance of 'mislabelled' eGFP-positive interneurons. The VSVG-coated retrovirus encoding *TVA* may have infected local interneurons in the dentate gyrus and either released the TVA protein into the cytosol or expressed it from the unintegrated viral mRNA, which got transported to the cell membrane rendering these interneurons susceptible to primary EnvA-pseudotyped RABV infection. This, combined with the fact that even low levels of TVA are sufficient to allow infection by EnvA-pseudotyped RABV led us to hypothesize that some of the interneurons labelled in our experiments with the *TVA*-encoding retrovirus and EnvA-pseudotyped RABV, were most likely due to pseudotransduction of TVA. Interestingly, the TVA produced by pseudotransduction remained stable on the plasma membrane for several weeks as direct labelling of interneurons was observed on injection of EnvA-pseudotyped RABV, 3 and even 5 weeks post retroviral injection. However, there were no detectable levels of DsRedExpress in the pseudotransduced neurons. One fact advocating the pseudotransduction hypothesis was that occurrence of 'eGFP-mislabelled' neurons was restricted to the site of injection (300-400 µM around the injected area) as opposed to ubiquitous labelling of eGFP-positive interneurons, along the septotemporal axis of the dentate gyrus, labelled by bona fide transsynaptic transport. In order to assess the amount of pseudotransduction, I compared the proportion of eGFP-labelled interneurons per double-transduced newborn granule neurons after injection of the *TVA*-encoding retrovirus with those obtained after injection of the *G*- and *TVA*-encoding retrovirus. A significantly lower proportion of eGFP-positive interneurons were present in mice injected with *TVA* retrovirus than that in mice injected with *G*- and *TVA*-encoding retrovirus. This means that a substantial proportion of interneurons labelled in our experiments with *G*- and *TVA*-encoding retrovirus is due to true retrograde transport of RABV between synaptically connected neurons. This inference is further strengthened by the fact that no long-range projections to the dentate gyrus were labelled on injecting the *TVA*-encoding retrovirus followed by EnvA-pseudotyped RABV at any time point tested.

These experiments confirmed that this strategy does not label neurons whose axons pass through the injection site.

Nevertheless, to eliminate the possibility of pseudotransduction and to unequivocally label local interneurons, I made use of transgenic mice engineered to express *TVA* under the hGFAP promoter. This promoter is active in parenchymal astrocytes as well as in aNSCs in the dentate gyrus and SEZ. In fact, these mice have been used in a previous study to demonstrate that GFAP-positive astrocytes in the SEZ are NSCs in the adult mammalian brain (Doetsch et al., 1999). Therefore the hypothesis was that injection of the EnvA-pseudotyped RABV into the SGZ of hGFAP-TVA mice would result in labelling of GFAP-positive aNSCs and their progeny. Injection of EnvA-pseudotyped RABV alone into the dentate gyrus of these mice resulted predominantly in labelling, by eGFP, of cells in the glial lineage and Dcx-positive immature neurons. The proportion of Dcx-positive neurons increased with time indicating that it was possible to label the progeny of GFAP-positive aNSCs in the dentate gyrus. Some eGFP-labelled mature granule neurons were also observed, pointing towards a high stability of TVA on the cell membrane. This was not relevant, however, because for the transsynaptic tracing experiments, a retrovirus was used which only transduced proliferating cells. Moreover, there were no local interneurons or long-range projections labelled with eGFP. In contrast, using a *G*-encoding retrovirus in combination with EnvA-pseudotyped RABV resulted in labelling of presynaptic partners of newborn neurons in the hGFAP-TVA mice. Pseudotransduction by G is not of concern because the pseudotransduced cells expressing glycoprotein on their cell membranes would never be directly infected by EnvA-pseudotyped RABV.

Using this alternative system, it was possible to label, with eGFP, local interneurons and mossy cells as well as long distance projections. Importantly, adapting the retrovirus-based approach to hGFAP-TVA mice yielded a similar pattern of presynaptic connectivity of newborn neurons compared to wild-type mice, thus confirming the overall applicability and specificity of the RABV-based monosynaptic tracing approach.

3.2 Identifying the presynaptic partners of newborn neurons in the adult dentate gyrus

3.2.1 Local connectivity

3.2.1.1 Hilar interneurons

The dentate gyrus comprises among granule neurons, hilar mossy cells and glial cells, a variety of local interneurons known to be connected to granule neurons. They all have GABA as their primary neurotransmitter. However, they are a remarkably heterogenuous mix divided into subclasses based on the location of their cell bodies, axonal and dendritic distributions, neurochemical markers expressed and physiological characteristics (Houser, 2007; Somogyi and Klausberger, 2005). Among these are the parvalbumin positive basket cells and axo-axonic cells that form synapses on cell bodies and axon initial segments of granule neurons, respectively. The cell bodies of these interneurons are located near the GCL although some are also found at the junction of granule cell and molecular layers while their axonal arbors are restricted to the GCL. Basket cells are distinguishable by their apical dendrites that ascend along the entire length of the ML. Their terminals form inhibitory synapses with cell bodies and proximal dendrites of granule neurons (Houser, 2007). Another prominent interneuron type in the dentate gyrus is the somatostatin-expressing neurons that have their cell bodies located in the hilus while their axons arborise in the outer ML. Somatostatin terminals synapse primarily with dendrites of granule neurons (Katona et al., 1999). Many of the somatostatin-expressing interneurons in the dentate gyrus are considered to be HIPP neurons as their axonal arbors are located in the region where the perforant path fibres terminate. Hilar interneurons also express the marker, Neuropeptide Y (NPY) and there is substantial co-localization of NPY and somatostatin in the hilus (Kohler et al., 1987). Given that their axons terminate in the outer ML or in the hilus, many of the NPY-expressing interneurons could be HIPP cells (Houser, 2007). Besides these, other prominent interneuron subtypes in the dentate gyrus are the Hilar Commissural-Association pathway-associated (HICAP) cells that have their cell bodies in the hilus and project to the inner third of the ML as well as MOPP cells with their cell bodies, axonal and dendritic trees restricted to the outer ML (Halasy and Somogyi, 1993). Áccordingly,

stereotaxic injection of the *G*- and *TVA*-encoding retrovirus followed by EnvA-pseudotyped RABV in the dentate gyrus enabled the visualisation of local monosynaptic inputs of adult-generated granule neurons, from a variety of dentate interneurons. The eGFP only-positive cell bodies immunoreactive for parvalbumin were typically located at the interface of the hilus and GCL and their axonal arbor spanning the GCL strongly suggesting that they may be fast-spiking basket cells (Freund and Buzsaki, 1996). I also observed co-localization of eGFP with somatostatin and their location within the hilus and dendritic arbors indicated that they may be HIPP neurons (Freund and Buzsaki, 1996). There were also eGFP-labelled cell bodies in the ML, their morphology and location indicating that they were MOPP cells but further neurochemical characterization still remains to be completed. Notably, the number of transsynaptically labelled interneurons increased with longer duration of EnvA-pseudotyped RABV infection. However, intervals longer than two weeks between EnvA-pseudotyped RABV injection and sacrifice resulted in some toxicity in the infected cells. Labelling of interneurons was observed between 3-5 weeks after retrovirus injection (i.e. birth of granule neurons) and even earlier in some experiments, corroborating previous work showing that local interneurons provide the first source of input to newborn granule neurons (Esposito et al., 2005).

3.2.1.2 Mossy cells

The transsynaptic tracing technique also revealed another neuron type in the hilus called the hilar mossy cell that is the local source of glutamatergic input to granule neurons in the dentate gyrus via the commissural/associational pathway. Surprisingly, eGFP-labelled mossy cells were detected as early as 10 days after retrovirus injection indicating that the first glutamatergic inputs to adult-born granule neurons may arise from hilar mossy cells while those from the entorhinal cortex appear only later. The mossy cell axons project to the ipsilateral and contralateral inner ML and also have collaterals in the hilus (Ribak et al., 1985). Although there were no eGFP-labelled mossy cells in the contralateral dentate gyrus, the ipsilateral dentate gyrus had several eGFP-labelled, large mossy cells, readily distinguishable by their triangular or multipolar cell bodies with thorny excrescences, which are large and complex spines present on their proximal dendrites (Amaral et al., 2007). These results indicate that the RABV can propagate across GABAergic as well as glutamatergic synapses.

3.2.1.3 Glial cells

The appearance of eGFP-positive astrocytes along dendrites of double-transduced granule neurons and oligodendroglia in the fimbria fornix indicate that there exist glia-neuron interactions that allow the transport of RABV. Astrocytes, via perisynaptic processes, can integrate and process synaptic information and control or modulate synaptic transmission and plasticity (Santello et al., 2012). It has been hypothesized that astrocytic perisynaptic processes may be involved in the development of dendritic spines on newborn granule neurons and that gliotransmission may assist in the synaptic integration of these neurons (N. Toni, personal communication). The presence of eGFP-positive astrocytes around newborn granule neurons suggests that astrocytic perisynaptic processes might play an important role in adult neurogenesis, however further investigation is required to ascertain this.

3.2.2 Influence of local interneurons and mossy cells on adult neurogenesis

Given that different types of GABAergic interneurons reside within the dentate gyrus in close proximity to aNSCs and have dendritic and axonal distribution restricted to its boundaries, it would not be too forward to consider that they may play an important role in the regulation of adult neurogenesis. Indeed, several studies have demonstrated the role of GABA in the proliferation and differentiation of type-2 cells that are the progeny of aNSCs in the dentate gyrus. Tonic GABA was shown to regulate hippocampal neurogenesis by demonstrating decreased proliferation in the dentate gyrus of mice lacking the $GABA_A$ receptor subunit $\alpha 4$, responsible for generating tonic inputs (Tozuka et al., 2005). Also, GABAergic input to Nestin-positive cells in the adult hippocampus has been shown to promote neuronal differentiation. The calcium influx generated by the depolarizing action of phasic GABA has been shown to stimulate the expression of proneural gene, NeuroD (Tozuka et al., 2005). There is some evidence that GABA may promote maturation of adult-generated dentate granule neurons by stimulating dendrite growth and spine density. Studies have shown that immature granule neurons treated with a $GABA_A$ receptor antagonist have shorter dendrites and decreased spine density (Sun et al., 2009) as opposed to neurons treated with a $GABA_A$ receptor agonist

which have longer dendrites (Ge et al., 2006). Although enough evidence points to the importance of GABA for regulation of adult neurogenesis, virtually nothing is known about the source of this GABA. For example, it has been suggested that stimulation of basket cells enhances tonic currents in adult-generated granule neurons (Ge et al., 2006) while another study suggested that neurogliaform cells or Ivy interneurons provide the initial source of GABAergic signalling to newborn neurons in the adult hippocampus (Markwardt et al., 2009). Recently it was demonstrated that tonic GABA released by parvalbumin-positive interneurons, in the adult dentate gyrus, maintained the quiescence of aNSCs and inhibited symmetrical self-renewing as well as astrogliogenic divisions through $GABA_A$ receptors containing the γ_2 subunit (Song et al., 2012). This regulation persisted under normal physiological conditions and in response to specific experiences. Since parvalbumin-positive interneurons are under direct modulation by dentate granule cells and by entorhinal cortex cells, the authors suggest that the parvalbumin interneuron-mediated coupling of local circuit activity to aNSC regulation may be an adaptive mechanism where high circuit activity maintains aNSCs quiescent while a decrease in neuronal activity propels them into activation (Song et al., 2012).

Modulation of interneurons by the inputs they receive in turn influences their inhibition of granule neurons. One such regulatory mechanism is the feed-forward inhibition of granule neurons, mediated by several types of interneurons. Distal dendrites of parvalbumin-positive interneurons (basket cells) are located in the outer two-thirds of the ML which harbors the afferents to the dentate gyrus, arising mainly from the entorhinal cortex. These interneurons are suitably positioned to provide feed-forward inhibition to the granule neurons, in response to excitatory inputs to their dendrites in the ML (Houser, 2007). MOPP cells that receive input directly from the entorhinal cortex are also known to provide feed-forward inhibition to granule neuron dendrites in the ML as their cell bodies and dendrites are ideally located to receive input from the perforant path (Ferrante et al., 2009). In addition to feed-forward inhibition, cell bodies of HIPP and HICAP cells are located in the hilus and they receive considerable input from granule neurons, providing feedback-inhibition of dentate granule neurons (Houser, 2007). Similarly, parvalbumin-positive interneurons (basket cells) are innervated by axon

collaterals of mossy fibres on their cell bodies and proximal dendrites, thus providing strong feedback inhibition of the granule neurons (Amaral et al., 2007; Houser, 2007) .

The role of mossy cells in modulating adult neurogenesis is not yet clear however it has been speculated that they are responsible for increasing the activity of granule neurons generated after status epilepticus (Pierce et al., 2007). Survival and integration of new neurons has been shown to be dependent on activation of NMDARs by glutamate, typically in the second to third week after neuronal birth (Tashiro et al., 2006). This time window coincides with the appearance of mossy cells in the monosynaptic tracing experiments in wild-type as well as hGFAP-TVA mice, suggesting that these cells might be the source of glutamate mediating NMDAR activation. Besides regulation of neurogenesis, hilar interneurons and mossy cells could also be involved in regulating the function of adult-generated neurons such as the proposed role of HIPP cells and mossy cells in the dynamic regulation of pattern separation (Myers and Scharfman, 2009). The RABV-based monosynaptic tracing technique allowed for the identification of different types of interneurons that directly innervate adult-generated granule neurons consistent with the GABA-dependent regulation of adult neurogenesis and possibly other functions as well as mossy cells as immediate presynaptic partners of newborn neurons.

3.2.3 Long-distance projections

Longer time intervals between retrovirus and EnvA-pseudotyped RABV injections (i.e. allowing further maturation of newborn granule neurons) allowed labelling of several long-range projections of dentate granule neurons. Long distance afferent input to the dentate gyrus arises from several different regions. These afferents regulate the activity of the dentate gyrus by influencing granule neurons, interneurons and progenitors. The major intrahippocampal long-range projection to dentate gyrus originates from the entorhinal cortex, the axons of which innervate granule neurons and form excitatory glutamatergic synapses onto their dendrites in the upper two-thirds of the ML (Amaral et al., 2007). The entorhinal cortex is a six layered structure, subdivided into lateral and medial entorhinal cortex (LEC and MEC, respectively). Fibres originating in the LEC

terminate in the outer one-third of the dentate ML and those from the MEC terminate in the middle one-third. Axons of neurons in the entorhinal cortex project to the ipsilateral dentate gyrus via the perforant path. These neurons are located almost exclusively in layer 2 of the entorhinal cortex (Witter, 2007). The perforant path is the first component of a trisynaptic, supposedly unidirectional loop that links the dentate gyrus, CA3 and CA1 subfields together. In the RABV-based transsynaptic tracing experiments, labelling of cells was observed exclusively in layer 2 of the entorhinal cortex (as identified by the location of the neurons in the entorhinal cortex). Notably, consistent with previous studies (Toni et al., 2007), labelling of this afferent system was observed only at the latest time point assessed, i.e., at least 5 weeks after the birth of dentate granule neurons.

Rabies virus-mediated transsynaptic tracing technique also identified a potentially novel afferent input to newborn granule neurons, originating in the subiculum. The subicular complex is a part of the hippocampal formation consisting of the subiculum, presubiculum and the parasubiculum (O'Mara, 2005). Using the anterograde neuronal tracer, Phaseolus vulgaris leucoagglutinin (PHA-L), it was demonstrated that fibres originating in the presubiculum and parasubiculum send a minor projection to the ML of the DG, interspersed between the lateral and medial perforant path projections (Kohler, 1985). The nature of postsynaptic neurons or the neurotransmitters used was however not known. The subicular complex receives input from the CA1 field of the hippocampus, the entorhinal cortex, hypothalamic nuclei, medial septum/nucleus of the diagonal band, anterior thalamic nuclei and minor projections from the brainstem. It, in turn, projects to many cortical and subcortical targets (O'Mara, 2005) and therefore, is considered a major output of the hippocampus. Retrograde tracing using EnvA-pseudotyped RABV revealed a subicular-dentate monosynaptic connection, suggesting that the subiculum may in fact be a presynaptic partner of adult-generated granule neurons. The subiculum has been implicated to play a role in spatial navigation, memory processing and control of response to stress (O'Mara, 2005). In light of the emerging role of newborn neurons in spatial learning, memory consolidation and mood regulation, it may be possible that the subicular projection to the dentate gyrus plays a role in modulating the function of adult-generated neurons. Therefore, it would be interesting to investigate the precise

nature of the subicular-dentate projection in order to better understand its functional implications.

The dentate gyrus also receives subcortical afferent inputs originating in the basal forebrain, namely, MS-NDB, the ventral tegmental area (VTA), locus coeruleus and the raphe nucleus (Amaral et al., 2007). There are two types of afferents originating in the MS-NDB, terminating on different cell types in the dentate gyrus. The cholinergic afferents preferentially innervate the dentate granule neurons while the GABAergic neurons terminate on interneurons (Leranth and Hajszan, 2007). Moreover, nicotinic AchRs are known receptors of RABV at the neuromuscular junction (Jackson and Wunner, 2007). Consistent with this, the RABV-based tracing technique labelled cholinergic (but not GABAergic) projections arising from the MS-NDB, indicating that cholinergic synapses in the CNS are also amenable to RABV propagation. However, no eGFP labelling was observed in the brainstem inputs such as those originating from the raphe nuclues, locus coeruleus or the VTA. The reasons for this could be (i) nature of neurotransmitter release at the terminal or (ii) inability of RABV for transsynaptic transfer at specific synapses. A previous study using the CVS strain of RABV to identify neurons involved in the olfactory pathway, described that the virus did not label neurons in the locus coeruleus, the source of noradrenergic fibres to the olfactory bulb and only weakly labelled the serotonergic afferents arising in the raphe nucleus (Astic et al., 1993). The authors argue that noradrenergic terminals are non-permissive to RABV transsynaptic transfer and also that the virus has low infection capacity for serotonergic fibres arising from raphe nucleus (Astic et al., 1993). The RABV G used in RABV-mediated monosynaptic tracing experiments belongs to the CVS strain, it might potentially explain the absence of labelling in the locus coeruleus and raphe nucleus. Moreover, it is known that axons of one class of neurons originating in the raphe nucleus release serotonin at non-synaptic sites, acting on neurons expressing 5-HT-1/2 receptors (Kosofsky and Molliver, 1987) while the axons of a second type of neuron forms synapses with GABAergic interneurons that express the 5-HT3 receptors (Halasy et al., 1992). The VTA provides a sparse dopaminergic input to the dentate gyrus. Dopamine fibres are found in close proximity of aNSCs and different cell types in the dentate gyrus respond to dopamine

by activation of distinct receptors (D1-D5), the exact mechanisms for which are not fully elucidated (Leranth and Hajszan, 2007). However, absence of labelling of neurons in the VTA in the RABV-mediated tracing technique may suggest that dopamine may be indirectly influencing newborn dentate granule neurons.

3.2.4 Role of afferents in adult neurogenesis

Neurotransmitters released by the afferent systems to the dentate gyrus have been shown to regulate the activity of aNSCs and also the integration of newborn neurons into the existing circuitry. As dentate granule neurons receive major excitatory innervations from the entorhinal cortex, glutamate plays an influential role in modulating adult neurogenesis at several levels. Cameron et al (1995) showed that NMDAR activation had a negative effect on proliferation of aNSCs while treatment with NMDAR antagonists or lesions of the entorhinal cortex increased the birth of neurons in the GCL (Cameron et al., 1995). It has also been shown that survival of newborn dentate granule neurons is competitively regulated by the relative levels of NMDAR activation (Tashiro et al., 2006). Furthermore, the influence of NMDAR activation on newborn neuron survival was restricted to the third week after birth, a critical period associated with synapse formation (Tashiro et al., 2006). Additionally, NMDAR-dependent plasticity of adult-born granule neurons, mediated by the NR2B subunit, has been shown to be important for fine contextual discrimination which supports the proposed role of dentate granule neurons in pattern separation (Kheirbek et al., 2012).

Influence of acetylcholine on adult neurogenesis was demonstrated by lesions in the basal forebrain cholinergic system which led to impaired dentate neurogenesis (Mohapel et al., 2005). Activation of the α7-nicotinic AchR has been reported to be critical in regulating the conversion of GABA-induced depolarization into hyperpolarization in adult-born neurons, which is in turn required for switching the initially excitatory action of GABA into an inhibitory one. Adult-generated neurons in mice lacking the α7-nicotinic AchR have severely truncated dendritic arbors in addition to a prolonged depolarizing chloride gradient (Campbell et al., 2010). One of the earliest connections observed in the EnvA-pseudotyped RABV-based tracing technique were cholinergic projections

arising from the MS-NDB, about 10-14 days after retrovirus injection, a time window coinciding with the acetylcholine-mediated reversal of the chloride gradient underlying the GABA switch (Deshpande et al., in preparation). Our study is the first to visualize the cholinergic projection from the MS-NDB onto adult-generated neurons and our data corroborates with other studies implicating nicotinic receptors in the development of adult-born neurons.

The effect of serotonin on neurogenesis is well known by several studies on antidepressant treatments (Santarelli et al., 2003). Serotonin is mainly produced by neurons in the brainstem raphe nuclei and is known to activate several receptors, most of which are expressed in the dentate gyrus. Serotonin is thought to regulate neurogenesis via 5-HT-1A receptors - agonists of 5-HT-1A have been shown to increase the number of BrdU-labelled cells in the rat dentate gyrus (Santarelli et al., 2003), while antagonists of 5-HT-1A reduced the number of newborn dentate granule neurons by about 30% (Radley and Jacobs, 2002). Other serotonin receptors that might be involved in serotonin-mediated increase in neurogenesis are 5-HT-4, 5-HT-6 and 5-HT-7 (Duman et al., 2001). All of them seem to act on neurogenesis indirectly by activating the cAMP-CREB cascade leading to increase in levels of BDNF. Brain DNF then may increase the release of serotonin thereby stimulating neurogenesis through increased activation of 5-HT-1A receptors (Duman et al., 2001). Since serotonin receptors are present on different cell types in the hippocampus, serotonin might not be acting directly on newborn granule neurons to regulate neurogenesis. The absence of labelling by the monosynaptic tracing technique of serotonergic neurons in the raphe nuclei is consistent with an indirect effect of serotonin on neurogenesis in the dentate gyrus.

Despite of the huge variety of neurotransmitters, the receptors and several pathways of regulation, the afferent connection to the dentate gyrus stems from a small number of neurons that terminate on a specific population of neurons, to exert their effects. The RABV-mediated transsynaptic tracing technique successfully allowed for the identification of some of these direct afferent systems to adult-born neurons while it is likely that some neuromodulatory afferents were in fact not labelled due to limitations of the technique.

In summary, the development of the presynaptic connectome of adult-generated neurons in the dentate gyrus of C57Bl6 as well as hGFAP-TVA transgenic mice exhibited a precise temporal pattern with local interneurons and mossy cells forming the first connections, followed by afferent innervation from the MS-NDB and finally glutamatergic innervation from the entorhinal cortex (**Fig.3.1**). The gradual incorporation of newborn neurons into the pre-existing circuits observed in this study further supports the notion that integration of adult-generated neurons is a highly regulated process that ensures the survival of only those neurons that have correctly integrated. This step-wise incorporation may have evolved to ascertain that the recruitment of newborn dentate gyrus granule neurons into the hippocampal trisynaptic circuit occurs only when they have reached functional maturity at the cellular level and have been incorporated accurately into the local circuit (Deshpande et al., in preparation).

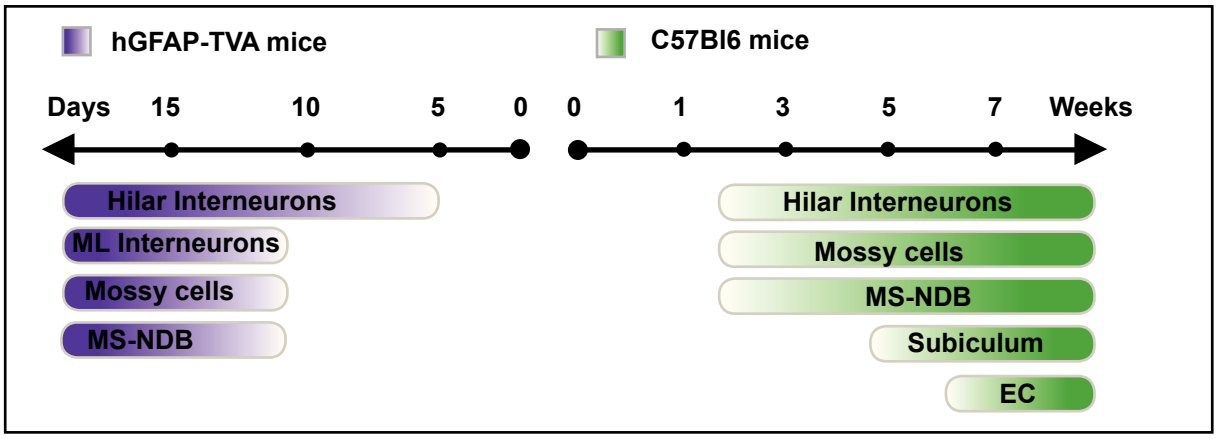

Fig. 3.1. Temporal pattern of presynaptic connectivity of newborn dentate granule neurons. Summary of the identity and location of RABV-labelled presynaptic neurons appearing during the course of maturation of adult-born DG neurons in hGFAP-TVA and C57BL/6 mice. ML=molecular layer; MS-NDB=medial septum and the nucleus of the diagonal band of Broca; EC=entorhinal cortex (Deshpande et al, in preparation).

3.3 Identification of the presynaptic partners of newborn neurons in the olfactory bulb

Due to the fact that there are multiple subtypes of newborn neurons in the adult olfactory bulb, in contrast to the dentate gyrus where there is a single type, assigning a specific population of presynaptic neurons to its postsynaptic newborn subtype is more difficult. Inspite of this, employing the RABV-mediated monosynaptic tracing technique

in the olfactory bulb provided interesting insights into presynaptic partners of adult-generated neurons. Considering that nearly 95% of newborn neurons arriving in the olfactory bulb are granule cells (only about 5% being PGCs) (Shepherd, 2003), it can be postulated that majority of the presynaptic neuron populations identified indeed form synapses onto granule cells.

3.3.1 Local connectivity and its influence on neurogenesis

The major excitatory (and regulatory) input to granule cells and PGCs in the olfactory bulb comes from the principle projection neurons, the mitral and tufted cells. This connection occurs mostly via reciprocal dendrodendritic synapses. Immunohistochemical studies with specific pre- and postsynaptic markers as well as ultrastructural evidence has confirmed the formation of the reciprocal dendrodendritic synapse between newborn granule cells and mitral cells, beginning at about 21 days after birth of granule cells in the SEZ (Whitman and Greer, 2007). Obviously, I expected that the RABV-mediated tracing technique would identify mitral and tufted cells as presynaptic partners of newborn bulbar interneurons. However, stereotaxic injection of the *G*- and *TVA*-encoding retrovirus in to the SEZ followed by EnvA-pseudotyped RABV injection into the RMS or olfactory bulb failed to label mitral or tufted cells, even after extended periods to allow for the formation of dendrodendritic synapses. However, it has been previously shown that electroporation of *G*- and *TVA*-encoding plasmids in the perinatal SEZ followed by postnatal injection of EnvA-pseudotyped RABV in the olfactory bulb resulted in the labelling of mitral cells (Arenkiel et al., 2011). One reason for this discrepancy could be that the pattern of synapse development in postnatal- and adult-generated neurons is different. There may be changes in the structure or function of axon terminals synapsing onto these two populations of granule cells resulting in the absence of mitral cell labelling in the adult olfactory bulb in our study. Another possibility is that the inherent nature of the dendrodendritic synapse may pose a hindrance to the trassynaptic transport of the rabies virus. In general, all studies involving the retrograde transsynaptic transport of RABV have focused on networks involving axodendritic connectivity of neurons. Rabies virus has been demonstrated to efficiently cross axodendritic synapses irrespective

of the neurotransmitter used (Ugolini, 2010). Mature granule cells receive synapses on their cell bodies and proximal domain of the apical dendrites as well as on their basal dendrites from centrifugal projections and axon collaterals of mitral and tufted cells. In the adult olfactory bulb, Whitman and Greer, using electron microscopy, have demonstrated the presence of glutamatergic synapses between axon terminals and GFP-encoding retrovirus-labelled newborn granule cells in the GCL (Whitman and Greer, 2007). However, they do not distinguish whether these axon terminals originate from centrifugal fibres or axon collaterals of mitral and tufted cells. Therefore, another explanation for the absence of labelling in mitral cells in this study could be that newborn granule cells may not be innervated by axon collaterals in the time window examined.

Our technique, however, did reveal monosynaptic connections of newborn granule cells (and PGCs) with other neurons in the olfactory bulb. Besides mitral and tufted cells, granule (and periglomerular) cells receive GABAergic input from within the bulb, the exact source of which was not clear. The most likely candidates are the inhibitory short-axon cells that form a heterogeneous population within the mouse olfactory bulb (Eyre et al., 2008). They have been characterised by the location of their cell bodies, structural features and neurochemical properties. They are called short-axon cells because contrary to projection neurons, their axonal arbors, albeit extensive, are largely restricted within the olfactory bulb. Many of these short-axon cells are immunoreactive for calcium binding proteins like calbindin, parvalbumin or for nitric oxide synthase, however, many of them do not co-localize with these markers (Kosaka and Kosaka, 2011). Moreover, very little is known about their axonal arborizations, their intrinsic electrical properties, their synaptic inputs, their postsynaptic targets and consequently their function in contributing to the odor information processing. Deep short-axon cells have their cell bodies in the GCL or IPL while superficial short-axon cells are located in the EPL or GL. Deep short-axon cells can be classified as Blanes cells, Golgi cells, vertical cells of Cajal, horizontal cells as well as some multipolar and bilpolar cells (Kosaka and Kosaka, 2010). One type of deep short-axon cell in the GCL having a stellate cell body and multiple dendrites, the Blanes cell, has been shown to monosynaptically inhibit granule cells through $GABA_A$ receptors (Pressler and Strowbridge, 2006). Persistent activation of these feed-forward

GABAergic interneurons mediates tonic inhibition of granule cells and therefore Blanes cells are positioned to disynaptically regulate mitral and tufted cell activity (**Fig.3.2;** Pressler and Strowbridge, 2006). The authors of this study also suggest that because Blanes cells may potentially innervate hundreds of granule cells, thus spiking activity in Blanes cells may represent a novel mechanism to generate synchronous activity in subpopulations of olfactory bulb neurons (Pressler and Strowbridge, 2006). By electron microscopy and electrophysiological recordings, Eyre et al (2008) have demonstrated that granule cells are indeed postsynaptic targets of deep short-axon cells (Eyre et al., 2008). Certain short-axon cells send interglomerular axons over long distances to form excitatory synapses with inhibitory periglomerular neurons (Aungst et al., 2003). Interglomerular excitation of PGCs has been shown to inhibit mitral cell activity in the on-centre-off-surround circuit (Aungst et al., 2003). A recent study also reported that a population of short-axon cells closely resembling the van Gehutchen cells may be presynaptic to postnatal-born granule cells and this connectivity could be significantly increased on odor stimulation, suggesting that short-axon cells may modulate the capacity of postnatally generated granule cells to integrate within the bulbar circuitry (Arenkiel et al., 2011). The RABV-mediated tracing technique described here, labelled

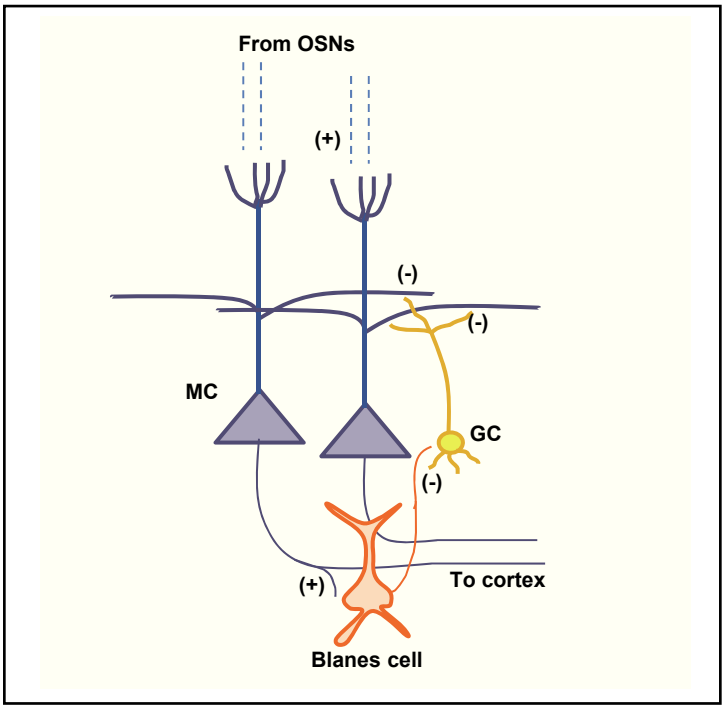

Fig. 3.2. Feedforward mechanism of disinhibition by Blanes cells.
Excitation of MC activates Blanes cells through glutamate release at axon terminals. Blanes cells make axonal GABAergic synapses onto GC (that normally inhibit MC at dendrodendritic synapses) inhibiting them. Inhibition of GC could lead to disinhibition of MC. (+) excitatory synapse; (-) inhibitory synapse; GC=granule cell; MC=mitral cells (adapted from Schoppa, N.E., 2006).

several morphologically distinct short-axon cells in different layers of the olfactory bulb. These include large, multipolar cells deep within the GCL and although neurochemical analysis is required to confirm the identity of these traced cells, their characteristics strongly suggest that they may be Blanes cells. Monosynaptic tracing also revealed eGFP-only cells in the IPL and the GL with extensive axonal arborisation in the EPL or GCL morphologically resembling superficial short-axon cells. Besides these, there were several eGFP-only short-axon cells lying in clusters within the GCL. This data would indicate that adult-generated granule cells (and PGCs) are also targets for innervation by short-axon cells. Further characterisation of these short-axon cells with respect to the neurochemical identity and firing pattern would shed light on which of these cells are involved in synapse formation on newborn neurons. Since very little is known about the function of short-axon cells in regulating granule cell and PGC activity, their influence on adult-generated bulbar interneurons can only be speculated. Similar to their role in mature circuits, short-axon cells may indirectly control the activity of mitral and tufted cells by inhibiting newborn granule cells as they integrate into the networks. More interestingly, similar to interneurons in the dentate gyrus, they may selectively control the integration of newborn granule cells by directing their activity in specific odor networks that favour synapse formation and survival (Arenkiel et al., 2011).

3.3.2 Long distance connectivity

Centrifugal input to the olfactory bulb arises from various brain regions. These can be divided into glutamatergic inputs from the AON, piriform cortex (belonging to the olfactory cortex), LEC and periamygdaloid cortex that are known to excite granule cells through AMPAR and NMDAR as well as modulatory inputs from the NDB, dorsal and medial raphe nuclei and locus coeruleus (Whitman and Greer, 2007). Rabies virus-mediated tracing labelled neurons located in the AON and the piriform cortex, on injecting the *G*- and *TVA*-encoding retrovirus in the SEZ followed by EnvA-pseudotyped RABV injection in the RMS or olfactory bulb. Using electron microscopy and immunohistochemical markers, it has been demonstrated that adult-generated granule cells express AMPAR on their cell body and basal dendrites and make asymmetric synapses with inputs

coming from centrifugal sources or perhaps axon collaterals of mitral and tufted cells (Whitman and Greer, 2007). The precise identity of these inputs however is not clear. In addition, this study also reports the presence of ChAT immunoreactive fibres adjacent to retrovirus-labelled newborn granule cells, suggesting that cholinergic inputs from NDB terminating in the GL and GCL may be involved in regulating the survival of new granule cells in the olfactory bulb (Whitman and Greer, 2007). Indeed, lesions in the cholinergic forebrain decreased the number of newborn neurons in the olfactory bulb and increased the number of apoptotic cells specifically in the GL indicating a role for the cholinergic system in survival of these neurons (Cooper-Kuhn et al., 2004). However, neither of the above studies have shown whether the effect of acetylcholine on neurogenesis is a direct or indirect one. With regard to this, no eGFP-positive neurons in the NDB were observed in the tracing experiments presented here. Further experiments will have to be designed to identify the nature of this cholinergic input on newborn neurons in the olfactory bulb. Similarly, no eGFP-labelled cells were observed in the raphe nucleus, locus coeruleus, LEC or periamygdaloid cortex. Olfactory neurogenesis is not affected by inhibition of serotonin reuptake inhibitors suggesting that newborn neurons may not receive input from the serotonergic neurons in the raphe nucleus (Malberg et al., 2000). The low or non-existent labelling by RABV of noradrenergic projections from the locus coeruleus could be explained by the fact that these projections occur largely via volume transmission and it might be that this special type of synapse is less conducive to RABV propagation (Ugolini, 2010). Moreover, since little is known about the innervation from afferent brain regions to newborn neurons in the olfactory bulb, it may be plausible that they do not make monosynaptic connections with adult-generated granule or PGCs. Equally important to consider is the fact that, like in the dentate gyrus, failure to label afferent connections to newborn bulbar interneurons from brainstem and other regions may also be due to inherent limitations of the technique.

3.3.3 Influence of afferents on adult neurogenesis

The formation of glutamatergic synapses onto the proximal dendrites of newborn granule cells occurs at early stages of maturation of before the appearance of distal

dendrodendritic synapses. It is well known that about 50% of the newborn neurons entering the olfactory bulb do not survive to integrate into the pre-existing circuits (Breton-Provencher and Saghatelyan, 2012). The peak of granule cell death lies exactly between the time of formation of glutamatergic input synapses on proximal dendrites and dendrodendritic reciprocal synapses. The first steps of synaptic integration of adult-generated neurons occurs before the formation of output synapses (Kelsch et al., 2008). Therefore, the timing of the development of input synapses has been speculated to be important in regulating the integration and survival of neurons in the olfactory network.

Moreover, the only output of granule cells occurs at dendrodendritic synapses, meaning that adult-generated granule cells are able to receive information before they can elicit a response. This is markedly different from the developing olfactory system where input synapses on newborn granule cells and the ability to fire action potentials appears simultaneously with the appearance of output dendrodendritic synapses (Kelsch et al., 2008). This sequential development of input and output synapses may be occurring to ensure that newborn granule cells receive correct cues before they can produce output signals to affect the performance of other cells. This 'silent' integration may constitute a unique form of plasticity in adult-generated neurons for odor information processing, to bring about the incorporation of new neurons with minimal disruption of pre-existing circuits. Interestingly, the axodendritic input to these cells occurs in two steps -first on the proximal domain and then on the basal dendrites - and it has been speculated that this may provide additional excitatory drive to tune the activity of granule cells (Kelsch et al., 2008). In this regard, it would be interesting to know the source of these two types of axodendritic inputs - whether they are different and what functions they may serve. Since the RABV-mediated tracing technique did not label mitral and tufted cells, it is not possible to comment on the temporal pattern of formation of input and output synapses of newborn granule cells. However, this technique did succeed in labelling axodendritic inputs and we now know that the centrifugal inputs to newborn bulbar interneurons arises directly from neurons in the AON and piriform cortex.

3.4 Conclusion and future prospects

Neural circuits comprise of complex, albeit specific, networks of neurons that connect different regions and act in an interdependent manner to execute the various functions of the mammalian brain. Newly generated neurons have to integrate into these neural circuits, establish connections with specific neurons while maintaining the integrity of the network. In this regard, the presynaptic input might be important not only for the incorporation of newborn neurons into pre-existing networks but also may help shape their postsynaptic output. The above work describes the application of a versatile dual virus-based technique, which exploits the ability of the retrovirus to selectively infect proliferating cells and that of the RABV for retrograde transsynaptic transfer, to unravel the presynaptic connectome of adult-generated neurons in the mouse brain. The presynaptic partners of newborn neurons, as revealed by this technique, comprise of a heterogeneous group that establishes its connectivity in a temporally defined pattern at different stages of maturation of the newly generated neuron. This technique revealed that the local presynaptic connectome is established prior to the long-distance connectome.

In the dentate gyrus, the earliest presynaptic partners of adult-generated granule neurons comprise of local interneurons in the GCL, hilus and ML expressing different interneuron markers like parvalbumin or somatostatin indicating that the early GABAergic connectivity is not restricted to a single type of interneuron. Interestingly, excitatory connectivity arising from mossy cells was also found to be established fairly early, i.e., 10 days after retrovirus injection. Moreover, monosynaptic tracing revealed that newborn dentate granule neurons receive input from the subicular complex. The function of this subicular-dentate connection is not known and it would be interesting to investigate the nature of subicular neurons to assess the influence of these neurons in modulating the activity of newborn neurons. Monosynaptic tracing also revealed long-distance connections, namely those arising from the cholinergic basal forebrain regions, MS-NDB

and the entorhinal cortex. Labelling of neurons in the entorhinal cortex was observed only at the latest time point assessed, i.e., at least 5 weeks after the birth of dentate granule neurons. Such step-wise development of innervation may ensure that the functional incorporation of newborn granule neurons into the classical hippocampal trisynaptic circuit takes place only when they have reached functional maturity on the cellular level and have been already incorporated into the local circuit (Deshpande et al., in preparation). A similar pattern of presynaptic connectivity compared to wild-type mice was observed in the dentate gyrus on adapting the retrovirus-based approach to hGFAP-TVA transgenic mice, thus confirming the overall applicability and specificity of this monosynaptic tracing approach.

Assessing the presynaptic connectivity of adult-generated neurons in the olfactory bulb was complicated by the fact that there is more than one type of newborn neuron in the olfactory bulb and the conspicuous absence of mitral and tufted cells. Nevertheless, like in the dentate gyrus, local and long-distance connections onto adult-generated neurons in the olfactory bulb could be revealed using this technique. Local connections were typically found to arise from a repertoire of short-axon cells in the GCL or GL, some of which are known to modulate granule cell activity through GABA. It would be interesting to further characterize this connectivity to establish the precise identities of these short-axon cells and their functions. Long-distance connectivity to newborn granule cells and PGCs was found to arise from the AON and piriform cortex.

Retrovirus-based targeting of newborn neurons for RABV infection described here can be used to map not only the connectivity of new neurons endogenously generated in the adult neurogenic areas but also to compare the nature and temporal development of the presynaptic inputs under different physiological stimuli or pathological conditions. The method can also be applied to study the incorporation of new neurons obtained following local reprogramming or transplantation (Vierbuchen, Ostermeier et al. 2010; Caiazzo, Dell'Anno et al. 2011). This approach would be especially valuable for manipulating connections selectively impinging onto adult-generated neurons, thereby

allowing us to precisely determine the contribution of specific populations of presynaptic neurons to the constant remodelling of the pre-existing network.

4 Methods

4.1 In vitro methods

4.1.1 Preparation and transduction of embryonic cortex cultures

Cultures were prepared from timed pregnant females at embryonic day 14 (E14). The day of the vaginal plug detection was considered day 0. Females were sacrificed and the abdomen was cut open to expose the uteri containing the embryos. After removal of the uterine tissue and placenta, embryos were transferred to a 60-cm dish containing ice-cold Hanks buffered salt solution with 10 mM Hepes buffer (HBSS-Hepes). Embryos were decapitated and the brain was isolated in a 60-cm dish with HBSS-Hepes under a dissecting binocular microscope (Leica). The hemispheres were separated and the meninges were removed. Cortices from both hemispheres were dissected out and transferred to a 15-ml tube containing ice-cold HBSS-Hepes. Under a tissue culture flow hood, the HBSS-Hepes was carefully aspirated with a Pasteur pipette and 5 ml E14 Plating medium was added to the cortices. The tissue was then mechanically dissociated using a fire-polished Pasteur pipette pre-wetted with seeding medium. The cell suspension was centrifuged at 1000 rpm for 5 minutes and the supernatant was discarded. The cell pellet was suspended in 3–5 ml Plating medium and the cell count was determined using an improved Neubauer chamber. Cells were seeded on poly-D-Lysine (PDL)-coated cover slips in a 24-well plate at a density of 250,000 cells in 500 µl E14 Plating medium per well. Cells were transduced with retrovirus 2 hours after plating. Twenty-four hours after transduction, 250 µl medium was removed from each well and replaced with E14 Differentiation medium for neuronal differentiation. The same procedure for medium change was repeated 24 hours later. Cells were fixed at different time intervals as required and processed for immunocytochemistry.

4.1.2 Preparation and transduction of postnatal astrocytes

Postnatal day 5-7 mouse pups were decapitated and brains were dissected out. The hemispheres were separated and the olfactory bulbs, meninges, striatum and hippocampi were removed. The remaining cortices were transferred to HBSS-Hepes in a 15-ml tube. The HBSS-Hepes was carefully aspirated with a Pasteur pipette and 5 ml Astrocyte Plating medium was added to the tube. The tissue was mechanically dissociated using a fire-polished Pasteur pipette. Dissociated tissue was centrifuged at 1000 rpm for 5 minutes at 4°C. Supernatant was discarded and the cell pellet was resuspended in 5 ml Astrocyte Plating medium reconstituted with epidermal growth factor (EGF) and basic fibroblast growth factor (bFGF) in a T25 flask.

Cells were seeded when they were nearly confluent (after ca. 1 week in culture). For seeding, the medium was discarded and the cell pellet was thoroughly washed with 1x Dulbecco's phosphate buffered saline (DPBS) to remove loosely attached oligodendrocyte precursors and debris. The DPBS was discarded and 3 ml 0.05% Trypsin-EDTA was added to the flask. The flask was incubated at 37°C for 4-5 minutes (or till cells were dissociated from the surface) and equal volumes of Astrocyte Plating medium was added to inhibit the trypsin. All the cells were carefully dissociated using a 5-ml pipette, transferred to a 15-ml tube and centrifuged at 1000 rpm for 5 minutes. Medium was discarded and the cell pellet was resuspended in 2 ml Astrocyte Plating medium. Cells were counted using an improved Neubauer chamber. Cells were seeded in a 24-well PDL-coated plate at a density of 50,000 cells/well in 500 µl Astrocyte plating medium reconstituted with EGF and FGF. Cells were transduced with retrovirus 2 hours after plating.

4.1.3 Treatment of cover slips and coating with PDL

Before coating, the glass cover slips were cleaned by shaking in a solution of 0.1M HCl for 1 h. Cover slips were then transferred to a beaker with acetone and placed in an ultrasonic bath for 20 minutes followed by shaking (ca.50 rpm) for 1h. Then cover slips were transferred to 70% ethanol solution on a shaker (ca.50 rpm) for 1 h. Finally, they were rinsed in 100% ethanol and dried on a paper towel under the laminar airflow.

For coating, cover slips were transferred to a 24-well plate (1 cover slip/well) and 500 µl PDL working solution was added to it. The plate was incubated for at least 2h or overnight at 37°C. The PDL was aspirated and cover slips were washed thoroughly with sterile double distilled water. Plates were dried under the laminar flow and stored at 4°C for no longer than one week (Heinrich et al., 2011).

4.1.4 Immunocytochemistry

For immunocytochemistry on E14 cortical cultures, cells were fixed in 4% Paraformaldehyde (PFA; 350 µl per well) for a maximum of 15 minutes and washed thoroughly with 1x PBS. Cover slips were covered with primary antibodies (see Table 1) in blocking buffer consisting of 0.1M PBS, 0.1% Triton-X-100 (Sigma) and 2% bovine serum albumin (BSA; Sigma) and incubated overnight at 4°C in a moistened chamber. Cover slips were washed in 1x PBS three times and incubated with specific secondary antibodies conjugated to fluorescent dyes (see Table 2) in blocking buffer for at least 1 hour at RT. Following incubation in the secondary antibodies, cover slips were washed again with 1xPBS (3x) and allowed to dry at room temperature (RT), after a brief wash in water to remove remnants of PBS. The cover slips were mounted on Superfrost glass slides (Roth) in Aqua Polymount (Polysciences) and allowed to dry at RT. The slides were stored at 4°C in boxes.

4.2 In vivo methods

4.2.1 Animals

All animal procedures were performed in accordance to the policies of the use of animals and humans in Neuroscience Research, revised and approved by the Society of Neuroscience and the state of Bavaria under license number 55.2-1-54-2531-144/07.

Eight to 12 week male and female C57Bl/6 J or C57Bl/6 N mice (18 − 25 g) were used for in vivo injections and in vitro cultures. Human GFAP-TVA transgenic mice (Jackson Labs; Strain name: STOCK Tg (GFAP-TVA)5Hev/J; Stock# 003528) expressing TVA under the human GFAP promoter generated by replacing the LacZ gene from the pGfa 2lac-1 plasmid with the tv-a cDNA from pSP73 (0.8) (Holland et al.,

1998; Holland and Varmus, 1998) were also used for in vivo injections. The transgene comprises of a 2.2 kb fragment of the hGFAP promoter, the quail TVA gene and part of the mouse protamine gene (MP-1) to supply an intron and polyadenylation site.

4.2.2 Genotyping

To identify the transgenic allele, animals were genotyped by PCR amplification of DNA of 3 week old mice. Tail biopsies of less than 5 mm length were used. The tails were incubated in 500 µl Lysis buffer in 1.5-ml tubes at 55°C overnight (or at least for 3 hours) on a shaker (Eppendorf) at 500 rpm. After lysis, hairs and tissue residues were removed by centrifugation at 10000 rpm for 5 minutes. The supernatant was transferred to a new 1.5-ml tube and the DNA was precipitated by adding 500 µl Isopropanol and centrifuging for 10 minutes at 12000 rpm, followed by a 70% ethanol wash. The supernatant was discarded and the pellet was dried for 1h at RT or alternatively for 30 minutes at 37°C. The DNA pellet was dissolved in 150 µl 10mM Tris-HCl buffer pH 8.0 followed by 1 − 2 hours shaking at 55°C. The DNA was stored at 4°C before PCRs. After PCR, 10 µl of the PCR product was analysed on a 2% agarose-TAE gel. The genotyping protocol and primers for genotyping the hGFAP-TVA mice were obtained from Jackson labs (http://jaxmice.jax.org/strain/003528.html).

Primer sequences for TVA genotyping:

TG1 #1046 5’ - CTG CTG CCC GGT AAC GTG ACC GG - 3’

TG2 #1047 5’ - GCC CTG GGG AAG GTC CTG CCC - 3’

Amplicon: TVA allele ~500 bp.

PCR Reaction			PCR Conditions			
Component	Vol (µl)	Final conc.	Step	Temp	Time	
ddH_2O	7.66		1	94°C	3min	
10xNEB Buffer	1.2	1x	2	94°C	30s	Repeat 2-4
dNTPs (25 mM)	0.24	0.5 mM	3	66°C	1min	for 30 cycles
Primer TG1 (20 pmol/µl)	0.5	1 pmol/µl	4	72°C	1min	
Primer TG2 (20 pmol/µl)	0.5	1 pmol/µl	5	72°C	10min	
NEB Taq Polymerase	0.3					
DNA	1.5					
Total	12					

4.2.3 Viral vector construction

4.2.3.1 Retroviral constructs

Moloney MLV-derived retroviral vectors were used to generate all the retroviral constructs. For initial validation of the system in vitro, a CMMP-TVA (kind gift from K. Conzelmann) retroviral vector and a pMX-Glycoprotein-IRES-Tomato retroviral vector was used. The transgenes in both the above vectors are driven directly under the viral Long Terminal Repeats (LTRs). The retroviral vector expressing TVA has no reporter while the G-encoding retrovirus has a tandem Tomato fluorescent reporter translated from an IRES. The other retroviral vectors used consist of a chicken-β-actin (CAG) promoter driving the expression of the transgenes which allows high and ubiquitous expression in all mammalian cells, an IRES and a DsRed or DsRedExpress2 reporter which allows identification of transduced cells by immunostaining for red fluorescent protein (RFP) flanked by Long Terminal Repeats (LTRs). The vectors used in this study are replication incompetent, self inactivating and have a lower extent of silencing which is beneficial for longer survival intervals. The vectors also have Ampicillin resistance for screening of transformed bacterial colonies.

pMX-Glyco-IRES-TdTomato

The *G* was subcloned from FuV-Glyco into pMX-IRES-TdTomato using XhoI and NotI to generate the retroviral construct, pMX-Glyco-IRES-TdTomato.

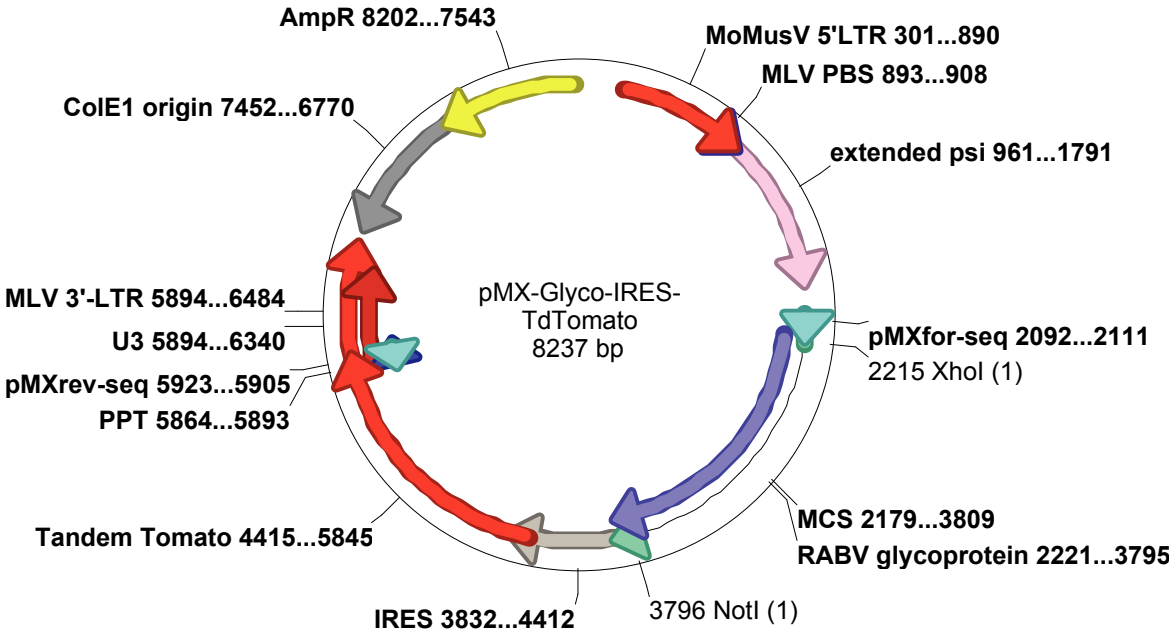

Fig. 4.1. pMX-Glyco-IRES-TdTomato retroviral construct

For RABV-mediated transsynaptic tracing, two retroviral vectors expressing the transgenes - the glycophosphoinositydol (GPI)-anchored form of the chicken TVA receptor (*TVA800*), the *G* from the CVS-11 strain of RABV and a *DsRed* or *DsRedExpress2* reporter were constructed. The second construct containing *DsRedExpress2* was designed to improve the detectability of the transduced cells for electrophysiological recordings.

CAG-Glyco-T2A-TVA-IRES-DsRed

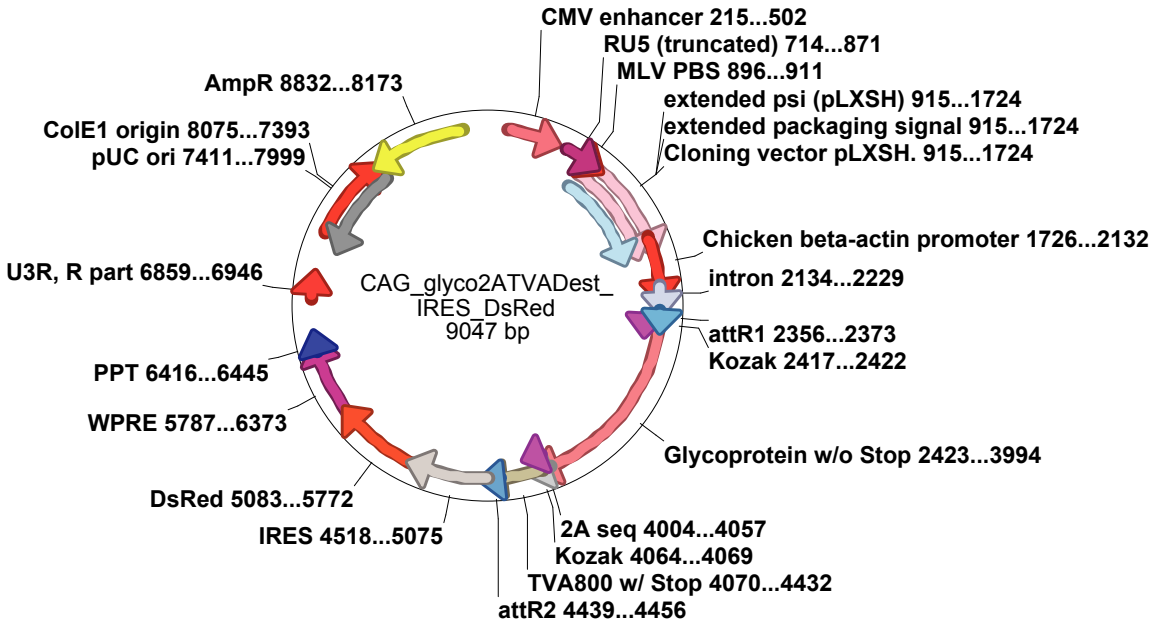

Fig. 4.2. CAG-Glyco-T2A-TVA-IRES-DsRed retroviral construct.

For the retroviral construct, cDNA for TVA800 was amplified by PCR using primers with NotI and AscI linkers and cloned into a mammalian expression vector to generate pCAG-TVA. The sequence of the self-cleaving 2A peptide from the virus Thosea asigna was introduced into pCAG-TVA at the NotI site to generate pCAG-2A-TVA. The translational stop codon was removed from the cDNA of G by targeted mutagenesis and ligated to the 2A sequence in pCAG-2A-TVA in the same reading frame, with specific restriction enzymes to generate pCAG-Glyco-2A-TVA. The Glyco-2A-TVA cassette was subcloned into the entry vector pENTR-1a (Invitrogen) using KpnI/XhoI and Gateway recombinational cloning was performed in an MMLV-based retroviral destination vector (kindly provided by P. Malatesta) using the LR clonase enzyme (Invitrogen) according to manufacturer's protocol to generate the *CAG-Glyco-2A-TVA-IRES-DsRed* polycistronic retroviral construct.

CAG-DsRedExpress-T2A-Glyco-IRES-TVA

For the retroviral vector with the DsRedExpress2 reporter, DsRedExpress2 was excised from the plasmid pIRES2DsedExpress2 (Clonetech) and replaced with the PCR-amplified cDNA for TVA800 to generate pIRES2-TVA using BstXI and NotI restriction enzymes. Primers were designed for the combined amplification of the 2A sequence and the cDNA for G (2A-Glyco) with SalI and SmaI linkers. The 2A-Glyco amplicon was cloned into pIRES2-TVA with these restriction enzymes. DsRedExpress2

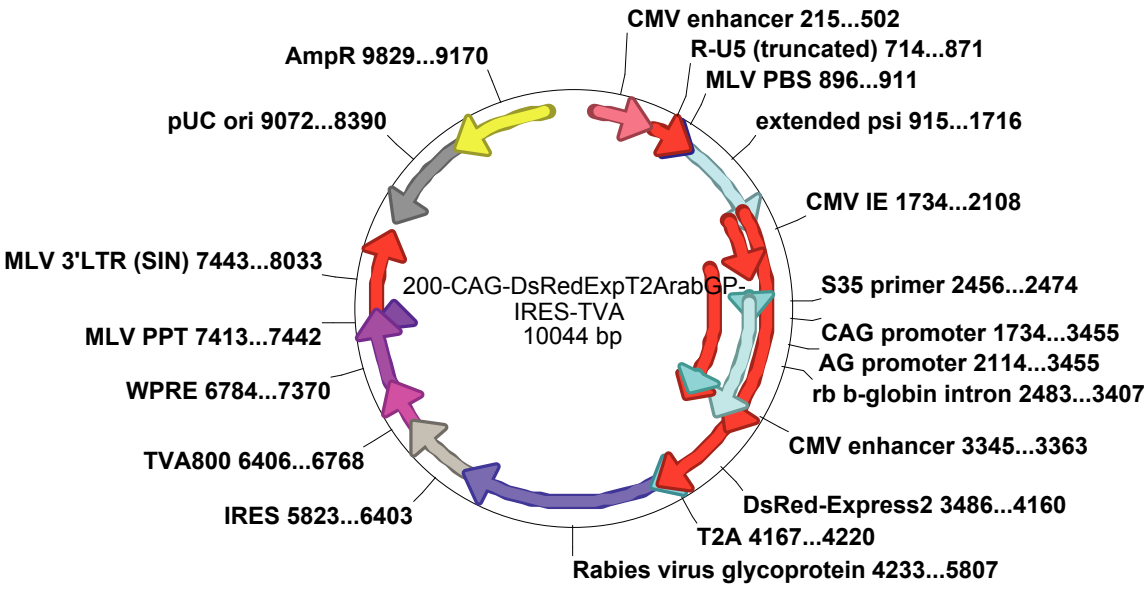

Fig. 4.3. CAG-DsRedExpress-T2A-Glyco-IRES-TVA retroviral construct.

without a translational stop codon was amplified by PCR from pIRES2-DsRedExpress2 and cloned in-frame into p2A-Glyco-IRES2-TVA using EcoRI and SalI. The entire DsRedExpress2-2A-Glyco-IRES2-TVA cassette was subcloned using SfiI/NotI into the CAG retroviral vector through the shuttle vector (pBKS-) to generate the polycistronic retroviral construct *CAG-DsRedExpress2-2A-Glyco-IRES2-TVA*.

CAG-DsRedExpress-IRES-TVA

For the control retroviral vector without the glycoprotein, the DsRedExpress2 reporter was excised from the plasmid pIRES2DsedExpress2 (Clonetech) and replaced with the PCR-amplified cDNA for TVA800 to generate pIRES2-TVA using BstXI and NotI restriction enzymes. The DsRedExpress2 from pIRES2DsedExpress2 was PCR amplified

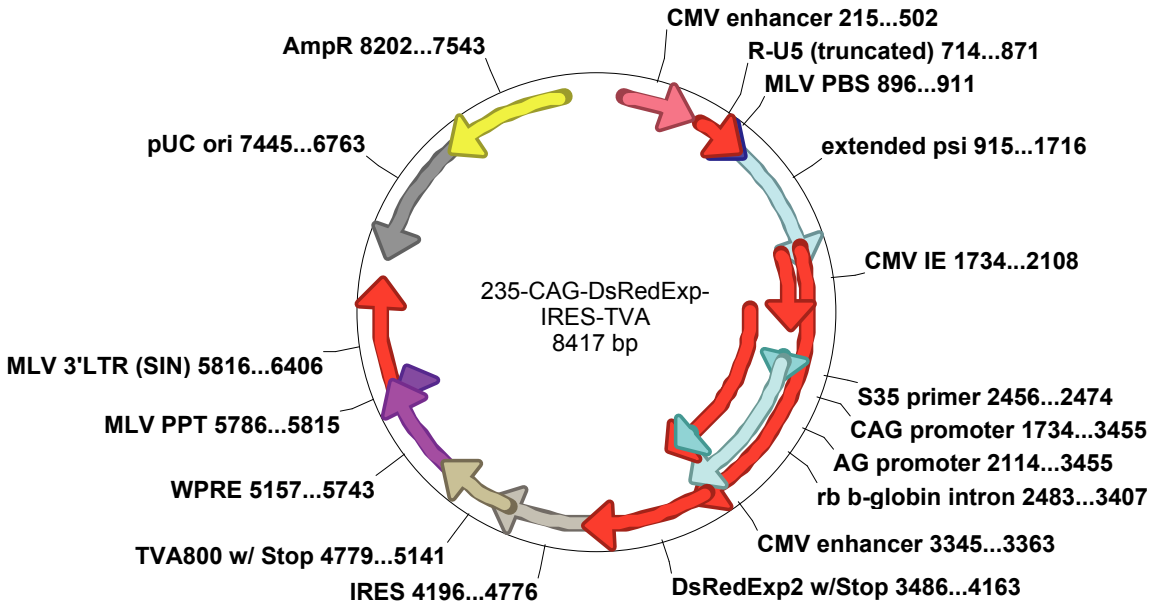

Fig. 4.4 CAG-DsRedExpress-IRES-TVA retroviral construct.

with EcoRI and SalI primers and cloned into pIRES2-TVA to generate pDsRedExp2-IRES2-TVA. The DsRedExp2-IRES2-TVA construct was then subcloned using SfiI/NotI into the CAG retroviral vector through the shuttle vector (pBKS-) to generate the control retroviral construct, *CAG-DsRedExpress2-IRES2-TVA* (*CAG-DsRedExpress-IRES-TVA* construct was generated in collaboration with Francesca Vigano).

CAG-Glyco-IRES-DsRed

The G from a lentiviral construct was cloned into pcDNA3.1 (with a modified MCS) using the restriction enzymes XhoI and NotI. The G from pcDNA3.1-Glyco was excised using SfiI/PmeI and ligated to the SfiI/PmeI digested CAG retroviral vector to generate the *CAG-Glyco-IRES-DsRed* construct.

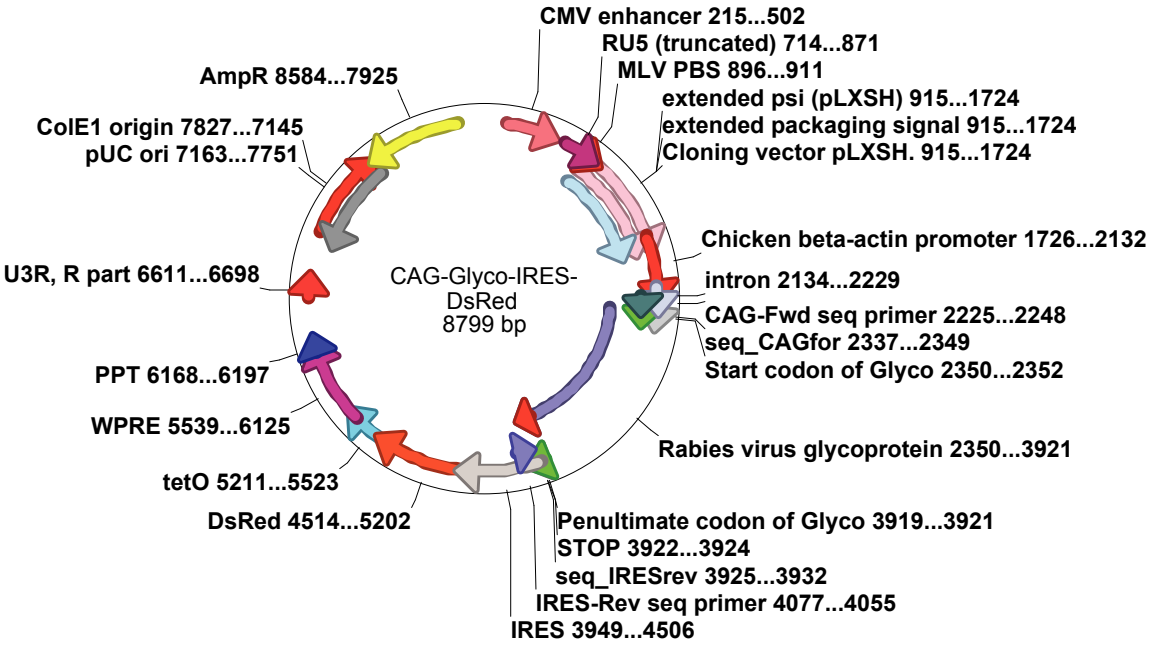

Fig. 4.5. CAG-Glyco-IRES-DsRed retroviral construct.

CAG-IRES-DsRedExpress2

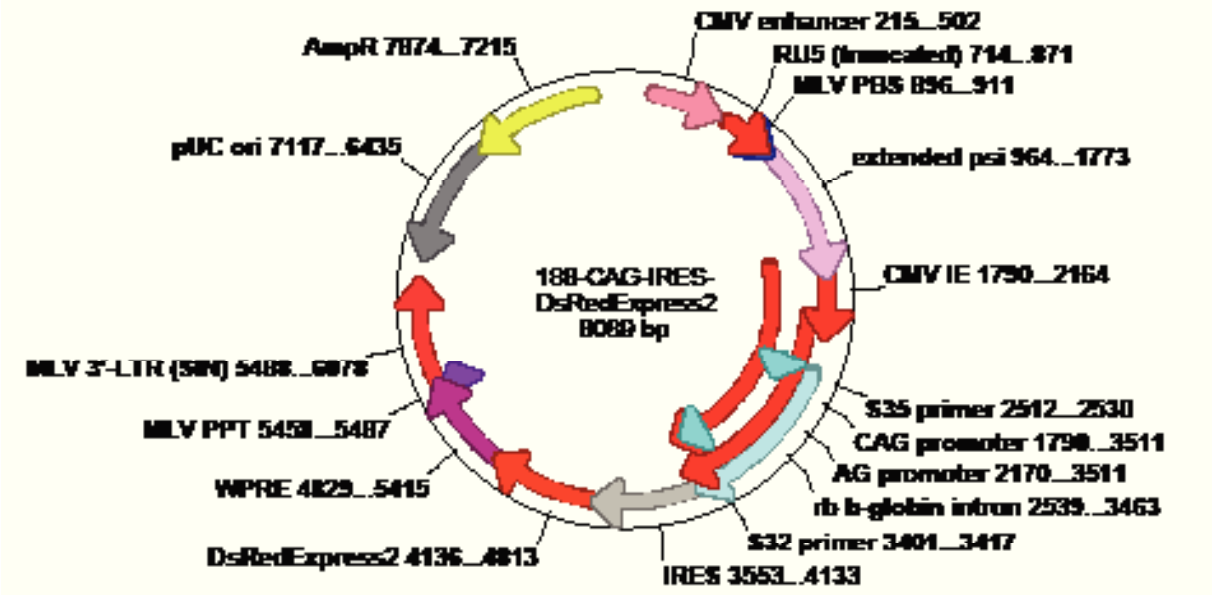

Fig. 4.6. CAG-IRES-DsRedExpress retroviral construct.

The control retrovirus was constructed by replacing the *DsRed* in the CAG retroviral vector with *DsRedExpress2* from pIRES2DsRedExpress2 (Clonetech) using BamHI and NotI.

4.2.3.2 Rabies virus constructs

Construction of the *G* gene-deleted eGFP-expressing RABV (SADΔG-eGFP) was as previously described by Wickersham et al (Wickersham et al., 2007a).

4.2.4 DNA preparation for retrovirus production (CsCl gradient)

A 250 ml bacterial culture was used to prepare pure supercoiled plasmid DNA for retroviral production. The culture was grown to about 90% confluency and harvested by centrifuging at 5000xg for 20 minutes and the supernatant was discarded. The pellet was resuspended in 10 ml Qiagen buffer 1 with RNAse. After complete resuspension, 10 ml Qiagen buffer 2 was added for lysing the bacterial cells, the tube was inverted gently several times and incubated at RT for 5 minutes. Ten ml of ice-cold Qiagen buffer 3 was added and the tube was shaken thoroughly to precipitate genomic DNA and proteins in the mixture. The mixture was filtered through a pre-wetted Whatman paper filter into a 50-ml tube. The plasmid DNA was precipitated by adding 20 ml Isopropanol to the filtrate (1:1), mixed and centrifuged at 8000xg for 1 hour at 4°C. The supernatant was drained off, the white pellet was washed carefully with ice-cold 70% ethanol and centrifuged again for 10 minutes at 8000xg. After draining off the ethanol, the wet pellet was dissolved in 15 ml Tris-EDTA buffer pH 8.0 (TE) and further purified using phenol extraction.

The suspension was poured into a MaxTract high density (Qiagen) 50-ml tube and 7.5 ml of phenol equilibrated with TE and 7.5 ml Chloroform was added to it. After mixing well, the mixture was centrifuged at 1500xg at room temperature (RT) for 20 min in a swing-out rotor. The upper aqueous phase was poured into a new 50-ml tube and 1.5 ml of 3M Sodium Acetate pH 5.2 and 15 ml Isopropanol was added to precipitate the plasmid DNA, mixed well and centrifuged at 8000xg for 1 hour at 4°C. The supernatant was drained off and the pellet was washed with ice-cold 70% ethanol. The DNA pellet

was air-dried until it was transparent. The dry pellet may be stored at -20°C before Cesium chloride (CsCl) gradient purification.

For the CsCl gradient preparation, the dry pellet was dissolved completely in 8 ml TE. The dissolved DNA was added to 10.5 g CsCl in a 50-ml tube and the salt was dissolved completely. Eight hundred µl of saturated Acridine Orange (AcOr; Sigma) was added and the solution was mixed until a fine precipitate was formed. Samples were warmed to 37°C for 15 minutes in a water bath and centrifuged at full speed in a swing-out rotor for 10 minutes. The supernatant was filled into an 11.2 ml OptiSeal tube (Beckmann) until the meniscus touched the mouth of the tube. Tubes were balanced precisely for the following ultracentrifugation step at 65000 rpm for 5.5 hours at 20°C and slow brake settings. After the ultracentrifugation, DNA bands were visualised using blue light on a DARK Reader transilluminator (DR-88M; Clare chemical research) and immediately extracted.

For collecting the DNA, the tube was fixed to a holder, in front of a UV-lamp. A 22-guage needle was used to pierce the shoulder of the tube to release the pressure to enable extraction of the DNA band. Then a second needle (22 guage) was inserted into the tube just below the lower DNA band which is the desired super-coiled form of plasmid, as seen under the blue light. The needle was connected to a 2-ml syringe and the DNA band (as much as possible) was sucked in and transferred to a 15-ml tube. The extracted plasmid DNA can be stored overnight at this stage at RT, in dark. To remove the AcOr from the DNA, an equal volume of n-butanol saturated with TE was added to the DNA, shaken well and centrifuged briefly in a swing-out rotor. The upper organic phase was removed and the extraction was repeated until the lower yellow aqueous phase was completely colourless (~5 – 6 times). An equal volume of diethylether was added, the solution was mixed and the upper, organic phase was separated to remove traces of n-Butanol from the aqueous phase. The ether evaporated during the next steps at RT. The mixture was transferred to 50-ml tubes and diluted with 2 volumes of sterile TE. One-tenth volume of 3M sodium acetate pH 5.2 and 2 volumes cold 100% ethanol (stored at -20°C) were added, the solution was mixed and incubated on ice for 1 – 2 hours or overnight at 4°C, followed by a centrifugation step at 10000xg for 1 hour

at 4°C. The supernatant was discarded and the pellet was washed with 10 ml cold 70% ethanol. The pellet was air-dried and the DNA was dissolved in 500-1000 µl of sterile 10 mM Tris-HCl pH 8.0, under sterile conditions. Vigorous shaking was avoided to prevent shearing of DNA. The DNA solution was transferred into a 1.5-ml tube and the amount of DNA was quantified. The quality of DNA was checked by confirmatory restriction enyzme digestion and loading on a 0.8% agarose-TAE gel.

4.2.5 Retrovirus Production

4.2.5.1 Cells

Human embryonic kidney (HEK) gpg293 cells were used for preparation of all retroviruses. The retrovirus preparation with gpg293 cells requires only the addition of the retroviral expression plasmid, as all other viral genes are integrated in the genome of these cells (Burns et al., 1993; Pear et al., 1993). All retroviruses used in this study were pseudotyped for Vesicular Stomatitis Virus glycoprotein (VSVG). Cells were grown in Basic medium and under a triple selection of antibiotics: 1 mg/ml Tetracycline (Sigma, repression of the VSVG production), 2 mg/ml Puromycin (Sigma, selection for the integrated VSVG gene and Tet-repressor that regulates VSVG expression) and 0.3 mg/ml G418 (=Geneticin, Gibco, selection for integrating MMLV genome (gagpol)). This medium was stored at 4°C and used within 6 weeks to avoid degradation of the antibiotics. When cells were nearly confluent, they were dissociated using 0.05% Trypsin-EDTA (Sigma) and passaged at a ratio of 1:3 to 1:5.

4.2.5.2 Retroviral Packaging

The HEK gpg293 cells were expanded in 175cm2 flasks to yield a sufficiently large number of cells for viral packaging. Cells were seeded in 10-cm culture dishes in Basic medium without Tetracycline (with Puromycin and G418) to induce VSVG expression. Up to 6 (or at least 3) 10-cm dishes were used for production of one retroviral vector batch. The day after seeding, the cells at 80-90% confluency were washed with Opti-MEM (Gibco) containing 10% FCS (6 ml per 10-cm dish) to remove any antibiotics. Two washing steps were performed to ensure complete removal of antibiotics, followed by a 1 hour incubation at 37°C. The cells were transfected using the following mix (Pear,

Nolan et al. 1993; Hack, Saghatelyan et al. 2005). For 6 dishes, 2x 50-ml tubes:

In Tube 1, 9 ml Opti-MEM (1.5 ml per 10-cm dish) and 360µl Lipofectamine 2000 (Invitrogen, 60µl per 10-cm dish), mix well. In Tube 2, 9 ml Opti-MEM and 150µg CsCl-purified DNA (24µg DNA per 10-cm dish), mix well. Solutions were allowed to settle for 5 minutes at RT. The contents of Tube 1 were added to Tube 2, mixed and incubated for 30 minutes under the tissue culture flow to allow formation of Lipofectamine-DNA complexes. Three ml of transfection mix was added drop-wise to each 10-cm dish. About 16-20 hours later, transfection medium was replaced with the Packaging medium (10 - 12ml of Packaging medium per 10-cm dish).

4.2.5.3 Retroviral Harvesting

The first medium collection (harvest) was performed 48 hours after transfection, the second harvest was done three days following transfection and a third harvest was done 4 days after. All centrifuge tubes, screw caps and rotor buckets were sterilized in 100% ethanol prior to harvesting. The culture medium was collected in 50-ml tubes and 10 ml Packaging medium was gently added on top of the transfected cells. The cells were returned to the incubator and the supernatant was filtered through a pre-wetted low-protein binding 0.45 µm Polyvinylidene fluoride (PVDF) filter (Millipore) into Beckmann ultracentrifugation tubes and balanced accurately with medium. This was followed by an ultracentrifugation step at 50000xg for 90 minutes at 4°C (Beckmann, SW40Ti rotor). After ultracentrifugation, the supernatant was carefully aspirated using a Pasteur pipette connected to a vacuum pump. The transparent pellet was soaked for at least 3 hours or overnight on ice in 80-100 µl TBS-5 buffer and resuspended carefully with a 200µl-pipette tip. Ten µl aliquots of the viral suspension were made in 0.5-ml safe-lock tubes (Eppendorf) on ice, under sterile conditions and stored at -80°C.

4.2.5.4 Retroviral titering

Dissociated E14 cortical cells were used for determination of retroviral titres. Cells were seeded at a density of 250,000 cells/well in 24-well plates on Poly-D-Lysine (PDL)-coated cover slips in 500 µl E14 Plating medium. Cells were transduced 2 hours after plating at following dilutions :

1µl virus in 500µl medium: 250 µl = 0.5 µl virus/well

50 µl = 0.1

5 µl = 0.01

1 µl = 0.002

Day after seeding and transduction, 500 µl E14 Differentiation medium was added to the cells. Cells were cultured for 72 hours, after which they were fixed in 4% PFA for 15 minutes at RT. Cells were then processed for GFP or RFP immunocytochemistry. Colonies were counted and viral titres were assessed using the following formula:

Virus titre (per ml) = no. of clones x 1000/ Dilution factor

In most cases, the 1 µl (0.002) or 5 µl (0.01) dilution allowed for counting of single colonies and to accurately assess the viral titre. Virus titering was done for each harvest and a viral titre of ~5-9 x 107 was considered optimal for in vivo injections.

4.2.6 Pseudotyped rabies virus production

The protocol for pseudotyped RABV production was obtained courtesy of Prof. K-K Conzelmann. Briefly, the RABV SADΔG-eGFP was amplified in BSR MG-on cells complementing the G deficiency of the virus upon induction of G expression by doxycycline as previously described (Finke et al., 2003). One million BSR MG-on cells in T25-flasks were infected at a multiplicity of infection (MOI) of 0.01 and G protein expression was induced immediately by adding 1µg/ml doxycycline. When almost all cells were infected as determined by fluorescence microscopy, supernatants were harvested, cleared from debris by centrifugation for 5 minutes at 1000 rcf at 4°C and stored in 1 ml aliquots at – 80°C.

Pseudotyping of SADΔG-eGFP(G) with EnvA was done by infection of BHK-EnvARGCD cells, expressing an ASLV-A envelope protein comprising the G cytoplasmic tail (Wickersham et al., 2007b) at a MOI of 1. Cells were thoroughly washed with fresh medium to remove cell-free input virus. Supernatant was harvested 72 hours post infection, cleared by centrifugation as above and stored in 1 ml aliquots at – 80°C. Titers

of SADΔG-eGFP(EnvA) were determined on HEK293T-TVA800 cells by serial dilutions and counting GFP-positive cells.

4.2.7 Stereotactic injections

For the stereotactic surgery, mice were anaesthetised by an intraperitoneal injection of 100-150 µl mix comprising of 1.0 ml Ketamine, 10%, (injected at approximately 100 mg/kg body weight; cp-pharma, Burgdorf, Germany), 0.25 ml Xylazine hydrochloride, 2% (injected at 5 mg/kg body weight; trade name Rompun, Bayer, Leverkusen, Germany) and 2.5 ml saline (0.9% sodium chloride ; Braun, Germany) with insulin needles (U-100, 1-ml, BD Micro Fine, PZN: 324870). Mice were fixed on the stereotactic apparatus (Stoelting) and the eyes were covered with an eye cream (Bepanthen Augen- und Nasensalbe) to prevent them from drying out. The top of the head was disinfected with 70% ethanol and a small midline incision was performed with a size-22 scalpel (Schreiber Instrumente). The bregma (the point on the skull where the coronal suture intersects the sagittal suture) was determined and the tip of a glass capillary was aligned directly at the bregma. The digital display of the stereotactic apparatus was set to 0.0 on the X, Y and Z axes at this point. The required stereotactic coordinates were set relative to bregma and a small craniotomy was performed using a drill (Foredom), keeping the meninges intact. A finely pulled capillary containing the viral suspension was attached to the stereotaxic apparatus and the bregma was set again. The digital display was adjusted to 0.0 in the X- and Y-axis. At the injection coordinates, the Z-axis was adjusted to 0.0 at the dura and the capillary of inserted into the brain to the required depth. Then 1-2 µl viral suspension was injected very slowly (5–10 minutes) using an air system (WPI, picopump, PV 820; connected to a Jun-Air compressor). A pulse generator (pulse/delay generator PDG 204) generated a pulse every 5 s to release minute amounts of the virus, which could be observed under the binocular microscope as lowering of the meniscus of the viral suspension in the capillary. Pulses were given at the lowest possible pressure and pulse length to gradually inject the virus into the brain. After the injections, the capillary was retained in the brain for 4-5 minutes before retracting, to allow the injected viral suspension to be absorbed. The skin incision was closed carefully with a suture thread

(Ethicon Vicryl, 4-0, SH-1 plus, 21.8mm 1/2c, 70cm filament) after retroviral injection to minimize inflammation in order to facilitate the subsequent EnvA-pseudotyped RABV injection. For recovery from anaesthesia, mice were put in an airing cupboard at 37°C. The following stereotactic coordinates were used relative to Bregma: for DG, caudal 2.0, lateral 1.6 and ventral 1.9-2.1; for SEZ, rostral 0.7, lateral 1.2 and ventral 1.6-2.0; for RMS, rostral 2.5, lateral 0.8 and ventral 3.2–3.0; for OB, rostral 4.5, lateral 0.8 and ventral 1.0-0.5.

4.2.8 Fixation and histology

For immunohistochemistry, animals were deeply anaesthetised by an intraperitoneal injection of 250-300 µl mix comprising of previously described anaesthetic with insulin needles and transcardially perfused, first with 1x PBS for 5 minutes and then with 4% PFA for 20-30 minutes. Brains were post-fixed in 4 % PFA for 1 hour, washed with 1x PBS and stored in 1x PBS at 4°C till sectioning. For histology, fixed brains were embedded in 4% agarose (in water or 1x PBS) and cut at the vibratome (Leica) at a thickness of 100 µm. For long term storage, vibratome sections were frozen at -20°C in storing solution.

4.2.9 Immunohistochemistry

Vibratome sections were incubated with primary antibodies at specific dilutions (see Table 1) in blocking buffer consisting of 0.1M PBS, 0.5% Triton-X-100 (Sigma) and 2% BSA (Sigma) overnight at 4°C. Following incubation in the primary antibody, sections were washed thrice in 1x PBS for 20 minutes each on a shaker and incubated in specific secondary antibodies conjugated to fluorescent dyes or biotin (see Table 2) in blocking buffer, for detection of antigen. For biotinylated secondary antibodies, detection was done by incubating the sections in Streptavidin linked to Alexa dyes. To visualize nuclei, 4', 6' Diamidino-2-phenylindole (DAPI; Sigma) was added to the secondary antibody solution at a concentration of 0.1 µg/ml. After incubation in secondary antibodies for 1-3 hours at RT, sections were washed in 1x PBS and mounted on glass slides (Thermoscientific). Slides were dried at RT, coated with Aqua Polymount and covered gently with cover slips (24x60 mm; Roth), taking care to avoid air bubbles. The mountant was allowed

to dry at RT for 4-6 hours and slides were stored at 4°C in boxes. Control experiments were carried out to ascertain specificity of primary antibodies used.

4.2.10 Confocal imaging and cell counting

Samples were imaged with a confocal laser-scanning microscope (LSM 710 module, Zeiss) equipped with 4 laser lines (405, 488, 561 and 633 nm) and 10x (NA 0.3), 25x (NA 0.8), 40x (NA 1.1) or 63x (NA 1.3) objective lens. Serial Z-stacks of 1µm (for 25x objective) and 0.5µm (for 40x objective) were taken and collapsed to obtain a maximum intensity projection of the scanned image.

Cell counting was performed by quantifying the number of double-transduced (eGFP-positive and DsRed-positive) or RABV-only transduced cells (eGFP-positive) per mouse. Phenotypic characterization of cells targeted by the EnvA-pseudotyped RABV in hGFAP-TVA mice was performed by colocalization with cell-type specific markers such as GFAP, Dcx, NeuN.

Image processing of the acquired images was performed with ImageJ (National Institutes of Health, Bethesda, United States) and the brightness of final images was uniformly adjusted with Photoshop (Adobe Systems Incorporated, San Jose, California, United States). For some figure panels, a manual alignment of adjacent fields of acquisition was performed.

4.2.11 Electrophysiological recordings of neuronal cultures

Dual perforated patch-clamp recordings were performed at room temperature with amphotericin-B (Calbiochem). Pipettes were tip-filled with internal solution and back-filled with internal solution containing 200 µg/ml amphotericin-B. The electrodes had resistances of 2–2.5 MOhms The external solution contained 150 mM NaCl, 3 mM KCl, 3 mM $CaCl_2$, 2 mM $MgCl_2$, 10 mM HEPES, and 5 mM glucose (pH 7.4) at an osmolarity of 310 mOsm. A continuous perfusion at a rate of 0.5 ml/min was maintained during experiments. Cells were visualized with an epifluorescence microscope (Axioskop2, Carl Zeiss) equipped with the appropriate filter sets and with a digital camera (AxioCam, Carl Zeiss) and virally transduced cells were selected on the basis of their fluorescence.

Recorded signals were sampled at 10 kHz with an Axopatch 200B amplifier (Axon Instruments, Foster City, CA, USA), filtered at 5 kHz and analyzed with Clampfit 9.2 software (Axon Instruments). Synaptic connectivity was investigated by means of pair recordings in voltage clamp mode. One neuron was stimulated at low frequency (0.05–0.1 Hz) by a 1 ms step-depolarization from −70 to +30 mV and the response was recorded from the other neuron.

4.2.12 Statistical analysis

Results are presented as means ± standard errors and significance was calculated with GraphPad Prism 5 (Graphpad Software, San Diego, CA) using the Student's t-test.

4.3 Materials

4.3.1 Primary antibodies

Table 1. Primary Antibodies

Antigen	Host species	Dilution	Company	Cell type labelled
Calbindin	mouse IgG1	1:500	Sigma	Short-axon cells, PGCs, DG granule neurons
Calretinin	rabbit	1:500	Millipore	Granule cells, mossy cells
Choline acetlytransferase (ChAT)	goat	1:100	Millipore	Cholinergic neurons
Doublecortin (Dcx)	rabbit	1:1000,	Abcam	Immature DG granule neurons
γ-Amino butyric acid (GABA)	rabbit	1:500	Sigma	interneurons
Glial fibrillary acidic protein (GFAP)	mouse IgG1 rabbit	1:500 1:500	Sigma Dako	aNSCs, astrocytes
Green fluorescent protein (GFP)	chicken	1:2000	Aves Lab	eGFP-labelled cells
Neuropeptide Y (NPY)	rabbit	1:1000	Abcam	interneurons
Parvalbumin	mouse IgG1	1:500	Sigma	interneurons
Rabies virus glycoprotein	Mouse IgG2a	1:200	ABD Serotec	G-encoding retrovirus infected cells
Rabies virus nucleoprotein	rabbit		Centocor	Rabies virus infected cells
Red fluorescent protein (RFP)	rabbit	1:1000	Rockland	DsRed/DsRedExpress2 or TdTomato-labelled cells
Reelin	mouse IgG1	1:400	MBL	Mitral cells
Somatostatin	rat	1:250	Millipore	interneurons
β-III-Tubulin (Tuj1)	mouse IgG2b	1:500	Sigma	Immature neurons
TVA	rat	1:100	Home made	TVA expressing cells

4.3.2 Secondary antibodies

Table 2. Secondary Antibodies

Species specificity	Fluorescence tag	Company	Dilution
Donkey α-Chick	FITC	Dianova	1:200
Donkey α-Goat	Cy3	Dianova	1:500
Goat α-Mouse IgG	Cy5	Dianova	1:500
Goat α-Mouse IgG	DyLight 649	Dianova	1:500
α-Mouse IgG2a	Biotin		1:200
Goat α-Mouse IgG2a	A488	Invitrogen	1:500
Donkey α-Rabbit	A488	Invitrogen	1:500
Donkey α-Rabbit	Cy3	Dianova	1:1000
Goat α-Rabbit	Cy5	Dianova	1:500-800
Goat α-Rabbit	DyLight 649	Dianova	1:500
Donkey α-Rat	A488	Invitrogen	1:500
Goat α-Rat	Cy3	Dianova	1:500
Donkey α-Rat	Cy5	Dianova	1:500-800
Goat α-Rat	A647	Invitrogen	1:500
Biotinylated secondary	Streptavidin A405	Invitrogen	1:200
Biotinylated secondary	Streptavidin A647	Invitrogen	1:200

4.3.3 Solutions

Table 3. Solutions

Solution	Components	Preparation	Use
Ampicillin stock, 100 mg/ml	1g Ampicillin Autoclaved ddH_2O	Dissolve powder in 10 ml autoclaved ddH_2O. Make 10x 1 ml aliquots and store at -20°C.	To prepare LB agar for screening bacterial colonies.
Ethylene-diamine-tetraacetic acid, disodium salt (EDTA), 0.5M pH 8.0	18.6g EDTA disodium salt powder 1N NaOH ddH_2O*	Dissolve powder in 50 ml ddH_2O and adjust the pH with NaOH. Top up the solution to a final volume of 100 ml. Autoclave.	Preparation of 50x TAE buffer.
Kanamycin stock, 50 mg/ml	0.5g Kanamycin Autoclaved ddH_2O	Dissolve powder in 10 ml autoclaved ddH_2O. Make 10x 1 ml aliquots and store at -20°C.	To prepare LB agar for screening bacterial colonies.
Loading buffer, 10X	0.021g Bromophenol Blue 0.021g Xylene Cyanol 2 ml 0.5M EDTA 5g glycerol ddH_2O	Dissolve components in ca. 10 ml ddH_2O.	For DNA gels.
Lysis buffer	1ml 1M Tris-HCl pH 8.5 100µl 0.5M EDTA 200µl 10% SDS 2ml 1M NaCl, Autoclaved ddH_2O Proteinase K	Dissolve all components in 6.6 ml autoclaved ddH_2O and store at RT. Add Proteinase K freshly just before lysis.	DNA preparation for genotyping.
Parafomaldehyde, 20% (20% PFA)	134g $NA_2HPO_4.2H_2O$ 100g PFA (Sigma) ~10ml NaOH, 32% ~7ml HCl, 37%	Dissolve $NA_2HPO_4.2H_2O$ in 1600 ml autoclaved ddH_2O and heat to 60°C while stirring. Stop heating and add PFA to the heated solution and dissolve completely by adding NaOH. Let the solution cool on ice and adjust pH to 7.4 with HCl. Store at -20°C.	Diluting to 4% PFA.
Parafomaldehyde, 4% (4% PFA)	20% PFA Autoclaved ddH_2O	Dilute 200 ml 20% PFA in 800 ml ddH_2O. Store at 4°C.	Fixative
Phosphate buffered saline, 0.15M (10x PBS)	400g NaCl 10g KCl 58.75g $Na_2HPO_4.2H_2O$ 10g K_2HPO_4	Dissolve components in upto 5 l ddH_2O and autoclave. pH of the solution should be ca.7.4. Store at RT.	Diluting to 1x PBS.
Phosphate buffered saline, 1x (1x PBS)	10x PBS Autoclaved ddH_2O	Dilute 100 ml 10x PBS to 1 l with ddH_2O. Store at RT	Washing for IHC and ICC.
Phosphate buffer, 0.25M (10x PB)	6.5g $NaH_2PO_4.H_2O$ 1.5g NaOH Autoclaved ddH_2O	Dissolve $NaH_2PO_4.H_2O$ in upto 40 ml autoclaved ddH_2O. Adjust pH to 7.4 using NaOH and make up volume to 50 ml with ddH_2O.	To prepare storing solution.

Table 3. Solutions *(continued)*

Solution	Components	Preparation	Use
Poly-D-Lysine (PDL) stock solution, 1 mg/ml	PDL powder ddH_2O Concentration: 1 mg/ml	Dissolve 50 mg PDL powder in sterile ddH_2O to make a stock solution of 1 mg/ml. Filter sterilize. Store 1 ml aliquots at -20°C.	Stock solution for coating of cover slips.
Poly-D-Lysine (PDL) working solution	1 ml PDL stock solution 50 ml ddH_2O	Add 1 ml stock solution to sterile ddH_2O. Filter-sterilize and store it at 4 °C for up to 2 weeks.	Coating of cover slipsfor primary cultures.
Storing solution	30ml Glycerol 30ml Ethyleneglycol 10ml 10x PB Autoclaved ddH_2O	Dissolve the components in 30 ml autoclaved ddH_2O while stirring. Store at 4°C.	To store vibratome sections.
Tris-Acetate-EDTA buffer (TAE), 50x	242g Tris base 57.1ml glacial acetic acid 100ml 0.5M EDTA ddH_2O	Dissolve Tris base in ca. 750 ml ddH_2O . Carefully add glacial acid acid and 0.5M EDTA and adjust the solution to a final volume of 1 l. Autoclave. pH should be ca.8.5.	To prepare 1xTAE electrophoresis buffer for DNA agarose gels.
Tris-Acetate-EDTA buffer** (TAE), 1x	20ml 50x TAE ddH_2O	Dilute 20 ml TAE stock in upto 1 l ddH_2O.	Running buffer for agarose gels.
Tris buffer saline (TBS-5)	20ml 1M Tris-Cl pH 7.8 10.4ml 5M NaCl 4ml 1M KCl 2ml 1M $MgCl_2$ Ultrapure ddH_2O	Add components to 300 ml ddH_2O and make up volume to 400 ml. Filter sterilize. Store at 4°C.	Buffer for suspension of viral pellet after ultracentrifugation.
Tris buffer, 1M pH 7.2	121g Tris base ddH_2O Conc. HCl	Dissolve Tris base in 800 ml ddH_2O. Adjust pH to 8.0 with HCl. Make up volume to 1 l. Autoclave.	To prepare RIPA buffer.
Tris buffer, 1M pH 8.0	121g Tris base ddH_2O Conc. HCl	Dissolve Tris base in 800 ml ddH_2O. Adjust pH to 8.0 with HCl. Make up volume to 1 l. Autoclave.	To prepare various tris-based buffers.
Tris buffer, 10mM pH 8.0	1.21g Tris base ddH_2O Conc. HCl	Dissolve Tris base in 800 ml ddH_2O. Adjust pH to 8.0 with HCl. Make up volume to 1 l. Autoclave.	Dissolving DNA from tails or for cloning.

4.3.4 Media

Table 4. Media for cell and bacterial culture.

Medium	Components	Notes
LB broth	Add 25g LB Broth (Roth) per litre of ddH_2O. Mix and autoclave liquid cycle for 30 min. Add antibiotic after cooling.	Growing bacteria for transformation or cloning.
LB Agar	Add 5g Bacto-tryptone, 2.5g Yeast extract, 5g NaCl* and 7.5g Agar to 500ml ddH_2O. Mix and autoclave liquid cycle for 20 min. Add antibiotic when agar cools to ca. 50-55°C.	Growing bacteria for transformation or cloning. Makes ca. 20x 10cm plates.
Basic medium for retroviral production	DMEM/high glucose/Glutamax (Gibco) 10% Fetal Calf Serum (FCS; Invitrogen) 1x Non-essential Amino Acids (NEAA; 100x, Gibco) 1x Sodium Pyruvate (100x; Gibco)	FCS is heat inactivated at 56°C for 30 min. Medium for growth and expansion of HEK gpg293 cells. Add Tetracycline, Puromycin, G418 and PenStrep. Filter sterilize. Store at 4°C.
Packaging medium	DMEM/high glucose/Glutamax 10% FCS 1x NEAA 1x Sodium Pyruvate	Medium for retroviral packaging after transfection. Without Tetracycline. Filter sterilize. Store at 4°C.
Opti-MEM, 10%	Opti-MEM (Gibco) 10% FCS	Medium for transfection for retroviral production.
Astrocyte Plating medium	DMEM:F12 (Gibco) 10% FCS 1x PenStrep (100x; Sigma) 10 ng/ml EGF (10 µg/ml; Invitrogen) 10 ng/ml bFGF (10 µg/ml; Invitrogen)	Medium for growing and seeding postnatal astrocytes. No filter steritization.
Astrocyte differentiation medium	DMEM:F12 (Gibco) 1x PenStrep (100x, Sigma) B27 supplement (Gibco)	Medium for growing seeded postnatal astrocytes 24h after transduction.
E14 Plating medium	DMEM-Glutamax (Gibco) 10% FCS 1x PenStrep (100x)	Medium for plating E14 cortical cells. No filter steritization.
E14 differentiation medium	DMEM-Glutamax (Gibco) 1x PenStrep (100x) B27 supplement	Medium for neuronal differentiation of E14 cortical culture. No filter steritization. Add 1ml B27 to 50ml medium.

* LB agar plates without NaCl used for growing retro- and lentiviral vectors.

5 Appendix

5.1 Appendix 1: List of abbreviations

AChR	acetylcholine receptor
AcOr	acridine orange
AMPA	α-amino-3-hydroxy-5-methyl-4-isoxazolepropionic acid receptor
aNSC	adult neural stem cell
AON	anterior olfactory nucleus
ARA-C	Arabinofuranosyl Cytidine
ASLV-A	avian sarcoma and leukosis virus type-A
BDNF	brain-derived neurotrophic factor
bFGF	basic fibroblast growth factor
BLBP	brain lipid-binding protein
BrdU	bromodeoxyuridine
BSA	bovine serum albumin
CAG	chicken-b-actin
cAMP	cyclic adenosine monophosphate
ChAT	choline acetyltransferase
cDNA	complementary deoxyribonucleic acid
CNS	central nervous system
CREB	cAMP response element-binding
CVS	challenged virus strain
DAPI	4',6-diamidino-2-phenylindole

Dcx	doublecortin
ddH2O	double-distilled water
DiI	1,1'-dioctadecyl-3,3,3',3'-tetramethyl-indocarbocyanine perchlorate
DNA	deoxyribonucleic acid
dNTP	deoxyNucleotide triphosphate
DPBS	Dulbecco's phosphate buffered saline
E14	embryonic day 14
EB	Evans blue
EDTA	ethylenediaminetetraacetic acid
EGF	epidermal growth factor
eGFP	enhanced green fluorescent protein
EnvA	envelope protein of ASLV-A
EPL	external plexiform layer
FCS	fetal calf serum
G	rabies virus glycoprotein
GABA	g-amino-butyric acid
GFAP	glial fibrillary acidic protein
GCL	granule cell layer
GL	glomerular layer
GPI	glycophosphatidylinositol
h	hours
HBSS	Hank's buffered salt solution
HEK	human embryonic kidney
HIPP	hilar perforant path-associated
HICAP	hilar commissural/associational pathway-associated
HMG	high mobility group
HRP	horseradish peroxidase
HSV	herpes simplex virus
5-HT	5-hydroxytryptophan
Hz	Hertz

IP	intermediate progenitors
IPSC	inhibitory postsynaptic currents
IRES	internal ribosomal entry site
KCC2	neuronal potassium chloride co-transporter
kHz	kiloHertz
L	rabies virus RNA-dependent RNA polymerase
l	litre
LEC	lateral entorhinal cortex
LGE	lateral ganglionic eminence
LOT	lateral olfactory tract
LTP	long term potentiation
LTR	long terminal repeat
M	rabies virus matrix protein
MCL	mitral cell layer
MCS	multiple cloning site
MEC	medial entorhinal cortex
ml	millilitre
mM	millmolar
MMLV	Moloney murine leukemia virus
MOI	multiplicity of infection
MOPP	molecular layer perforant path-associated
mOsm	milliosmoles
MP-1	mouse protamine-1 gene
mRNA	messenger ribonucleic acid
MS	medial septum
ms	millisecond
N	rabies virus nucleoprotein
n	number of samples
NCAM	neural cell adhesion molecule
NDB	nucleus of the diagonal band of Broca

NSC	neural stem cell
NKCC1	sodium potassium chloride co-transporter
NMDAR	N-Methyl-D-aspartate receptor
NPY	neuropeptide Y
P	rabies virus phosphoprotein
PBS	phosphate buffered saline
PCR	polymerase chain reaction
PFA	paraformaldehyde
PGC	periglomerular cell
PHA	Phasolus vulgaris agglutinin
PrV	pseudorabies virus
PSA-NCAM	polysialated-neural cell adhesion molecule
PVDF	Polyvinylidene fluoride
RABV	EnvA-pseudotyped rabies virus
RFP	red fluorescent protein
RITC	Rhodamine isothiocyanate
RMS	rostral migratory stream
RNA	ribonucleic acid
rpm	rotations per minute
RT	room temperature
s	second
SAD	street alabama dufferin
SEZ	subependymal zone
SGZ	subgranular zone
SRY	Sex-determining region Y
TAP	transit amplifying precursor
TBS	tris buffered saline
TE	tris-HCl EDTA
TG1	TVA transgene primer 1
TG2	TVA transgene primer 2

TH	tyrosine hydroxylase
TTC	tetanus toxin
TVA	tumor virus A
VGLUT	vesicular glutamate transporter
VSV	vesicular stomatitis virus
VSVG	vesicular stomatitis virus glycoprotein
VTA	ventral tegmental area
WGA	wheat germ agglutinin
µM	micrometer

5.2 Appendix 2: List of figures

Fig. 1.1 Sites of neurogenesis in the adult brain.

Fig. 1.2 Trisynaptic loop of hippocampal circuitry.

Fig. 1.3 Schematic of afferent inputs to the dentate gyrus.

Fig. 1.4 Hippocampal neurogenesis.

Fig. 1.5 Cellular organization of the olfactory bulb.

Fig. 1.6 Schematic of afferent inputs to the olfactory bulb.

Fig. 1.7 Subependymal zone neurogenesis.

Fig. 1.8 Transneuronal transfer of tracer using conventional methods.

Fig. 1.9 Transneuronal transfer of tracer using viral tracers.

Fig. 1.10 Rabies virion.

Fig. 1.11 Monosynaptic tracing technique.

Fig. 2.1 Graphical abstract.

Fig. 2.2 First generation of retroviral constructs and RABV vector.

Fig. 2.3 Transduction of E14 cortical cultures.

Fig. 2.4 Mechanism of 2A peptide co-translational cleavage.

Fig. 2.5 Glycoprotein expression from retroviral constructs.

Fig. 2.6 Glycoprotein expression from retroviral constructs.

Fig. 2.7 Monoclonal antibody against TVA.

Fig. 2.8 Transduction of E14 cortical cultures and synaptic connectivity.

Fig. 2.9 Transduction of E14 cortical culture with G-pseudotyped RABV.

Fig. 2.10 Transduction of postnatal astrocytes with RABV.

Fig. 2.11 Transduction of postnatal astrocytes with SAD L16 RABV.

Fig. 2.12 Implementation of the tracing technique in the adult dentate gyrus.

Fig. 2.13 Voluntary exercise increases neurogenesis.

Fig. 2.14 Transsynaptic tracing in the adult dentate gyrus.

Fig. 2.15 Transsynaptic tracing in the adult dentate gyrus.

Fig. 2.16 Location of transsynaptically labelled neurons.

Fig. 2.17 Axonal arborisation of EnvA-pseudotyped RABV-traced dentate interneurons.

Fig. 2.18 Phenotypic characterisation of EnvA-pseudotyped RABV-traced interneurons.

Fig. 2.19 Dependence of EnvA-pseudotyped RABV infection on TVA expression.

Fig. 2.20 Cell poplulations infected with G-pseudotyped RABV.

Fig. 2.21 Transsynaptically traced putative mossy cells.

Fig. 2.22 EnvA-pseudotyped RABV-labelled glial cells.

Fig. 2.23 Monosynaptically traced neurons in the basal forebrain.

Fig. 2.24 Monosynaptically traced cortical projections.

Fig. 2.25 Transsynaptically traced neurons in the subiculum.

Fig. 2.26 Pseudotransduction of TVA.

Fig. 2.27 Pseudotransduction of TVA.

Fig. 2.28 Pseudotransduction of TVA.

Fig. 2.29 Cell types labelled with EnvA-pseudotyped RABV in hGFAP-TVA mice.

Fig. 2.30 Cell types labelled with EnvA-pseudotyped RABV in hGFAP-TVA mice.

Fig. 2.31 Cell types labelled with EnvA-pseudotyped RABV in hGFAP-TVA mice.

Fig. 2.32 Schematic of monosynaptic tracing in hGFAP-TVA mice.

Fig. 2.33 EnvA-pseudotyped RABV-traced neurons in the dentate gyrus of

hGFAP-TVA mice.

Fig. 2.34 EnvA-pseudotpyed RABV-traced putative mossy cells in hGFAP-TVA mice.

Fig. 2.35 Cholinergic projections to adult-generated neurons in hGFAP-TVA mice.

Fig. 2.36 Implementation of the tracing technique in the adult olfactory bulb.

Fig. 2.37 Adult-generated granule cells in the olfactory bulb.

Fig. 2.38 Adult-generated periglomerular cells in the olfactory bulb.

Fig. 2.39 EnvA-pseudotpyed RABV-traced neurons in the olfactory bulb.

Fig. 2.40 EnvA-pseudotpyed RABV-traced neurons in the olfactory bulb.

Fig. 2.41 EnvA-pseudotpyed RABV-traced neurons in the olfactory bulb.

Fig. 2.42 Absence of mitral cell labelling by RABV.

Fig. 2.43 Monosynaptically traced long-distance projections to adult-generated neurons in the olfactory system.

Fig. 3.1 Temporal pattern of presynaptic connectivity of newborn dentate granule neurons.

Fig. 3.2 Feedforward mechanism of disinhibition by Blanes cells.

6 Bibliography

Ahn, S. and A. L. Joyner (2005). “In vivo analysis of quiescent adult neural stem cells responding to Sonic hedgehog.” Nature 437(7060): 894-897.

Aimone, J. B., W. Deng, et al. (2011). “Resolving new memories: a critical look at the dentate gyrus, adult neurogenesis, and pattern separation.” Neuron 70(4): 589-596.

Alme, C. B., R. A. Buzzetti, et al. (2010). “Hippocampal granule cells opt for early retirement.” Hippocampus 20(10): 1109-1123.

Alonso, M., G. Lepousez, et al. (2012). “Activation of adult-born neurons facilitates learning and memory.” Nat Neurosci.

Altman, J. (1969). “Autoradiographic and histological studies of postnatal neurogenesis. IV. Cell proliferation and migration in the anterior forebrain, with special reference to persisting neurogenesis in the olfactory bulb.” J Comp Neurol 137(4): 433-457.

Altman, J. and G. D. Das (1965). “Autoradiographic and histological evidence of postnatal hippocampal neurogenesis in rats.” J Comp Neurol 124(3): 319-335.

Alvarez-Buylla, A. and D. A. Lim (2004). “For the long run: maintaining germinal niches in the adult brain.” Neuron 41(5): 683-686.

Amaral, D. G., H. E. Scharfman, et al. (2007). “The dentate gyrus: fundamental neuroanatomical organization (dentate gyrus for dummies).” Prog Brain Res 163: 3-22.

Anderson, S. A., D. D. Eisenstat, et al. (1997). “Interneuron migration from basal forebrain to neocortex: dependence on Dlx genes.” Science 278(5337): 474-476.

Arenkiel, B. R. (2011). “Genetic approaches to reveal the connectivity of adult-born neurons.” Front Neurosci 5: 48.

Arenkiel, B. R., H. Hasegawa, et al. (2011). “Activity-induced remodeling of olfactory bulb microcircuits revealed by monosynaptic tracing.” PLoS One 6(12): e29423.

Astic, L., D. Saucier, et al. (1993). “The CVS strain of rabies virus as transneuronal tracer in the olfactory system of mice.” Brain Res 619(1-2): 146-156.

Aungst, J. L., P. M. Heyward, et al. (2003). “Centre-surround inhibition among olfactory bulb glomeruli.” Nature 426(6967): 623-629.

Bardy, C., M. Alonso, et al. (2010). “How, when, and where new inhibitory neurons release neurotransmitters in the adult olfactory bulb.” J Neurosci 30(50): 17023-17034.

Barkho, B. Z., H. Song, et al. (2006). “Identification of astrocyte-expressed factors that modulate neural stem/progenitor cell differentiation.” Stem Cells Dev 15(3): 407-421.

Barnard, R. J., D. Elleder, et al. (2006). "Avian sarcoma and leukosis virus-receptor interactions: from classical genetics to novel insights into virus-cell membrane fusion." Virology 344(1): 25-29.

Bates, P., J. A. Young, et al. (1993). "A receptor for subgroup A Rous sarcoma virus is related to the low density lipoprotein receptor." Cell 74(6): 1043-1051.

Beier, K. T., A. Saunders, et al. (2011). "Anterograde or retrograde transsynaptic labeling of CNS neurons with vesicular stomatitis virus vectors." Proc Natl Acad Sci U S A 108(37): 15414-15419.

Belluzzi, O., M. Benedusi, et al. (2003). "Electrophysiological differentiation of new neurons in the olfactory bulb." J Neurosci 23(32): 10411-10418.

Ben-Ari, Y. and E. Cherubini (1991). "Zinc and GABA in developing brain." Nature 353(6341): 220.

Bergami, M. and B. Berninger (2012). "A fight for survival: the challenges faced by a newborn neuron integrating in the adult hippocampus." Dev Neurobiol 72(7): 1016-1031.

Bergami, M., R. Rimondini, et al. (2008). "Deletion of TrkB in adult progenitors alters newborn neuron integration into hippocampal circuits and increases anxiety-like behavior." Proc Natl Acad Sci U S A 105(40): 15570-15575.

Bergmann, O., J. Liebl, et al. (2012). "The age of olfactory bulb neurons in humans." Neuron 74(4): 634-639.

Bolteus, A. J. and A. Bordey (2004). "GABA release and uptake regulate neuronal precursor migration in the postnatal subventricular zone." J Neurosci 24(35): 7623-7631.

Bonaguidi, M. A., M. A. Wheeler, et al. (2011). "In vivo clonal analysis reveals self-renewing and multipotent adult neural stem cell characteristics." Cell 145(7): 1142-1155.

Bovetti, S., Y. C. Hsieh, et al. (2007). "Blood vessels form a scaffold for neuroblast migration in the adult olfactory bulb." J Neurosci 27(22): 5976-5980.

Breton-Provencher, V., M. Lemasson, et al. (2009). "Interneurons produced in adulthood are required for the normal functioning of the olfactory bulb network and for the execution of selected olfactory behaviors." J Neurosci 29(48): 15245-15257.

Breton-Provencher, V. and A. Saghatelyan (2012). "Newborn neurons in the adult olfactory bulb: unique properties for specific odor behavior." Behav Brain Res 227(2): 480-489.

Brill, M. S., J. Ninkovic, et al. (2009). "Adult generation of glutamatergic olfactory bulb interneurons." Nat Neurosci 12(12): 1524-1533.

Burns, J. C., T. Friedmann, et al. (1993). "Vesicular stomatitis virus G glycoprotein pseudotyped retroviral vectors: concentration to very high titer and efficient gene transfer into mammalian and nonmammalian cells." Proc Natl Acad Sci U S A 90(17): 8033-8037.

Caiazzo, M., M. T. Dell'Anno, et al. (2011). "Direct generation of functional dopaminergic neurons from mouse and human fibroblasts." Nature 476(7359): 224-227.

Cajal, S. R. Y. (1928). Degeneration and Regeneration of the Nervous System. . New York, Hafner.

Callaway, E. M. (2008). "Transneuronal circuit tracing with neurotropic viruses." Curr Opin Neurobiol 18(6): 617-623.

Calvo, C. F., R. H. Fontaine, et al. (2011). "Vascular endothelial growth factor receptor 3 directly regulates murine neurogenesis." Genes Dev 25(8): 831-844.

Cameron, H. A., B. S. McEwen, et al. (1995). "Regulation of adult neurogenesis by excitatory input and NMDA receptor activation in the dentate gyrus." J Neurosci 15(6): 4687-4692.

Cameron, H. A., C. S. Woolley, et al. (1993). "Differentiation of newly born neurons and glia in the dentate gyrus of the adult rat." Neuroscience 56(2): 337-344.

Campbell, N. R., C. C. Fernandes, et al. (2010). "Endogenous signaling through alpha7-containing nicotinic receptors promotes maturation and integration of adult-born neurons in the hippocampus." J Neurosci 30(26): 8734-8744.

Card, J. P., L. Rinaman, et al. (1993). "Pseudorabies virus infection of the rat central nervous system: ultrastructural characterization of viral replication, transport, and pathogenesis." J Neurosci 13(6): 2515-2539.

Card, J. P., L. Rinaman, et al. (1990). "Neurotropic properties of pseudorabies virus: uptake and transneuronal passage in the rat central nervous system." J Neurosci 10(6): 1974-1994.

Carleton, A., L. T. Petreanu, et al. (2003). "Becoming a new neuron in the adult olfactory bulb." Nat Neurosci 6(5): 507-518.

Carleton, A., C. Rochefort, et al. (2002). "Making scents of olfactory neurogenesis." J Physiol Paris 96(1-2): 115-122.

Charlton, K. M. and G. A. Casey (1979). "Experimental rabies in skunks: immunofluorescence light and electron microscopic studies." Lab Invest 41(1): 36-44.

Choi, J. and E. M. Callaway (2011). "Monosynaptic inputs to ErbB4-expressing inhibitory neurons in mouse primary somatosensory cortex." J Comp Neurol 519(17): 3402-3414.

Claiborne, B. J., D. G. Amaral, et al. (1986). "A light and electron microscopic analysis of the mossy fibers of the rat dentate gyrus." J Comp Neurol 246(4): 435-458.

Clelland, C. D., M. Choi, et al. (2009). "A functional role for adult hippocampal neurogenesis in spatial pattern separation." Science 325(5937): 210-213.

Conzelmann, K. K., J. H. Cox, et al. (1990). "Molecular cloning and complete nucleotide sequence of the attenuated rabies virus SAD B19." Virology 175(2): 485-499.

Cooper-Kuhn, C. M., J. Winkler, et al. (2004). "Decreased neurogenesis after cholinergic forebrain lesion in the adult rat." J Neurosci Res 77(2): 155-165.

Creer, D. J., C. Romberg, et al. (2010). "Running enhances spatial pattern separation in mice." Proc Natl Acad Sci U S A 107(5): 2367-2372.

Crews, F. T. and K. Nixon (2003). "Alcohol, neural stem cells, and adult neurogenesis." Alcohol Res Health 27(2): 197-204.

Desmaisons, D., J. D. Vincent, et al. (1999). "Control of action potential timing by intrinsic subthreshold oscillations in olfactory bulb output neurons." J Neurosci 19(24): 10727-10737.

Dietzschold, B., J. Li, et al. (2008). "Concepts in the pathogenesis of rabies." Future Virol 3(5): 481-490.

Doetsch, F., I. Caille, et al. (1999). "Subventricular zone astrocytes are neural stem cells in the adult mammalian brain." Cell 97(6): 703-716.

Donnelly, M. L., L. E. Hughes, et al. (2001). "The 'cleavage' activities of foot-and-mouth disease virus 2A site-directed mutants and naturally occurring '2A-like' sequences." J Gen Virol 82(Pt 5): 1027-1041.

Donnelly, M. L., G. Luke, et al. (2001). "Analysis of the aphthovirus 2A/2B polyprotein 'cleavage' mechanism indicates not a proteolytic reaction, but a novel translational effect: a putative ribosomal 'skip'." J Gen Virol 82(Pt 5): 1013-1025.

Duman, R. S., S. Nakagawa, et al. (2001). “Regulation of adult neurogenesis by antidepressant treatment.” Neuropsychopharmacology 25(6): 836-844.

Elleder, D., D. C. Melder, et al. (2004). “Two different molecular defects in the Tva receptor gene explain the resistance of two tvar lines of chickens to infection by subgroup A avian sarcoma and leukosis viruses.” J Virol 78(24): 13489-13500.

Encinas, J. M., T. V. Michurina, et al. (2011). “Division-coupled astrocytic differentiation and age-related depletion of neural stem cells in the adult hippocampus.” Cell Stem Cell 8(5): 566-579.

Ennis, M., L. A. Zimmer, et al. (1996). “Olfactory nerve stimulation activates rat mitral cells via NMDA and non-NMDA receptors in vitro.” Neuroreport 7(5): 989-992.

Eriksson, P. S., E. Perfilieva, et al. (1998). “Neurogenesis in the adult human hippocampus.” Nat Med 4(11): 1313-1317.

Esposito, M. S., V. C. Piatti, et al. (2005). “Neuronal differentiation in the adult hippocampus recapitulates embryonic development.” J Neurosci 25(44): 10074-10086.

Etessami, R., K. K. Conzelmann, et al. (2000). “Spread and pathogenic characteristics of a G-deficient rabies virus recombinant: an in vitro and in vivo study.” J Gen Virol 81(Pt 9): 2147-2153.

Evinger, C. and J. T. Erichsen (1986). “Transsynaptic retrograde transport of fragment C of tetanus toxin demonstrated by immunohistochemical localization.” Brain Res 380(2): 383-388.

Eyre, M. D., M. Antal, et al. (2008). “Distinct deep short-axon cell subtypes of the main olfactory bulb provide novel intrabulbar and extrabulbar GABAergic connections.” J Neurosci 28(33): 8217-8229.

Ferrante, M., M. Migliore, et al. (2009). “Feed-forward inhibition as a buffer of the neuronal input-output relation.” Proc Natl Acad Sci U S A 106(42): 18004-18009.

Finke, S., R. Mueller-Waldeck, et al. (2003). “Rabies virus matrix protein regulates the balance of virus transcription and replication.” J Gen Virol 84(Pt 6): 1613-1621.

Freund, T. F. and G. Buzsaki (1996). “Interneurons of the hippocampus.” Hippocampus 6(4): 347-470.

Ge, S., E. L. Goh, et al. (2006). “GABA regulates synaptic integration of newly generated neurons in the adult brain.” Nature 439(7076): 589-593.

Ge, S., D. A. Pradhan, et al. (2007). “GABA sets the tempo for activity-dependent adult neurogenesis.” Trends Neurosci 30(1): 1-8.

Geering, B., J. Schmidt-Mende, et al. (2011). “Protein overexpression following lentiviral infection of primary mature neutrophils is due to pseudotransduction.” J Immunol Methods 373(1-2): 209-218.

Gheusi, G., H. Cremer, et al. (2000). “Importance of newly generated neurons in the adult olfactory bulb for odor discrimination.” Proc Natl Acad Sci U S A 97(4): 1823-1828.

Godement, P., J. Vanselow, et al. (1987). “A study in developing visual systems with a new method of staining neurones and their processes in fixed tissue.” Development 101(4): 697-713.

Goldman, S. A. and F. Nottebohm (1983). “Neuronal production, migration, and differentiation in a vocal control nucleus of the adult female canary brain.” Proc Natl Acad Sci U S A 80(8): 2390-2394.

Gould, E., A. J. Reeves, et al. (1999). “Hippocampal neurogenesis in adult Old World primates.”

Proc Natl Acad Sci U S A 96(9): 5263-5267.

Gritti, A., L. Bonfanti, et al. (2002). "Multipotent neural stem cells reside into the rostral extension and olfactory bulb of adult rodents." J Neurosci 22(2): 437-445.

Haas, D. L., S. S. Case, et al. (2000). "Critical factors influencing stable transduction of human CD34(+) cells with HIV-1-derived lentiviral vectors." Mol Ther 2(1): 71-80.

Hack, M. A., A. Saghatelyan, et al. (2005). "Neuronal fate determinants of adult olfactory bulb neurogenesis." Nat Neurosci 8(7): 865-872.

Hafting, T., M. Fyhn, et al. (2005). "Microstructure of a spatial map in the entorhinal cortex." Nature 436(7052): 801-806.

Halasy, K., R. Miettinen, et al. (1992). "GABAergic Interneurons are the Major Postsynaptic Targets of Median Raphe Afferents in the Rat Dentate Gyrus." Eur J Neurosci 4(2): 144-153.

Halasy, K. and P. Somogyi (1993). "Subdivisions in the multiple GABAergic innervation of granule cells in the dentate gyrus of the rat hippocampus." Eur J Neurosci 5(5): 411-429.

Harrison, P. J., H. Hultborn, et al. (1984). "Labelling of interneurones by retrograde transsynaptic transport of horseradish peroxidase from motoneurones in rats and cats." Neurosci Lett 45(1): 15-19.

Heinrich, C., S. Gascon, et al. (2011). "Generation of subtype-specific neurons from postnatal astroglia of the mouse cerebral cortex." Nat Protoc 6(2): 214-228.

Henze, D. A., L. Wittner, et al. (2002). "Single granule cells reliably discharge targets in the hippocampal CA3 network in vivo." Nat Neurosci 5(8): 790-795.

Holland, E. C., W. P. Hively, et al. (1998). "A constitutively active epidermal growth factor receptor cooperates with disruption of G1 cell-cycle arrest pathways to induce glioma-like lesions in mice." Genes Dev 12(23): 3675-3685.

Holland, E. C. and H. E. Varmus (1998). "Basic fibroblast growth factor induces cell migration and proliferation after glia-specific gene transfer in mice." Proc Natl Acad Sci U S A 95(3): 1218-1223.

Houser, C. R. (2007). "Interneurons of the dentate gyrus: an overview of cell types, terminal fields and neurochemical identity." Prog Brain Res 163: 217-232.

Hsia, A. Y., J. D. Vincent, et al. (1999). "Dopamine depresses synaptic inputs into the olfactory bulb." J Neurophysiol 82(2): 1082-1085.

Huh, Y., M. S. Oh, et al. (2010). "Gene transfer in the nervous system and implications for transsynaptic neuronal tracing." Expert Opin Biol Ther 10(5): 763-772.

Imayoshi, I. and R. Kageyama (2011). "The role of Notch signaling in adult neurogenesis." Mol Neurobiol 44(1): 7-12.

Imayoshi, I., M. Sakamoto, et al. (2008). "Roles of continuous neurogenesis in the structural and functional integrity of the adult forebrain." Nat Neurosci 11(10): 1153-1161.

Jackson, A. C. (2002). "Rabies pathogenesis." J Neurovirol 8(4): 267-269.

Jackson, A. C., Wunner, W.H. (2007). Rabies, Elsevier.

Johansson, C. B., S. Momma, et al. (1999). "Identification of a neural stem cell in the adult mammalian central nervous system." Cell 96(1): 25-34.

Kaplan, M. S. and D. H. Bell (1984). "Mitotic neuroblasts in the 9-day-old and 11-month-old

rodent hippocampus." J Neurosci 4(6): 1429-1441.

Kaplan, M. S. and J. W. Hinds (1977). "Neurogenesis in the adult rat: electron microscopic analysis of light radioautographs." Science 197(4308): 1092-1094.

Katona, I., L. Acsady, et al. (1999). "Postsynaptic targets of somatostatin-immunoreactive interneurons in the rat hippocampus." Neuroscience 88(1): 37-55.

Kee, N., C. M. Teixeira, et al. (2007). "Preferential incorporation of adult-generated granule cells into spatial memory networks in the dentate gyrus." Nat Neurosci 10(3): 355-362.

Kelly, R. M. and P. L. Strick (2000). "Rabies as a transneuronal tracer of circuits in the central nervous system." J Neurosci Methods 103(1): 63-71.

Kelsch, W., C. W. Lin, et al. (2008). "Sequential development of synapses in dendritic domains during adult neurogenesis." Proc Natl Acad Sci U S A 105(43): 16803-16808.

Kempermann, G., H. G. Kuhn, et al. (1997). "More hippocampal neurons in adult mice living in an enriched environment." Nature 386(6624): 493-495.

Kheirbek, M. A., L. Tannenholz, et al. (2012). "NR2B-Dependent Plasticity of Adult-Born Granule Cells is Necessary for Context Discrimination." J Neurosci 32(25): 8696-8702.

Kim, E. J., J. L. Ables, et al. (2011). "Ascl1 (Mash1) defines cells with long-term neurogenic potential in subgranular and subventricular zones in adult mouse brain." PLoS One 6(3): e18472.

Klingen, Y., K. K. Conzelmann, et al. (2008). "Double-labeled rabies virus: live tracking of enveloped virus transport." J Virol 82(1): 237-245.

Knoth, R., I. Singec, et al. (2010). "Murine features of neurogenesis in the human hippocampus across the lifespan from 0 to 100 years." PLoS One 5(1): e8809.

Kobbert, C., R. Apps, et al. (2000). "Current concepts in neuroanatomical tracing." Prog Neurobiol 62(4): 327-351.

Kohler, C. (1985). "Intrinsic projections of the retrohippocampal region in the rat brain. I. The subicular complex." J Comp Neurol 236(4): 504-522.

Kohler, C., L. G. Eriksson, et al. (1987). "Co-localization of neuropeptide tyrosine and somatostatin immunoreactivity in neurons of individual subfields of the rat hippocampal region." Neurosci Lett 78(1): 1-6.

Kosaka, K., K. Toida, et al. (1998). "How simple is the organization of the olfactory glomerulus?: the heterogeneity of so-called periglomerular cells." Neurosci Res 30(2): 101-110.

Kosaka, T. and K. Kosaka (2010). "Heterogeneity of calbindin-containing neurons in the mouse main olfactory bulb: I. General description." Neurosci Res 67(4): 275-292.

Kosaka, T. and K. Kosaka (2011). ""Interneurons" in the olfactory bulb revisited." Neurosci Res 69(2): 93-99.

Kosofsky, B. E. and M. E. Molliver (1987). "The serotoninergic innervation of cerebral cortex: different classes of axon terminals arise from dorsal and median raphe nuclei." Synapse 1(2): 153-168.

Kriegstein, A. and A. Alvarez-Buylla (2009). "The glial nature of embryonic and adult neural stem cells." Annu Rev Neurosci 32: 149-184.

Kuhn, H. G., H. Dickinson-Anson, et al. (1996). "Neurogenesis in the dentate gyrus of the adult rat: age-related decrease of neuronal progenitor proliferation." J Neurosci 16(6): 2027-2033.

Kukekov, V. G., E. D. Laywell, et al. (1999). “Multipotent stem/progenitor cells with similar properties arise from two neurogenic regions of adult human brain.” Exp Neurol 156(2): 333-344.

Kuypers, H. G. and G. Ugolini (1990). “Viruses as transneuronal tracers.” Trends Neurosci 13(2): 71-75.

Lazarini, F., M. A. Mouthon, et al. (2009). “Cellular and behavioral effects of cranial irradiation of the subventricular zone in adult mice.” PLoS One 4(9): e7017.

Lentz, T. L., T. G. Burrage, et al. (1982). “Is the acetylcholine receptor a rabies virus receptor?” Science 215(4529): 182-184.

Leranth, C. and M. Frotscher (1983). “Commissural afferents to the rat hippocampus terminate on vasoactive intestinal polypeptide-like immunoreactive non-pyramidal neurons. An EM immunocytochemical degeneration study.” Brain Res 276(2): 357-361.

Leranth, C. and T. Hajszan (2007). “Extrinsic afferent systems to the dentate gyrus.” Prog Brain Res 163: 63-84.

Leutgeb, J. K., S. Leutgeb, et al. (2007). “Pattern separation in the dentate gyrus and CA3 of the hippocampus.” Science 315(5814): 961-966.

Lever, A. M., P. M. Strappe, et al. (2004). “Lentiviral vectors.” J Biomed Sci 11(4): 439-449.
Li, Y., Y. Mu, et al. (2009). “Development of neural circuits in the adult hippocampus.” Curr Top Dev Biol 87: 149-174.

Lie, D. C., S. A. Colamarino, et al. (2005). “Wnt signalling regulates adult hippocampal neurogenesis.” Nature 437(7063): 1370-1375.

Lisman, J. (2011). “Formation of the non-functional and functional pools of granule cells in the dentate gyrus: role of neurogenesis, LTP and LTD.” J Physiol 589(Pt 8): 1905-1909.

Lledo, P. M., M. Alonso, et al. (2006). “Adult neurogenesis and functional plasticity in neuronal circuits.” Nat Rev Neurosci 7(3): 179-193.

Lledo, P. M., F. T. Merkle, et al. (2008). “Origin and function of olfactory bulb interneuron diversity.” Trends Neurosci 31(8): 392-400.

Lledo, P. M., A. Saghatelyan, et al. (2004). “Inhibitory interneurons in the olfactory bulb: from development to function.” Neuroscientist 10(4): 292-303.

Lois, C. and A. Alvarez-Buylla (1994). “Long-distance neuronal migration in the adult mammalian brain.” Science 264(5162): 1145-1148.

Lois, C., J. M. Garcia-Verdugo, et al. (1996). “Chain migration of neuronal precursors.” Science 271(5251): 978-981.

Lopez-Garcia, C., A. Molowny, et al. (1988). “Delayed postnatal neurogenesis in the cerebral cortex of lizards.” Brain Res 471(2): 167-174.

Lugert, S., O. Basak, et al. (2010). “Quiescent and active hippocampal neural stem cells with distinct morphologies respond selectively to physiological and pathological stimuli and aging.” Cell Stem Cell 6(5): 445-456.

Lugert, S., M. Vogt, et al. (2012). “Homeostatic neurogenesis in the adult hippocampus does not involve amplification of Ascl1(high) intermediate progenitors.” Nat Commun 3: 670.

Luskin, M. B. (1993). “Restricted proliferation and migration of postnatally generated neurons derived from the forebrain subventricular zone.” Neuron 11(1): 173-189.

Ma, D. K., M. A. Bonaguidi, et al. (2009). “Adult neural stem cells in the mammalian central

nervous system." Cell Res 19(6): 672-682.

Mak, G. K., E. K. Enwere, et al. (2007). "Male pheromone-stimulated neurogenesis in the adult female brain: possible role in mating behavior." Nat Neurosci 10(8): 1003-1011.

Malberg, J. E., A. J. Eisch, et al. (2000). "Chronic antidepressant treatment increases neurogenesis in adult rat hippocampus." J Neurosci 20(24): 9104-9110.

Markwardt, S. J., J. I. Wadiche, et al. (2009). "Input-specific GABAergic signaling to newborn neurons in adult dentate gyrus." J Neurosci 29(48): 15063-15072.

Marshel, J. H., T. Mori, et al. (2010). "Targeting single neuronal networks for gene expression and cell labeling in vivo." Neuron 67(4): 562-574.

Martin, L. A., S. S. Tan, et al. (2002). "Clonal architecture of the mouse hippocampus." J Neurosci 22(9): 3520-3530.

Masiulis, I., S. Yun, et al. (2011). "The interesting interplay between interneurons and adult hippocampal neurogenesis." Mol Neurobiol 44(3): 287-302.

Mebatsion, T., M. Konig, et al. (1996). "Budding of rabies virus particles in the absence of the spike glycoprotein." Cell 84(6): 941-951.

Mebatsion, T., F. Weiland, et al. (1999). "Matrix protein of rabies virus is responsible for the assembly and budding of bullet-shaped particles and interacts with the transmembrane spike glycoprotein G." J Virol 73(1): 242-250.

Merkle, F. T., Z. Mirzadeh, et al. (2007). "Mosaic organization of neural stem cells in the adult brain." Science 317(5836): 381-384.

Miller, M. W. and R. S. Nowakowski (1988). "Use of bromodeoxyuridine-immunohistochemistry to examine the proliferation, migration and time of origin of cells in the central nervous system." Brain Res 457(1): 44-52.

Ming, G. L. and H. Song (2005). "Adult neurogenesis in the mammalian central nervous system." Annu Rev Neurosci 28: 223-250.

Ming, G. L. and H. Song (2011). "Adult neurogenesis in the mammalian brain: significant answers and significant questions." Neuron 70(4): 687-702.

Miyamichi, K., F. Amat, et al. (2011). "Cortical representations of olfactory input by trans-synaptic tracing." Nature 472(7342): 191-196.

Mizrahi, A. and L. C. Katz (2003). "Dendritic stability in the adult olfactory bulb." Nat Neurosci 6(11): 1201-1207.

Mohapel, P., G. Leanza, et al. (2005). "Forebrain acetylcholine regulates adult hippocampal neurogenesis and learning." Neurobiol Aging 26(6): 939-946.

Molyneaux, B. J., P. Arlotta, et al. (2007). "Neuronal subtype specification in the cerebral cortex." Nat Rev Neurosci 8(6): 427-437.

Mongiat, L. A. and A. F. Schinder (2011). "Adult neurogenesis and the plasticity of the dentate gyrus network." Eur J Neurosci 33(6): 1055-1061.

Morshead, C. M., B. A. Reynolds, et al. (1994). "Neural stem cells in the adult mammalian forebrain: a relatively quiescent subpopulation of subependymal cells." Neuron 13(5): 1071-1082.

Moser, E. I. (2011). "The multi-laned hippocampus." Nat Neurosci 14(4): 407-408.

Myers, C. E. and H. E. Scharfman (2009). "A role for hilar cells in pattern separation in the

dentate gyrus: a computational approach." Hippocampus 19(4): 321-337.

Nakashiba, T., J. D. Cushman, et al. (2012). "Young Dentate Granule Cells Mediate Pattern Separation, whereas Old Granule Cells Facilitate Pattern Completion." Cell 149(1): 188-201.

Nassi, J. J. and E. M. Callaway (2007). "Specialized circuits from primary visual cortex to V2 and area MT." Neuron 55(5): 799-808.

Nissant, A. and M. Pallotto (2011). "Integration and maturation of newborn neurons in the adult olfactory bulb--from synapses to function." Eur J Neurosci 33(6): 1069-1077.

Norgren, R. B., Jr. and M. N. Lehman (1998). "Herpes simplex virus as a transneuronal tracer." Neurosci Biobehav Rev 22(6): 695-708.

O'Mara, S. (2005). "The subiculum: what it does, what it might do, and what neuroanatomy has yet to tell us." J Anat 207(3): 271-282.

Osakada, F., T. Mori, et al. (2011). "New rabies virus variants for monitoring and manipulating activity and gene expression in defined neural circuits." Neuron 71(4): 617-631.

Palmer, T. D., A. R. Willhoite, et al. (2000). "Vascular niche for adult hippocampal neurogenesis." J Comp Neurol 425(4): 479-494.

Parveen, Z., M. Mukhtar, et al. (2003). "Cell-type-specific gene delivery into neuronal cells in vitro and in vivo." Virology 314(1): 74-83.

Pear, W. S., G. P. Nolan, et al. (1993). "Production of high-titer helper-free retroviruses by transient transfection." Proc Natl Acad Sci U S A 90(18): 8392-8396.

Petreanu, L. and A. Alvarez-Buylla (2002). "Maturation and death of adult-born olfactory bulb granule neurons: role of olfaction." J Neurosci 22(14): 6106-6113.

Pierce, J. P., M. Punsoni, et al. (2007). "Mossy cell axon synaptic contacts on ectopic granule cells that are born following pilocarpine-induced seizures." Neurosci Lett 422(2): 136-140.

Pinto, L. and M. Gotz (2007). "Radial glial cell heterogeneity--the source of diverse progeny in the CNS." Prog Neurobiol 83(1): 2-23.

Pressler, R. T. and B. W. Strowbridge (2006). "Blanes cells mediate persistent feedforward inhibition onto granule cells in the olfactory bulb." Neuron 49(6): 889-904.

Prevosto, V., W. Graf, et al. (2009). "Posterior parietal cortex areas MIP and LIPv receive eye position and velocity inputs via ascending preposito-thalamo-cortical pathways." Eur J Neurosci 30(6): 1151-1161.

Radley, J. J. and B. L. Jacobs (2002). "5-HT1A receptor antagonist administration decreases cell proliferation in the dentate gyrus." Brain Res 955(1-2): 264-267.

Reynolds, B. A. and S. Weiss (1992). "Generation of neurons and astrocytes from isolated cells of the adult mammalian central nervous system." Science 255(5052): 1707-1710.

Rhodes, C. H., A. Stieber, et al. (1987). "Transneuronally transported wheat germ agglutinin labels glia as well as neurons in the rat visual system." J Comp Neurol 261(3): 460-465.

Ribak, C. E., L. Seress, et al. (1985). "The development, ultrastructure and synaptic connections of the mossy cells of the dentate gyrus." J Neurocytol 14(5): 835-857.

Rochefort, C., G. Gheusi, et al. (2002). "Enriched odor exposure increases the number of newborn neurons in the adult olfactory bulb and improves odor memory." J Neurosci 22(7): 2679-2689.

Ruda, M. and J. D. Coulter (1982). "Axonal and transneuronal transport of wheat germ agglutinin

demonstrated by immunocytochemistry." Brain Res 249(2): 237-246.

Sahay, A., K. N. Scobie, et al. (2011). "Increasing adult hippocampal neurogenesis is sufficient to improve pattern separation." Nature 472(7344): 466-470.

Salin, P., M. Castle, et al. (2008). "High-resolution neuroanatomical tract-tracing for the analysis of striatal microcircuits." Brain Res 1221: 49-58.

Sanai, N., T. Nguyen, et al. (2011). "Corridors of migrating neurons in the human brain and their decline during infancy." Nature 478(7369): 382-386.

Santarelli, L., M. Saxe, et al. (2003). "Requirement of hippocampal neurogenesis for the behavioral effects of antidepressants." Science 301(5634): 805-809.

Santello, M., C. Cali, et al. (2012). "Gliotransmission and the tripartite synapse." Adv Exp Med Biol 970: 307-331.

Sawachenko, P., Gerfen, CR (1985). "Plant lectins and bacterial toxins as tools for tracing neuronal connections. ." Trends Neurosci 8: 378-384.

Scharfman, H. E. (2007). "The CA3 "backprojection" to the dentate gyrus." Prog Brain Res 163: 627-637.

Schmidt, B., D. F. Marrone, et al. (2012). "Disambiguating the similar: the dentate gyrus and pattern separation." Behav Brain Res 226(1): 56-65.

Schnell, M. J., J. P. McGettigan, et al. (2010). "The cell biology of rabies virus: using stealth to reach the brain." Nat Rev Microbiol 8(1): 51-61.

Schoppa, N. E. (2006). "A novel local circuit in the olfactory bulb involving an old short-axon cell." Neuron 49(6): 783-784.

Shepherd, G. M. (2003). Synaptic Organization of the Brain, Oxford Univeristy Press.

Shingo, T., C. Gregg, et al. (2003). "Pregnancy-stimulated neurogenesis in the adult female forebrain mediated by prolactin." Science 299(5603): 117-120.

Sibbe, M., E. Forster, et al. (2009). "Reelin and Notch1 cooperate in the development of the dentate gyrus." J Neurosci 29(26): 8578-8585.

Sidman, R. L., I. L. Miale, et al. (1959). "Cell proliferation and migration in the primitive ependymal zone: an autoradiographic study of histogenesis in the nervous system." Exp Neurol 1: 322-333.

Somogyi, P. and T. Klausberger (2005). "Defined types of cortical interneurone structure space and spike timing in the hippocampus." J Physiol 562(Pt 1): 9-26.

Song, H., C. F. Stevens, et al. (2002). "Astroglia induce neurogenesis from adult neural stem cells." Nature 417(6884): 39-44.

Song, J., K. Christian, et al. (2012). "Modification of hippocampal circuitry by adult neurogenesis." Dev Neurobiol.

Song, J., C. Zhong, et al. (2012). "Neuronal circuitry mechanism regulating adult quiescent neural stem-cell fate decision." Nature.

Stanfield, B. B. and J. E. Trice (1988). "Evidence that granule cells generated in the dentate gyrus of adult rats extend axonal projections." Exp Brain Res 72(2): 399-406.

Stepien, A. E., M. Tripodi, et al. (2010). "Monosynaptic rabies virus reveals premotor network organization and synaptic specificity of cholinergic partition cells." Neuron 68(3): 456-472.

Suh, H., A. Consiglio, et al. (2007). “In vivo fate analysis reveals the multipotent and self-renewal capacities of Sox2+ neural stem cells in the adult hippocampus.” Cell Stem Cell 1(5): 515-528.

Sultan, S., N. Mandairon, et al. (2010). “Learning-dependent neurogenesis in the olfactory bulb determines long-term olfactory memory.” FASEB J 24(7): 2355-2363.

Sun, B., B. Halabisky, et al. (2009). “Imbalance between GABAergic and Glutamatergic Transmission Impairs Adult Neurogenesis in an Animal Model of Alzheimer’s Disease.” Cell Stem Cell 5(6): 624-633.

Tanapat, P., L. A. Galea, et al. (1998). “Stress inhibits the proliferation of granule cell precursors in the developing dentate gyrus.” Int J Dev Neurosci 16(3-4): 235-239.

Tashiro, A., H. Makino, et al. (2007). “Experience-specific functional modification of the dentate gyrus through adult neurogenesis: a critical period during an immature stage.” J Neurosci 27(12): 3252-3259.

Tashiro, A., V. M. Sandler, et al. (2006). “NMDA-receptor-mediated, cell-specific integration of new neurons in adult dentate gyrus.” Nature 442(7105): 929-933.

Tavazoie, M., L. Van der Veken, et al. (2008). “A specialized vascular niche for adult neural stem cells.” Cell Stem Cell 3(3): 279-288.

Thanos, S., M. Vidal-Sanz, et al. (1987). “The use of rhodamine-B-isothiocyanate (RITC) as an anterograde and retrograde tracer in the adult rat visual system.” Brain Res 406(1-2): 317-321.

Thoulouze, M. I., M. Lafage, et al. (1998). “The neural cell adhesion molecule is a receptor for rabies virus.” J Virol 72(9): 7181-7190.

Toni, N., D. A. Laplagne, et al. (2008). “Neurons born in the adult dentate gyrus form functional synapses with target cells.” Nat Neurosci 11(8): 901-907.

Toni, N., E. M. Teng, et al. (2007). “Synapse formation on neurons born in the adult hippocampus.” Nat Neurosci 10(6): 727-734.

Tozuka, Y., S. Fukuda, et al. (2005). “GABAergic excitation promotes neuronal differentiation in adult hippocampal progenitor cells.” Neuron 47(6): 803-815.

Tronel, S., L. Belnoue, et al. (2012). “Adult-born neurons are necessary for extended contextual discrimination.” Hippocampus 22(2): 292-298.

Tuffereau, C., J. Benejean, et al. (1998). “Low-affinity nerve-growth factor receptor (P75NTR) can serve as a receptor for rabies virus.” EMBO J 17(24): 7250-7259.

Ugolini, G. (1995). “Specificity of rabies virus as a transneuronal tracer of motor networks: transfer from hypoglossal motoneurons to connected second-order and higher order central nervous system cell groups.” J Comp Neurol 356(3): 457-480.

Ugolini, G. (2008). “Use of rabies virus as a transneuronal tracer of neuronal connections: implications for the understanding of rabies pathogenesis.” Dev Biol (Basel) 131: 493-506.

Ugolini, G. (2010). “Advances in viral transneuronal tracing.” J Neurosci Methods 194(1): 2-20.

Ugolini, G., H. G. Kuypers, et al. (1987). “Retrograde transneuronal transfer of herpes simplex virus type 1 (HSV 1) from motoneurones.” Brain Res 422(2): 242-256.

Ugolini, G., H. G. Kuypers, et al. (1989). “Transneuronal transfer of herpes virus from peripheral nerves to cortex and brainstem.” Science 243(4887): 89-91.

van Praag, H., G. Kempermann, et al. (1999). “Running increases cell proliferation and neurogenesis in the adult mouse dentate gyrus.” Nat Neurosci 2(3): 266-270.

Ventura, R. E. and J. E. Goldman (2007). “Dorsal radial glia generate olfactory bulb interneurons in the postnatal murine brain.” J Neurosci 27(16): 4297-4302.

Vierbuchen, T., A. Ostermeier, et al. (2010). “Direct conversion of fibroblasts to functional neurons by defined factors.” Nature 463(7284): 1035-1041.

Wall, N. R., I. R. Wickersham, et al. (2010). “Monosynaptic circuit tracing in vivo through Cre-dependent targeting and complementation of modified rabies virus.” Proc Natl Acad Sci U S A 107(50): 21848-21853.

Warrell, M. J. and D. A. Warrell (2004). “Rabies and other lyssavirus diseases.” Lancet 363(9413): 959-969.

Weible, A. P., L. Schwarcz, et al. (2010). “Transgenic targeting of recombinant rabies virus reveals monosynaptic connectivity of specific neurons.” J Neurosci 30(49): 16509-16513.

Whitman, M. C., W. Fan, et al. (2009). “Blood vessels form a migratory scaffold in the rostral migratory stream.” J Comp Neurol 516(2): 94-104.

Whitman, M. C. and C. A. Greer (2007). “Synaptic integration of adult-generated olfactory bulb granule cells: basal axodendritic centrifugal input precedes apical dendrodendritic local circuits.” J Neurosci 27(37): 9951-9961.

Whitman, M. C. and C. A. Greer (2009). “Adult neurogenesis and the olfactory system.” Prog Neurobiol 89(2): 162-175.

Wickersham, I. R., S. Finke, et al. (2007). “Retrograde neuronal tracing with a deletion-mutant rabies virus.” Nat Methods 4(1): 47-49.

Wickersham, I. R., D. C. Lyon, et al. (2007). “Monosynaptic restriction of transsynaptic tracing from single, genetically targeted neurons.” Neuron 53(5): 639-647.

Witter, M. P. (2007). “The perforant path: projections from the entorhinal cortex to the dentate gyrus.” Prog Brain Res 163: 43-61.

Yassa, M. A. and C. E. Stark (2011). “Pattern separation in the hippocampus.” Trends Neurosci 34(10): 515-525.

Yoshihara, Y., T. Mizuno, et al. (1999). “A genetic approach to visualization of multisynaptic neural pathways using plant lectin transgene.” Neuron 22(1): 33-41.

Yoshimura, S., Y. Takagi, et al. (2001). “FGF-2 regulation of neurogenesis in adult hippocampus after brain injury.” Proc Natl Acad Sci U S A 98(10): 5874-5879.

Zhao, C., E. M. Teng, et al. (2006). “Distinct morphological stages of dentate granule neuron maturation in the adult mouse hippocampus.” J Neurosci 26(1): 3-11.

List of publications

This dissertation will be published as follows:

1. **Aditi Deshpande***, Matteo Bergami*, Alexander Ghanem, Karl-Klaus Conzelmann, Alexandra Lepier, Magdalena Götz, Benedikt Berninger. "*Retrograde monosynaptic tracing of connections onto adult-born neurons reveals a blueprint for incorporation into pre-existing circuits*" In preparation.

Other publications:

2. Ruth Beckervordersandforth-Bonk, **Aditi Deshpande,** Magdalena Götz. "*The combination of hGFAP and Prominin1 labels neural stem cells in the adult dentate gyrus*." In preparation.

3. Felipe Ortega, Sergio Gascon, Giacomo Masserdotti, **Aditi Deshpande**, Christiane Simon, Chichung Lie, Leda Dimou, Benedikt Berninger. "*Oligodendrogliogenic and neurogenic adult subependymal zone neural stem cells constitute distinct lineages and exhibit differential responsiveness to Wnt signalling.*" Nature cell biology. In revision.

4. Sergio Gascon, Felipe Ortega, Aditi Deshpande, Marisa Karow, Christophe Heinrich, Giacomo Masserdotti, Alex Lepier, Benedikt Berninger and Magdalena Götz. Contrasting effect of persistent and transient CREB-mediated transcription on neuronal reprogramming.

4. Cheryl M Travasso, Mona Anand, Mansi Samarth, **Aditi Deshpande**, Chandan Kumar-Sinha. "*Human papillomavirus genotyping by multiplex pyrosequencing in cervical cancer patients from India*." J Biosci. 2008 Mar;33(1):73-80.

Acknowledgements

"*I feel a very unusual sensation - if it's not indigestion, I think it must be gratitude.*"

- Benjamin Disraeli.

Working towards obtaining the highest degree education can offer has been an enjoyable journey, albeit long and oft tenuous. My accomplishment would lose merit if I did not thank all those who made it possible, bearable and even fun. I am truly grateful to Magdalena, especially for giving me an opportunity to pursue a PhD in her lab, despite knowing about my morbid fear of working with animals, and also for following my project with great interest and guiding me in the right direction whenever necessary. Her enthusiasm for science and her work are undoubtedly an inspiration. I am indebted to my supervisor, Benedikt, for believing that I could be a good PhD student for him as well as his support, patience and encouragement at all times.

I am thankful to Mark Hübener for his suggestions and guidance during my TAC meetings; to Karl-Klaus Conzelmann for unlimited quantities of rabies virus, for allowing me to work in his lab and for our discussions about my results during the TAC meetings and at the Gene Centre. I would also like to thank the Graduate School of Systemic Neurosciences for funding me for various conferences.

I would like to thank Alex Lepier for all the retrovirus-related help, from designing cloning strategies to preparing the viruses for me. I also would like to thank all other lab members who were always forthcoming in their assistance to me when required. Especially Matteo Bergami - for his intellectual and experimental help with my project; Monika Brill - for teaching me how to inject in vivo and Pratibha Tripathi - for being a good friend when I was new to the lab and to Munich. I am much obliged to Lana Polero for making my life so much easier by taking care of all the small things when I first came to Munich and the big things like contract extensions, reimbursements, visa etc.

I take this opportunity to thank all the technicians in the lab. Special mention to - Tatiana for teaching me to make primary cultures and for making cultures or stainings for me anytime I asked, always with a smile; to Ines for all her help in cloning, CsCl DNA preparation and many, many things she took care of when I asked; to Carmen for offering to help me (and then helping) with my experiments when I was busy writing the thesis and manuscript. A big thank you to

Simone and Detlef for making the retroviruses that I so often required.

I so greatly appreciate my amazing and patient friends - Leo, Andromachi, Felipe and Sergio - not only for always helping me but also for tolerating my idiosyncratic behaviour, bordering on misanthropic, and making me feel like I belong inspite of it. I am grateful to Giacomo for his ever-helpful nature and his wife Chiara, who makes the world's best crostata! I extend the same sentiment towards Christiane for patiently solving the countless problems I ran to her with, work-related or otherwise, and Francesca, for being a very good friend.

Lastly, this thesis would not have been possible without encouragement from my family - especially from my mother, with her frighteningly unwavering confidence in me, yearly visits to Munich and so many care packages sent from India; from my father, patiently supporting me in every single decision I make (and those that I don't) and from my brother, Anoop, my very silent pillar of strength. For that, I shall be eternally grateful.

Aditi.

Eidestattliche Erklärung

Ich erkläre hiermit, dass ich diese Dissertation selbstständig ohne Hilfe Dritter und ohne Benutzung anderer als der angegebenen Quellen und Hilfsmittel verfasst habe. Alle den benutzten Quellen wörtlich oder sinngemäß entnommenen Stellen sind als solche einzeln kenntlich gemacht.

Ich bin mir bewusst, dass eine falsche Erklärung rechtliche Folgen haben wird.

_____

Ort, Datum, Unterschrift